

FREQUENCY INDEPENDENT ANTENNAS INTERACTED ULTRA-WIDE
BAND (UWB) ARTIFICIAL MAGNETIC CONDUCTOR (AMC) FOR 5G
MILLIMETER WAVE WIRELESS COMMUNICATION APPLICATIONS

by

Xuehe Wang

A dissertation submitted to the faculty of
The University of North Carolina at Charlotte
in partial fulfillment of the requirements
for the degree of Doctor of Philosophy in
Electrical Engineering

Charlotte

2019

Approved by:

Dr. Ryan S. Adams

Dr. M.A Hassan

Dr. Thomas P. Weldon

Dr. Pinku Mukherjee

ABSTRACT

XUEHE WANG. Frequency Independent Antennas Interacted Ultra-Wide Band (UWB) Artificial Magnetic Conductor (AMC) for 5G Millimeter Wave Wireless Communication Applications. (Under the direction of DR. RYAN S. ADAMS)

This dissertation introduces the design and simulation work of a novel of UWB (Ultra-Wide Band) mushroom surface Artificial Magnetic Conductor, which acts as a reflector that interacts with frequency independent rectangular spiral antenna to enhance the radiation of certain directions by transforming absorption of unwanted radiation into reflection. This research proposed is designed to have a wider working bandwidth or better performance compared with the mushroom surface AMCs currently exist.

In this document, the background of the project, as well as the literature review of metamaterials' history and progress, is presented, as well as that of the electromagnetic waves and antennas.

The contributions made in the field of the theoretical research as well as applications are introduced, special of the millimeter wave spectrum which is very promising in the 5G wireless communication technologies.

This document first reviews the progress of Artificial Magnetic Conductors, then gives a theoretical explanation of why the AMCs may still work with the antennas although in their reactive near field regions. The theoretical models applied to explain the performance of the AMCs are summarized and discussed with the author's own discoveries in this field.

Using the theory summarize, a number of AMCs are designed and demonstrate to show their in-phase band and/or the performance with the wideband antennas. This document shows the work that first pushes the research of AMCs clearly into the spectrum of millimeter waves for 5G wireless communications and ultra-wideband performance. The performance of those AMCs is demonstrated with the wideband

spiral antennas.

Finally, the future work is proposed to push the research forward, for example, some on-chip structures for the 5G communications, and using the AMC as a great enhancer of the Multiple In Multiple Out antenna system which is of great importance in the 5G technologies.

ACKNOWLEDGEMENTS

To my mother, Ms. Yanwe Han, who loves me with all her life.

To my father, Mr. Jiashen Wang, who passed away more than 20 years ago.

To all my beloved ones.

To my beloved motherland of Manchuria.

I wish to give my special thanks to my committee members, especially my advisor, a great teacher, mentor, and friend of mine, Dr. Ryan Adams. For the Department of I would like to thanks to the GASP awarded by the Graduate School and the fundings by the Department of Electrical and Computer Engineering, which greatly helps me to propose this research.

I also would like to thank my labmates, Dr. Kathry Smith, Mr. Naveet Yadav, Mr. Dip Dhakhar, and Mr. Mohammad Fazeli, My Friend Dr. Chen Zhao who all helped me a lot in my study and research.

Thank Lord Jesus Christ for walking me through all the way to the United States and the life here.

TABLE OF CONTENTS

LIST OF FIGURES	ix
LIST OF TABLES	xv
CHAPTER 1: Introduction	1
1.1. Overview of the research	1
1.2. Broadband Topology - The Planar Frequency Independent Antennas	3
1.3. Artificial Magnetic Conductors	4
1.4. Motivation of Research	5
1.5. Dissertatoin Roadmap	6
LIST OF ABBREVIATIONS	1
CHAPTER 2: Electromagnetic Waves	8
2.1. Maxwell's Equations	11
2.2. Electromagnetic Wave Interaction with Materials	13
2.2.1. Response to Electric Stimulus: Relative Permittivity	15
2.2.2. Response to Magnetic Stimulus: Relative Permeability	18
2.3. Boundary Conditions	22
2.3.1. Fields in linear materials	23
2.3.2. Fields at a material interface	24
CHAPTER 3: Background: Antennas	28
3.1. Antenna Theory	28
3.2. Frequency Independent Antenna	39

CHAPTER 4: Literature Review: on Metamaterials Development	42
4.1. Introduction of Metamaterials	42
4.2. The prehistory of metamaterials	42
4.3. Founders of Metamaterial Techniques	43
4.4. Progress of Metamaterials	46
4.5. Artificial Magnetic Conductor	56
4.6. Mushroom AMC Design Equations	59
4.7. Restrictive Conditions of Mushroom AMC Design	61
CHAPTER 5: Artificial Magnetic Conductor Design	65
5.1. Design Analysis	65
5.2. Artificial Magnetic Conductor Design	67
5.3. The Artificial Atom Model	68
5.4. The Intrinsic Impedance Model	69
5.5. Artificial Magnetic Conductor Design Examples	71
5.5.1. Non-Mushroom AMCs	77
5.5.2. Millimeter Wave AMCs for 5G Applications	81
CHAPTER 6: Ultra Wideband Antennas Design and Feeding Methods	87
6.1. Traditional Rectangular Spiral Antenna	87
6.2. Varieties of Feeding Method	87
6.3. Offset Dual Layer Spiral Antennas	92
6.3.1. Example of Offset Dual Layer Spiral Antennas	94
6.3.2. Offset Dual Layer Rectangular Spiral Antenna	96
6.4. Results and Conclusion	101

	viii
CHAPTER 7: Ultra Wideband Antenna for 5G Millimeter Spectrum with AMC	103
7.1. Ultra Wideband Antenna for 5G Millimeter Spectrum	103
7.1.1. Circular Millimeter Wave Antenna	104
7.1.2. Rectangular Millimeter Wave Antenna	104
7.1.3. Spiral Antennas with 5G Millimeter Wave AMCs	105
CHAPTER 8: Summary and Perspection	119
8.1. Summary	119
8.2. Future Work	120
REFERENCES	121

LIST OF FIGURES

FIGURE 2.1: EM Wave Propagation Model in Free-space with E and H Fields Plotted	9
FIGURE 2.2: Electromagnetic Wave Spectrum Figure by NASA [6]	10
FIGURE 2.3: The Bohr Model of An Atom	14
FIGURE 2.4: The Bohr Model of An Atom and the Magnetic Moment Associated	14
FIGURE 2.5: Electrons Jumping Between Atoms	15
FIGURE 2.6: The equivalent polarized moments model associated with an individual atom	17
FIGURE 2.7: Formation of an electric field within a bulk dielectric material.	17
FIGURE 2.8: Formation of an magnetic field within a bulk dielectric material.	18
FIGURE 2.9: Image Currents associated with infinite planar boundaries with perfect electric conductors (PEC) and perfect magnetic conductors (PMC)	22
FIGURE 2.10: Field Vectors at an Interface Between Two Media	24
FIGURE 3.1: Different Kinds of Antennas	29
FIGURE 3.2: Wire in a Spherical Coordinate System	30
FIGURE 3.3: Patch Antenna Model	34
FIGURE 3.4: Patch Antenna Return Loss	34
FIGURE 3.5: Monopole and Dipole Antenna Models	35
FIGURE 3.6: Dual Band WLAN Antenna	35
FIGURE 3.7: Dual Band WLAN Antenna Return Loss	36

FIGURE 3.8: Single Frequency Antenna Return Loss Resonance Zoomed in	37
FIGURE 3.9: Narrow Band Antenna Return Loss Resonance Zoomed in	37
FIGURE 3.10: Waveguide Antenna Structure	38
FIGURE 3.11: Waveguide Antenna Return Loss	38
FIGURE 3.12: Monopole Antenna Return Loss	38
FIGURE 3.13: Dipole Antenna Return Loss	39
FIGURE 3.14: Frequency Independent Antenna Structures	41
FIGURE 4.1: Pendry's Metamaterials Schematic Figures	45
FIGURE 4.2: Leonhardt's Ideal Model of an Invisibility Cloak	47
FIGURE 4.3: Ideal DNG Performance for Visible Light	52
FIGURE 4.4: Simulation Structure and Result of the Negative Permittivity Ibeam Resonantor	53
FIGURE 4.5: Simulation Structure and Result of the Negative Permeability Ring Resonantor	54
FIGURE 4.6: Simulation Structure and Result of the DNG Resonantor	55
FIGURE 4.7: Mushroom Unit Cell Physical Structure	57
FIGURE 4.8: Mushroom Unit Cell Acting as DNG Material	58
FIGURE 4.9: Mushroom Unit Cell(s) and Equivalent Circuit	59
FIGURE 4.10: New Equivalent Circuit of Mushroom Surface When g gets bigger	63
FIGURE 5.1: Twisted Mushroom	67
FIGURE 5.2: Mushroom AMC Unit for Reference	71
FIGURE 5.3: Mushroom AMC Unit With Crossed Ground	72

FIGURE 5.4: Mushroom AMC Unit With Crossed Mushroom Top Patch	72
FIGURE 5.5: Mushroom AMC Unit With Air Substrate and RO4350 Superstrate	73
FIGURE 5.6: Malta Cross Mushroom AMC Unit	73
FIGURE 5.7: Malta Cross With Holes Mushroom AMC Unit	74
FIGURE 5.8: Disconnected Malta Cross With Holes Mushroom AMC Unit	74
FIGURE 5.9: Malta Cross With Holes Mushroom and Middle Patch AMC Unit	75
FIGURE 5.10: Less Removed Malta Cross With Holes Mushroom and Middle Patch AMC Unit	75
FIGURE 5.11: Hollowed Exponential Wire Structure AMC Unit	75
FIGURE 5.12: Cruciferous Wire Structure AMC Unit	76
FIGURE 5.13: Wire Doji/Shuriken Structure AMC Unit	76
FIGURE 5.14: Hollowed Malta Crossl Wire Structure AMC Unit	77
FIGURE 5.15: Hollowed Wire Net Structure AMC Unit	77
FIGURE 5.16: Patch to Patch AMC Unit	78
FIGURE 5.17: Patch to Patch Structure AMC width Reflection Phase	79
FIGURE 5.18: Nesting Rectangular Ring Structure AMC	79
FIGURE 5.19: Three Rings Structure AMC	80
FIGURE 5.20: Crossed Circular Rings Structure AMC	80
FIGURE 5.21: Four Rings Eight Wings Structure AMC	81
FIGURE 5.22: Typical 3D Radiation Pattern to Show How AMC Works as a Reflector	84
FIGURE 5.23: Wired Axe Top Millimeter Wave AMC	85

FIGURE 5.24: Wired Axe Top Cross Ground Millimeter Wave AMC	85
FIGURE 5.25: Four Spears Top with Cross Ground Millimeter Wave AMC	86
FIGURE 5.26: Vertical Cross Millimeter Wave AMC	86
FIGURE 6.1: Return Loss of the Rectangular Spiral Antenna over the Mushroom Surface	88
FIGURE 6.2: Rectangular Planar Spiral Antenna	89
FIGURE 6.3: Rectangular Planar Spiral Antenna Return Loss	89
FIGURE 6.4: 3D Radiation Patterns of 3.5GHz	90
FIGURE 6.5: Vertical Transformer Design	91
FIGURE 6.6: Vertical Transformer Radiation Pattern With/Without AMC Mushroom Surface	92
FIGURE 6.7: Integrated Transformer Design	93
FIGURE 6.8: Integrated Transformer Radiation Pattern With/Without AMC Mushroom Surface	94
FIGURE 6.9: Full Layer on Top Transformer Design	95
FIGURE 6.10: Full Addon Layer on Top Radiation Pattern With/Without AMC Mushroom Surface	96
FIGURE 6.11: Millimeter Wave Offset Dual Layer Circular Spiral Antenna	97
FIGURE 6.12: Offset Dual Layer Circular Spiral Antenna Fed with Perpendicular Coax Cable	97
FIGURE 6.13: Return Loss of the Millimeter Wave Offset Dual Layer Circular Spiral Antenna	98
FIGURE 6.14: Return Loss of the Offset Dual Layer Rectangular Spiral Antenna	98
FIGURE 6.15: Circular 3D Radiation Patterns of the Millimeter Circular Spiral Antenna at 30GHz	99

FIGURE 6.16: Millimeter Wave Offset Dual Layer Rectangular Spiral Antenna	100
FIGURE 6.17: Rectangular Spiral Antenna Fed with Perpendicular Coax Cable	100
FIGURE 6.18: 3D Radiation Patterns of The Offeset Rectangular Dual Layer Spiral Antenna	101
FIGURE 6.19: Offset Dual Layer Circular Antenna System Three View	102
FIGURE 6.20: Offset Dual Layer Circular Antenna System Three View	102
FIGURE 7.1: 5G Millimeter Wave Circular Spiral Antenna	103
FIGURE 7.2: 5G Millimeter Wave Rectangular Spiral Antenna	104
FIGURE 7.3: Return Loss of Millimeter Wave Circular Spiral Antenna	105
FIGURE 7.4: Impedance of Millimeter Wave Circular Spiral Antenna	105
FIGURE 7.5: Gain of Millimeter Wave Circular Spiral Antenna 10GHz - 50GHz	106
FIGURE 7.6: Return Loss of Millimeter Wave Chamfered Rectangular Spiral Antenna	107
FIGURE 7.7: Impedance of Millimeter Wave Chamfered Rectangular Spiral Antenna	107
FIGURE 7.8: Gain of Millimeter Wave Chamfered Rectangular Spiral Antenna 10GHz - 50GHz	108
FIGURE 7.9: Retrurn Loss Comparison for a Wire Bowtie Antenna with and without Mushroom AMC	110
FIGURE 7.10: Impedance Comparison for a Wire Bowtie Antenna with and without Mushroom AMC	111
FIGURE 7.11: Return Loss Comparison for a Frequency Independent Antenna with and without Mushroom AMC	112
FIGURE 7.12: Impedance Comparison for a Frequency Independent Antenna with and without Mushroom AMC	113

FIGURE 7.13: Patch to Patch Millimeter Wave AMC	114
FIGURE 7.14: Gains With Patch to Patch AMC	115
FIGURE 7.15: Vertical Cross Millimeter Wave AMC	116
FIGURE 7.16: Gains With The Vertical Cross AMC	117
FIGURE 7.17: The Structure of Return Losses of the Wire Bowtie Antennas	118
FIGURE 7.18: AMC Phase of Reflection and Gain With Bowtie	118

LIST OF TABLES

TABLE 2.1: Parameters Associated with Maxwell's Equations	13
TABLE 3.1: Different Types of Frequency Independent Antenna	40
TABLE 5.1: Thresholds of Distance	83
TABLE 6.1: Parameters for Rectangular Spiral Antenna Prototype	87
TABLE 6.2: Parameters for Offset Dual Layer Circular Spiral Antenna	95
TABLE 6.3: Parameters for Offset Dual Layer Rectangular Spiral Antenna	99
TABLE 7.1: Parameters for Offset Dual Layer Rectangular Spiral Antenna	104
TABLE 7.2: Parameters for Offset Dual Layer Rectangular Spiral Antenna	106
TABLE 7.3: Parameters for Patch to Patch AMC	113
TABLE 7.4: Parameters for Vertical Crossed Rings AMC	114

CHAPTER 1: Introduction

1.1 Overview of the research

The design and analysis of electromagnetic structures and circuits have been of increasing interest since Maxwell published his seminal work in 1865 [2]. In more recent years, electromagnetic structures have evolved even more rapidly because of the numerous applications for them, such as the communication systems, biomedical imaging, RADAR systems and so forth. A couple of years ago only, the 5th generation (5G) standard has been proposed that pushes the frequency of operation for many of these critical applications upward into the spectrum region of a millimeter wave.

In the purpose of helping to push this work forward, it is critical for us to have a full understanding of the behavior of those metamaterials in the presence of high-frequency electromagnetic waves over a broad bandwidth. To assist in this understanding, researchers have proposed many models that effectively describe the mechanisms that are in play when electromagnetic waves come in contact with materials commonly found in nature. These models include such designs as the Frequency Selective Surfaces, the Artificial Magnetic Conductors, and the Photonic Crystals. Each of these models has found broad applicability to materials that are periodic in structure. To realize their function of design, they usually contain both conductive and non-conductive components. These and other classes of materials generally all fall under the category of Metamaterials. The metamaterial, in one word, is a concept covers all kinds of materials that are not naturally foundable.

It has been demonstrated extensively in the literature that the metamaterial model for electromagnetic interaction with periodic structures is an effective one, and has led to incredible advances in device design and implementation. These structures

form the basis for such applications as cloaking, superluminal behavior, magnetic conductors, and left-handed propagation in which the phase velocity points in the opposite direction to the Poynting vector. Each of these phenomena is considered to be essentially impossible using bulk traditional materials, but have been done numerous times under the auspices of the metamaterial model.

While great success has been achieved in developing and using the metamaterial model, numerous gaps still exist in the development of stopping us from going really deep. For example, the interaction of these materials with antennas is still in its infancy, especially when the periodic metamaterial structure is placed in the near field of a wideband antenna, sometimes, those metamaterials act as a part of the medium in which the antenna presents, however, in some other cases, the metamaterials involve begin to act as an add-on component to the radiation body which interrupts the radiation field pattern and changes it completely. Among them, the wideband behavior represents a particular problem for this model as typically the unique behavior of metamaterials is caused by a resonance condition which is, by very nature, narrow band. So the challenge here is to attempt to incorporate narrow band material performance into a wideband scenario. In this work proposed, we will focus on the application of Artificial Magnetic Conductor (AMC) Frequency Selective Surfaces (FSS) to the near field of wideband antennas, especially with frequency independent topologies.

Briefly speaking the metamaterials are a novel series of structures that have special performance when interacting with electromagnetic fields and waves. As mentioned, those materials can be applied in many fields to realize functions that traditional materials are not able to. For example, an invisibility cloak can hide the items under the cover of it from the eyes of people or the detection devices by guiding the incident electromagnetic waves. A Double Negative Material can make the incident wave to travel backward although it is not a mirror.

It can be concluded that the future of metamaterials is beyond today's imagination. It will make something we now think as nothing but magic tricks to come true. No surprise that metamaterials are considered as the greatest discovery after the discovery of metal by some experts in this field.

The artificial magnetic conductor is one of the most promising types among the metamaterials. An AMC is used to perform as a Perfect Magnetic Conductor within a certain bandwidth call the bandwidth of operation.

Since AMC has only a few decades of history, there are a lot of points of interest to look into. New properties to be discovered, and new structures to be come up with, and what else functions they can have.

The research proposed in this proposal is based on a type of applications of the AMC. It is called Ultra-wideband (UWB) Artificial Magnetic Conductor (AMC) and is demonstrated by the interaction with frequency independent antennas. In this chapter, we hereby briefly lay out the roadmap of the proposed research work.

1.2 Broadband Topology - The Planar Frequency Independent Antennas

Broadband topologies performance of Artificial Magnetic Conductor is demonstrated with a type of antennas which operate across a very wide bandwidth. The type of antenna selected for this demonstration is the frequency independent antenna, which has gained its popularity for decades in the modern world. A Frequency Selective Surface Artificial Magnetic Conductor interacted frequency independent antenna is supposed to be a planar one in order to make sure different parts of the antenna to have the same distance from the Artificial Magnetic Conductor surface. In other words, to fulfill the design requirements of the proposed work discussed in the following chapters, we need the frequency independent antenna to be planar.

The performance of the electromagnetic field is very sensitive in the near-field regions, any change of the conductive area of interaction may lead to a completely altered field distribution. As a result, the selection of the frequency independent

antenna must be very careful.

Typically, the frequency independent antenna's radiation towards the upper and lower halves of the space are equal. However, some of these applications require semi-sphere radiation. Hence, radiation of the other half of the space called the unwanted radiation needs to be eliminated. Current designs applied mostly use a honeycomb cavity to absorb the unwanted radiation and as a result, half of the energy is lost in vain, and methods need to be taken to solve this problem.

1.3 Artificial Magnetic Conductors

Per Maxwell's equations discussed in the following chapters, a perfect magnetic conductor should be able to reflect the electric field parallel to it without changing its direction. However, since no natural PMC material has been found yet, researchers develop a special type of structures which can mimic the performance of PMC when operated on certain bandwidths, and those materials are named as artificial magnetic conductors(AMC). Methods of making artificial magnetic conductors can be varied as long as they can successfully perform like or similar to a PMC within the frequency band of operation. As a result, the structure of AMCs that have close performances may be very different in their structures.

The mushroom surface structure is an AMC deeply researched nowadays, of which band is defined per the phase shift of fields reflected, i.e., the working band is determined by the continuous upper and lower frequencies between which the phase shift of E field of perpendicularly incident plane waves lies within $\pm 90^\circ$. For the same field, PMC gives a 0° phase shift (the equivalence is an image current that has equal value and same direction that doubles the radiation) and PEC(Perfect Electric Conductor) gives a $\pm 180^\circ$ (the equivalence is an image current that has same value but opposite direction, which almost cancels the radiation) .Consequently, a $\pm 90^\circ$ phase shift means a conductor performance more like a PMC than a PEC.

In that way, the AMC mushroom surface structure is able to replace the absorbing

cavity located below the wide-band antenna. And by doing this, a part of the energy radiated to the unwanted half of the space can be reflected and turned into the radiation we need. That means if the total radiation energy remains the same, the power receiver can be increased, and we can reduce the input power to the antenna if the current radiation power is already sufficient for the applications.

Researchers have made a lot of contributions in the development of the Artificial Magnetic Conductor, such as a series of models of explanation the interaction between the electromagnetic fields and the AMC. However, these models are not that universal and are not able to guide the further practice of AMC.

1.4 Motivation of Research

Among the Frequency Selective Surface Artificial Magnetic Conductors, the mushroom surfaces interact with antennas reflectors have been introduced in for a few decades, however, not only the mechanism is not clear, but also the working bandwidth is not yet satisfying. They either operate across only a narrow band or need an extra element to perform a wide-band function, which required external energy and cost. [33]

An efficient way of designing mushroom surface AMC needs to be found which helps to enhance the performance of a frequency independent antenna across the entire required working bandwidth. As is proposed here in this document.

Ideal Perfect Magnetic Conductor has no limitation of working bandwidth, expanding the working bandwidth of mushroom surface AMCs wider helps us to find methods of making an AMC more closer to a PMC.

In order to advance the application of the Frequency Selective Surface Artificial Magnetic Conductor, the work proposed here intends to fulfill these proposes:

1. Improvement of the current designs of Mushroom AMC, to enhance the performance and expand the bandwidth of operation.
2. Figure out the universal mechanism of the Artificial Magnetic which will be

applied for guiding the further development of Artificial Magnetic Conductor design.

3. Using the universal mechanism figured out to design non-mushroom Frequency Selective Surface Artificial Magnetic Conductor.

The novel mushroom structure design is the first step and it needs to fulfill the following requirements.

1. The mushroom surface AMC needs to have a better performance than any current designs, which means either a wider band or smother curve of the phase of reflection.

2. The mushroom surface AMC needs to be able to work for the entire required bandwidth of operation of the frequency independence antennas interact with it.

3. The mushroom surface AMC needs to have the performance list above all by itself, no extra power supply or components are allowed in the system.

4. The fabrication of the mushroom surface AMC should not need to be more complicated than the current exist designs of Mushroom AMC.

5. The cost of fabrication cannot be more than the current exist designs of mushroom AMC.

6. The structure of the mushroom AMC needs to be reasonably simple.

In order to solve all the problems and fulfill the requirements above, the work in this document is proposed.

1.5 Dissertatoin Roadmap

The rest of this proposal document is organized as follows. In order to make the background to be clearly stated, it has been divided into three chapters. Background knowledge needed for the proposed research is discussed and the open literature is reviewed inside each of these chapters. There are two major parts of the rest chapters, the first part of Chapter 2 - Chapter 3, is about the background of the proposed research. Chapter 4 is a literature review of the current achievement researcher have made in Chapter 5 is about the proposed work.

Chapter 2 reviews the theoretical background electromagnetic fields and waves, as well as Maxwell's equations.

Chapter 3 goes over the theory background related to the antennas and frequency independent antenna.

Chapter 4 introduces the background, especially the open literature on the history of development and achievements in general of metamaterials.

Chapter 5 summarizes the theory of AMC design, as well as the models used to explain the performance of Artificial magnetic conductors. In this chapter, a number of different AMCs designed according to the theory discovered are also introduced and evaluated. Another contribution of great importance discussed in this chapter is the reason why the AMC can work with the antennas within their reactive near field region, methods of effectively reducing the unwanted interactions are also proposed and evaluated.

Chapter 6 shows the design procedure of wideband antennas which are used for demonstration purpose of the AMCs. Varieties of feeding methods are raised and evaluated, with the final decision of feeding method/antenna structure selection.

Chapter 7 mainly focuses on the antenna and AMCs which work for the millimeter wave in the coming 5G wireless communication technologies, in this chapter, ultra wideband and wideband AMCs are presented and evaluated in details. Meanwhile, the basic wideband antennas are modified to better demonstrate the function of the AMCs. Finally, this chapter also shows what will happen when the wideband millimeter-wave AMCs are interacting with narrowband/single frequency antennas. It is a persuasive way to prove that the design is universally applicable.

Chapter 8 summarizes the work presented in the entire document, discusses the possible applications. At last, this chapter proposes some future work that may help the AMCs to be more practical, and meanwhile, push the research and application of 5G millimeter wave wireless communication technologies forward.

CHAPTER 2: Electromagnetic Waves

Prior to the 19th century, it was generally thought that electricity and magnetism were completely separate phenomena, each with its own behavior. This notion persisted until Oersted observed a connection between the two fields in 1820 [1] and Michael Faraday further defined that relationship in his seminal set of experiments beginning in 1831 to form what is now known as Faraday's law [1]. Faraday conclusively demonstrated that a time-varying magnetic flux density gives rise to an electric field. This set of experiments defined the topic of electromagnetic induction and led to the development of devices such as transformers and motors.

These early efforts created a partial connection between electricity and magnetism, but the relationship remained weak until the complete description was proposed by James Clerk Maxwell who asserted that a time-varying electric flux density gives rise to a magnetic field. This contribution closed the loop on electricity and magnetism and represents one of the greatest technical accomplishments of the 19th century. The equations that we now, rightly, call Maxwell's equations combined for the first time the behavior of electricity and magnetism into a complete theory and has led to numerous breakthroughs since.

While devices such as transformers and motors may be postulated under the slow-time-varying assumption, fields that change rapidly with time lead to the more exotic phenomena of wave behavior. These electromagnetic waves have the potential to deliver energy over very large distances and very long time periods; on a galactic scale, the distances are measured in millions of light years. When these waves propagate in free space, the only acceptable mode is the Transverse ElectroMagnetic (TEM) mode in which the electric field vector points perpendicular to the magnetic field vector,

and both are oriented perpendicular to the direction of propagation. This relationship is illustrated in Figure 2.1. In this case, the solution to the wave equation leads to sinusoidal behavior in space, where the period of the sinusoidal response is called the wavelength λ and the speed of the wave is the phase velocity; in the vacuum, the phase velocity is the speed of light in free-space, c .

Every other electromagnetic wave mode represents variations of this initial model.

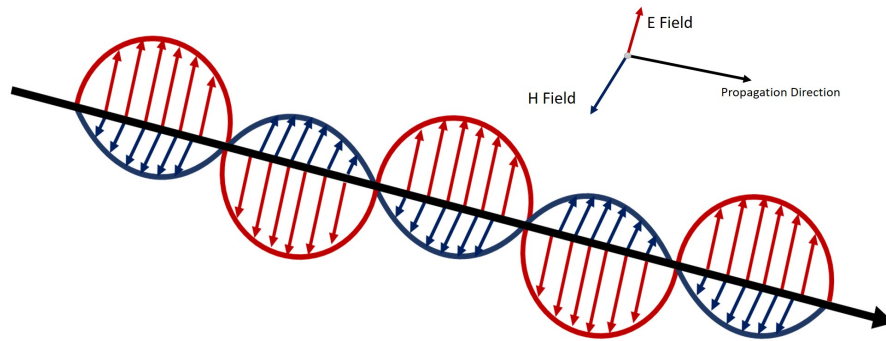


Figure 2.1: EM Wave Propagation Model in Free-space with E and H Fields Plotted

Electromagnetic waves come in varieties of forms, from Cosmic ray to ultraviolet, and from visible light to long wave radio, the electromagnetic waves cover a huge spectrum, as shown in the Figure2.2 of EM wave spectrum by NASA. The wavelength of EM waves varies from 10^{-16} to the scale of several kilometers.

Applications based on electromagnetic waves

Electromagnetic waves have been utilized for a multitude of purposes for all of recorded history. For example, electromagnetic wave generators include such things as torches, candles, and fires all the way to the cotton filament light bulb, fluorescent lights, and light emitting diodes each perform the same basic purpose: provide illumination in the visible spectrum. Additional applications of electromagnetic waves have only been considered in the last two centuries, however.

More recently, additional exotic and dynamic applications of these waves are devel-

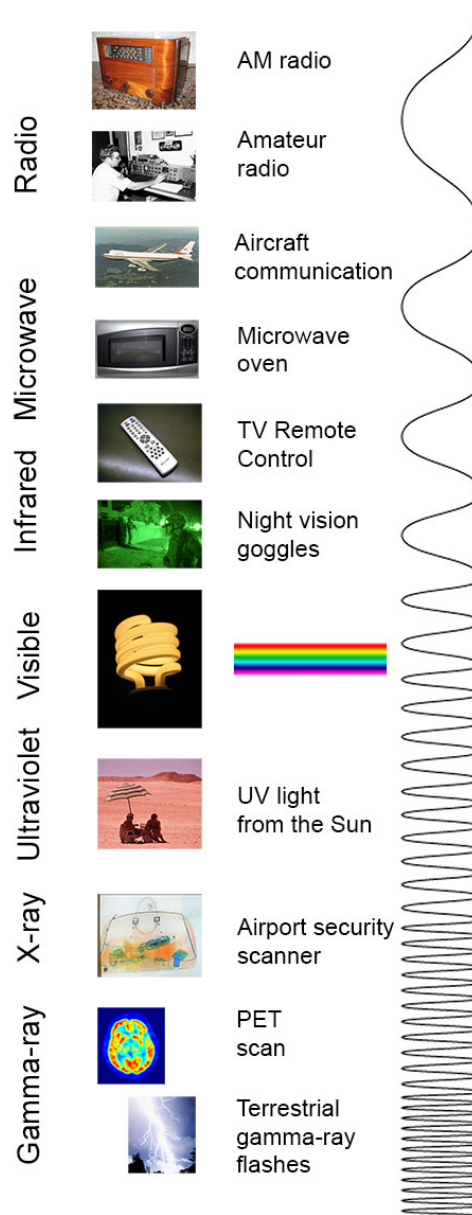


Figure 2.2: Electromagnetic Wave Spectrum Figure by NASA [6]

oped continuously. For example, the UltraViolet (UV) spectrum is used as a source for so-called black light lamps that are helpful in the application of insecticides. The Infrared (IR) spectrum is used to heat food, to detect objects, as well as various medical treatments. Microwave ovens are widely used in homes and offices making cooking faster and safer.

2.1 Maxwell's Equations

While Maxwell originally published his equations utilizing the mathematical tool of quaternions [2], around the transition from the 19th to the 20th centuries, Oliver Heaviside proposed an alternative form of these equations that makes use of vector notation. This notation has been refined since that time to be expressed in a very compact form. The point form of these equations can be decomposed into two sets that, together, satisfy the requirements of the Helmholtz theorem; Helmholtz postulated that both the curl and divergence of each vector field must be defined in order to fully define the field. The curl equations are given by

$$\begin{aligned}\nabla \times \bar{E} &= -\frac{\partial \bar{B}}{\partial t} - \bar{J}_m && \text{Faraday's Law} \\ \nabla \times \bar{H} &= \frac{\partial \bar{D}}{\partial t} + \bar{J}_e && \text{Ampere's Law}\end{aligned}$$

These equations clearly demonstrate the relationship between electric and magnetic fields through the curl and time derivative. Similarly, the divergence equations are given by

$$\begin{aligned}\nabla \cdot \bar{B} &= \rho_m && \text{Solenoidal Law} \\ \nabla \cdot \bar{D} &= \rho_e && \text{Gauss's Law}\end{aligned}$$

In these equations, the magnetic current \bar{J}_m and magnetic charge ρ_m are included. Although these quantities are not physically present in nature, they may be assumed to be present as quivalent parameters.

To conclude the development, two constitutive relations exist; one to relate the electric field with electric flux density, and another to relate the magnetic field with

magnetic flux density. In general, these constitutive relations are expressed as

$$\bar{B} = \mu_o(\bar{H} + \bar{M})$$

$$\bar{D} = \epsilon_o\bar{E} + \bar{P}$$

where $\mu_o = 4\pi \times 10^{-7}$ and $\epsilon_o = 8.854 \times 10^{-12}$. While these constitutive relations are fully generalizable, they may be simplified in cases where the material is defined as **simple**. Such materials have the properties of **linearity**, **homogeneity**, and **isotropy**. Under this assumption, the constitutive relations simplify to

$$\bar{B} = \mu_o\mu_r\bar{H} = \mu\bar{H}$$

$$\bar{D} = \epsilon_o\epsilon_r\bar{E} = \epsilon\bar{E}$$

where μ_r and ϵ_r are unitless scaling factors.

When time-harmonic waves are assumed, the field quantities each are proportional to $e^{j\omega t}$, and so all time-derivatives may be replaced with multiplication with $j\omega$. In this case, Maxwell's Equations simplify to

$$\nabla \times \bar{H} = j\omega\bar{D} + \bar{J}_e \quad \text{Ampere's Law}$$

$$\nabla \times \bar{E} = -j\omega\bar{B} - \bar{J}_m \quad \text{Faraday's Law}$$

$$\nabla \cdot \bar{B} = \rho_m \quad \text{Solenoidal Law}$$

$$\nabla \cdot \bar{D} = \rho_e \quad \text{Gauss's Law}$$

Time-harmonic waves satisfy the same constitutive relations stated above. Each of the parameters used above, and the units associated with them, are summarized in Table 2.1.

Table 2.1: Parameters Associated with Maxwell's Equations

Parameter	Definition	Unit
\vec{H}	Magnetic Field	A/m
\vec{E}	Electric Field	V/m
\vec{B}	Magnetic Flux Density	Wb/m ²
\vec{D}	Electric Flux Density	C/m ²
\vec{J}_m	Magnetic Current Density	V/m ²
\vec{J}_e	Electric Current Density	A/m ²
ρ_m	magnetic Charge Density	Wb/m ³
ρ_e	Electric Charge Density	C/m ³
M	Bulk Magnetization	A/m
P	Bulk Material Polarization	V/m
μ_o	Permeability of Free-Space	H/m
ϵ_o	Permittivity of Free-Space	F/m

2.2 Electromagnetic Wave Interaction with Materials

The previous section presented the basic equations associated with electromagnetic wave propagation and defined pertinent quantities associated with them. In this section, we wish to discuss in greater detail the direct interaction of electromagnetic waves with non-vacuum material media. The mechanisms which occur with traditional simple materials will create a framework for a discussion of the specific contributions later in this work.

We begin with a simple model for the basic structure of an atom. While more complicated, and correspondingly more accurate, models are commonly used to describe atomic behavior, the simple Bohr model is sufficient for our purposes. This first-order model assumes that the structure of an atom is equivalent to a tiny “solar system” as illustrated in Figure 2.4. In this model, the protons and neutrons of a given atom form a dense nucleus that represents the “sun”, and the electrons that orbit this nucleus in a circular or elliptical path represent the “planets.” Note that in its native state, this atom is electrically neutral, and the electron orbits are centered on the nucleus, so no appreciable net field extends beyond the electron orbits. Also,

please be aware of that, in order to avoid misunderstanding of any specific material, the Bohr atom model presented here is intentionally made to be one that is different from any existing atoms.

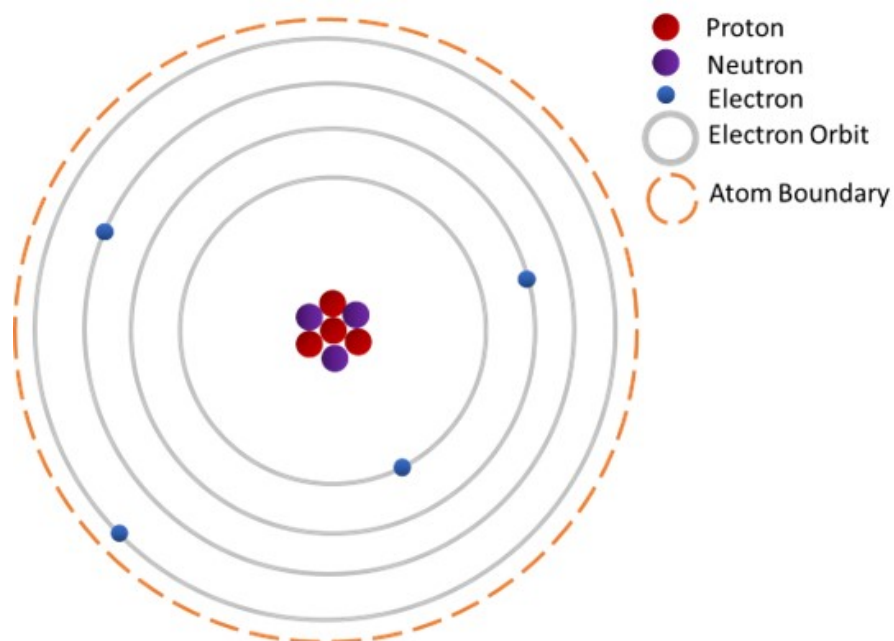


Figure 2.3: The Bohr Model of An Atom

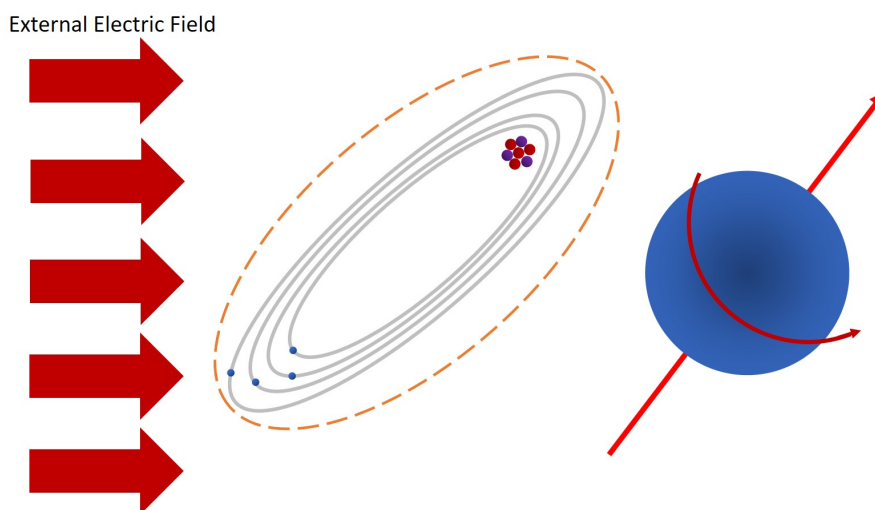


Figure 2.4: The Bohr Model of An Atom and the Magnetic Moment Associated

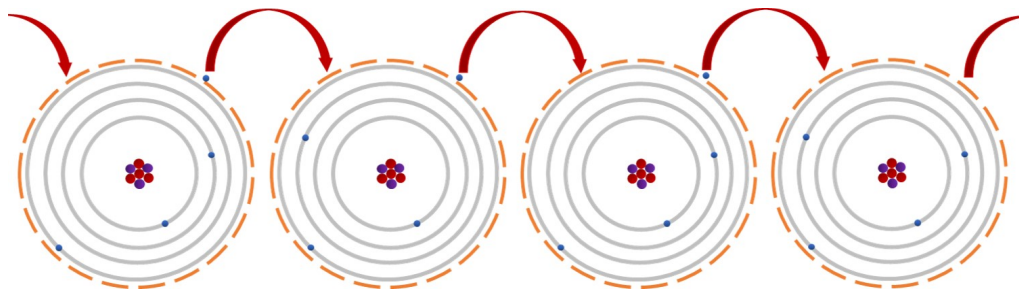


Figure 2.5: Electrons Jumping Between Atoms

2.2.1 Response to Electric Stimulus: Relative Permittivity

Now, let's consider this atom in isolation, and without anything nearby, and assume that an electric field impinges upon it from some external source. This outside field will cause the electron orbit to become more elliptical, with more time spent farther from the nucleus than in its unperturbed state. Additionally, the external field tends to push the nucleus in the opposite direction; both effects are illustrated in Figure 2.4. This modified atomic structure exhibits a finite net distance between the positively charged nucleus and the center of mass of the electron orbit, forming a very small electric dipole. While the separation distance between positive and negative charges is small, it may not be neglected as it will cause deviations in the electric field in the near vicinity of the atom.

This notion may be extended to bulk materials in which an extremely large number of atoms are oriented in some meaningful structure. In the case of a bulk material, so many atoms are present that it is not practical to treat each atom individually. Instead, it is common to convert the dipole moment of each atom into an approximate continuum of electric dipole moments and consider only the volume density of discrete dipole moments across the material. This averaging of moments lead to the concept of macroscopic electromagnetics, and it is only a valid assumption under one condition: **The interatomic spacing must be significantly smaller than the wavelength of the incident electric field.** For very high frequencies, or very large atomic

spacings, this approximation breaks down, and the model must extend to include each atom in the material.

The situation of Figure 2.5 may be extended by consideration of a line of several atoms within an arbitrary material. This scenario is depicted in Figure 2.5. In most materials, the valence electrons are not perfectly attached to a single atom. This is especially true for the transition metals and semiconducting materials that have been properly doped to add electrons to the conduction band. Even very tightly bound electrons can “jump” from one atom to another if sufficient energy is applied. This scenario is shown in Figure 2.5. This effect is treated as a loss within the material, and the relative permittivity is expressed as a complex value as,

$$\epsilon = \epsilon_o \epsilon_r - j \frac{\sigma}{\omega} \quad (2.1)$$

where σ is the electric conductivity and represents the tendency of a material’s electrons to move between atoms; larger values of σ arise from atoms with weak bonds to their electrons, and small values of σ are associated with atoms with very strongly bonded electrons.

Finally, we can represent the electric moment generated by an atom with a polarized particle which has a positive charge at one end and negative on the other named a polarized electric moment model. Similarly, when we’re talking about the permeability of a material, we can simplify the atomic structure by assuming the magnetic moment the electron motion current produces to have a structure of a bar magnet, and we may call it as the polarized magnetic moment model. Both the models of the electric/magnetic moments are shown as in Figure2.6, with an electric moment on the left, and a magnetic moment on the right.

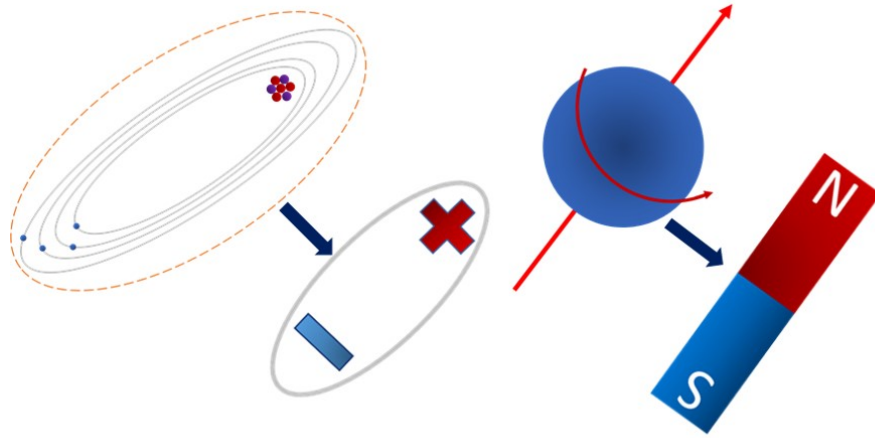


Figure 2.6: The equivalent polarized moments model associated with an individual atom

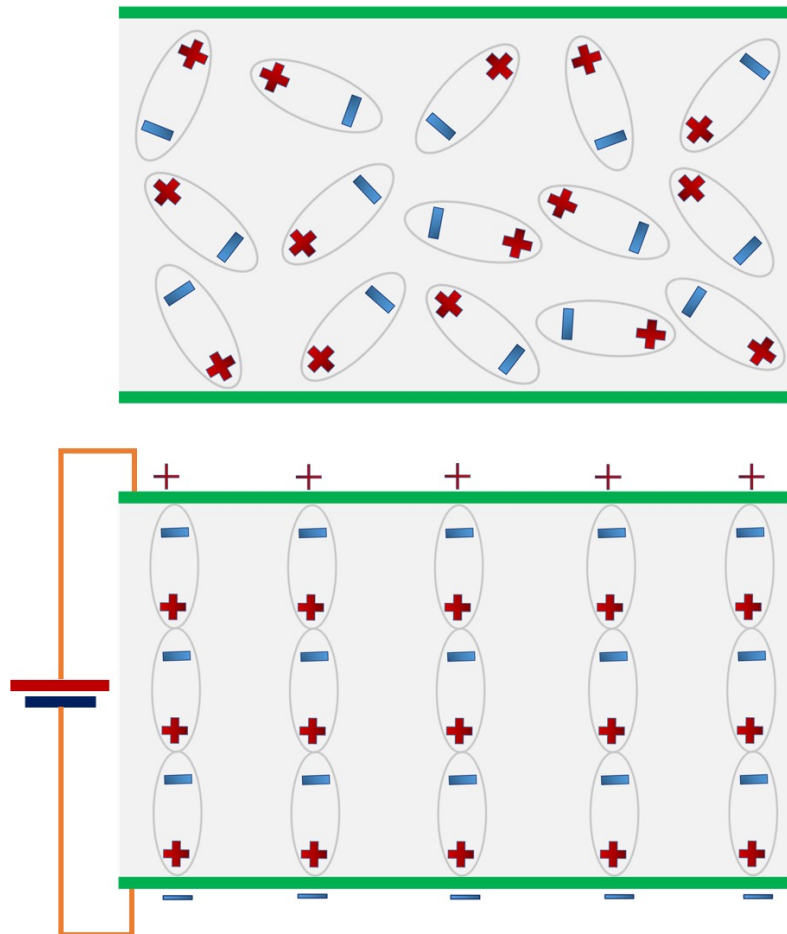


Figure 2.7: Formation of an electric field within a bulk dielectric material.

2.2.2 Response to Magnetic Stimulus: Relative Permeability

The model we used for the discussion of permeability is the polarized magnetic moment model. By definition, permeability, although has a similar name to permittivity, is the medium's ability to assist the form a magnetic field inside instead of resisting it. The measurement of permeability is the degree of magnetization obtained in response to an applied magnetic field, and the unit in SI for permeability is H/m, H is short for Henry here. The procedure of the magnetic field formed in a medium is shown as in Figure 2.8. The value of permeability also varies with temperature, external field frequency, humidity are some other factors like permittivity does, so the same material can have different permeabilities under different circumstances.

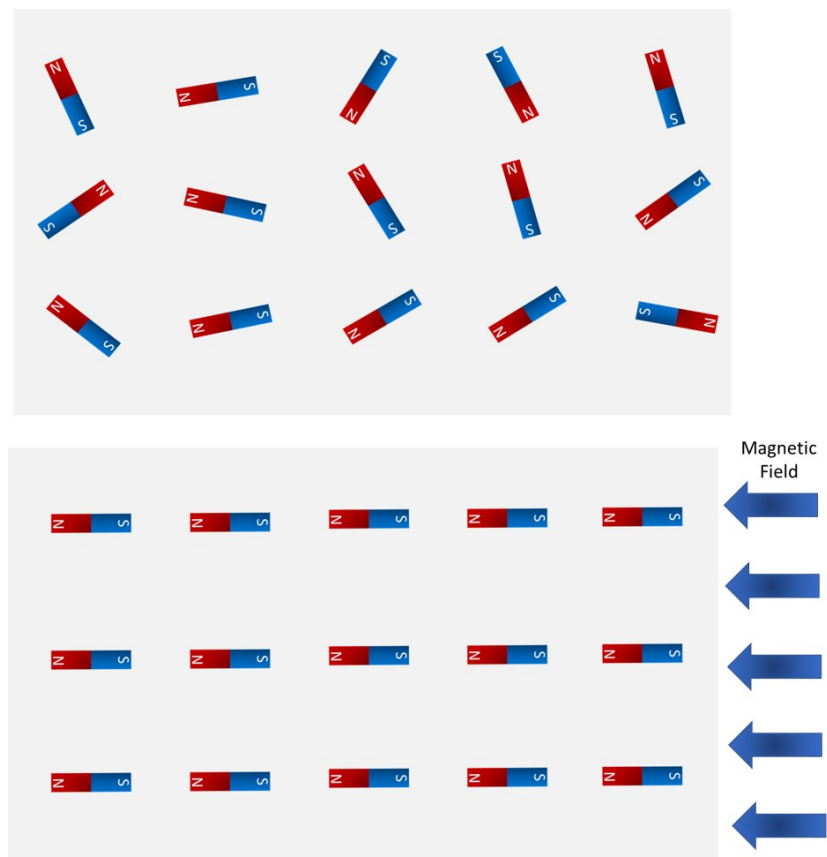


Figure 2.8: Formation of an magnetic field within a bulk dielectric material.

The value of permeability varies with temperature, external field frequency, hu-

midity are some other factors. As a result, the same material can have different permeabilities under different circumstances. It can be concluded from the definition that the difficulty of field formation decreases with the permeability gets bigger. Meanwhile, we have some questions for further discussion.

Since the permeability is defined to be the capability of a medium to enhance/help the formation of magnetic field internally, However, the free-space still have a permeability of $\mu_0 = 4\pi \times 10^{-7}$ H/m, it doesn't look reasonable at first glance, if there is nothing, then there shouldn't be any support for the formation of magnetic field, in other words, the free-space permeability should be 0. Hence, this is another topic we should pay attention to.

Similar to the discussion of the free space permittivity, scientists and engineers also came up with all kinds of answers to this question but the debate still continues. The answer which seems to be most persuasive is this, the free-space permeability shows the intrinsic capability for the magnetic field to form itself. Therefore, when the magnetic field enters a free-space, it generated a magnetic field there with its own pace, no promotion, and no resistance for the "medium", either.

Permeability is applied mostly to measure how well a medium can promote or resist the forming of a magnetic field internally. All mediums are classified into three types The analysis seems to contain some intrinsic contradiction, too, like that of the permittivity. And to simplify the discussion here, we use the relative permittivity instead of the real permittivity. In this system, $\epsilon_{r0} = 1$, $\epsilon_{rSi} = 11.7$, and so on. In the simulation software we used in our research named HFSS, this question is skipped, in HFSS, the datasheet shows that the ϵ_r of PEC is defined as 1 as if treated as the free-space. However, it is not true. When the material of a 3D structure is set to be PEC, the solver of HFSS turns off the internal field solver of it. Therefore, the HFSS skipped this question while running simulations. The simulation results solved in this way are still a good match for the measurement results in the real world.

Unfortunately again, we may not skip this question by ignoring it in our theoretical discussion, and we have to find an answer we think it is right. By reviewing the open literature, we found two answers that are the most popular, and they are literally bipolar, one is 0, the other is ∞ . I personally vote for the later one.

The discussion of the permeability of PMC is somehow different from that of PEC. The most important difference is that we can easily find a material that acts almost like a PEC, say, a piece of polished copper or silver. However, PMC has a completely distinct story, as it does not exist in nature. Hence, all the properties of the PMC need to be “derived” from the PEC, through the application of electromagnetic symmetry. Figure 2.9 shows the reaction of PEC and PMC when external E field and H field are applied, in which red for electric fields and blue for magnetic fields. And the reactions are described as the creation of image field, solid lines are for the external fields while the dash lines are for the image fields. To summarize, by the creation of the image field, a PEC cancels the parallel E field and perpendicular H field, and simultaneously, it doubles the perpendicular E Field and parallel field. Therefore, we know from the electromagnetic symmetry that a PMC cancels the perpendicular E field and parallel H field, and doubles the parallel E field and the perpendicular H field through image field creation.

As concluded from the discussion of permittivity, we know that PEC doesn’t allow the existence of internal electric fields and the permittivity if defined to be ∞ . From the electromagnetic symmetry, PMC doesn’t allow magnetic fields to occur inside, and since the permeability is defined as the capability of assisting the magnetic field to form, the permeability of a PMC, μ_{PMC} , is 0. Mathematically, the permeability is a multiplier in the equation of magnetic field formation, 0 in value means not associate magnetic field is formed, which matches the physical description.

Field, electric or magnetic, carries energy, the permeability of a medium changes the distribution of the energy, some part of the energy is re-guided, while the other

part may be turned into other forms, for example, heat. As a result, the permeability, as the permittivity, is also a complex number, and since μ_0 is real, μ_r is also complex. Since μ is a function of the angular frequency, the complex permittivity goes as $\mu = \hat{\mu}_\omega$, and the relationship between \bar{B} and \bar{H} is expressed as.

$$\bar{B}e^{-j\omega t} = \hat{\mu}_\omega \bar{H}e^{-j\omega t}$$

When \bar{B} is generated due to the externally applied \bar{H} , a delay in phase occurs, which is represented by δ , now we have,

$$\hat{\mu} = \left| \frac{\bar{B}}{\bar{H}} \right| e^{j\delta}$$

To separate the real and imaginary parts of the complex permittivity,

$$\hat{\mu}_\omega = \mu_r(\omega) + j\mu_i(\omega) = \left| \frac{\bar{B}}{\bar{H}} \right| (\cos\delta + j\sin\delta)$$

Where $\mu_r(\omega)$, $\mu_i(\omega)$, δ are the real part of permeability, the imaginary part of permeability, and the angle of loss, respectively. We may consequently define a equation,

$$\tan\delta = \frac{\mu_i}{\mu_r}$$

,to express the magnetic loss.

Different materials come with different permittivity/permeability combinations, some of which are quite common. However, there are also other combinations that are rare, or even cannot be found in nature, those materials are named as metamaterials, and will be discussed in details in the following chapter.

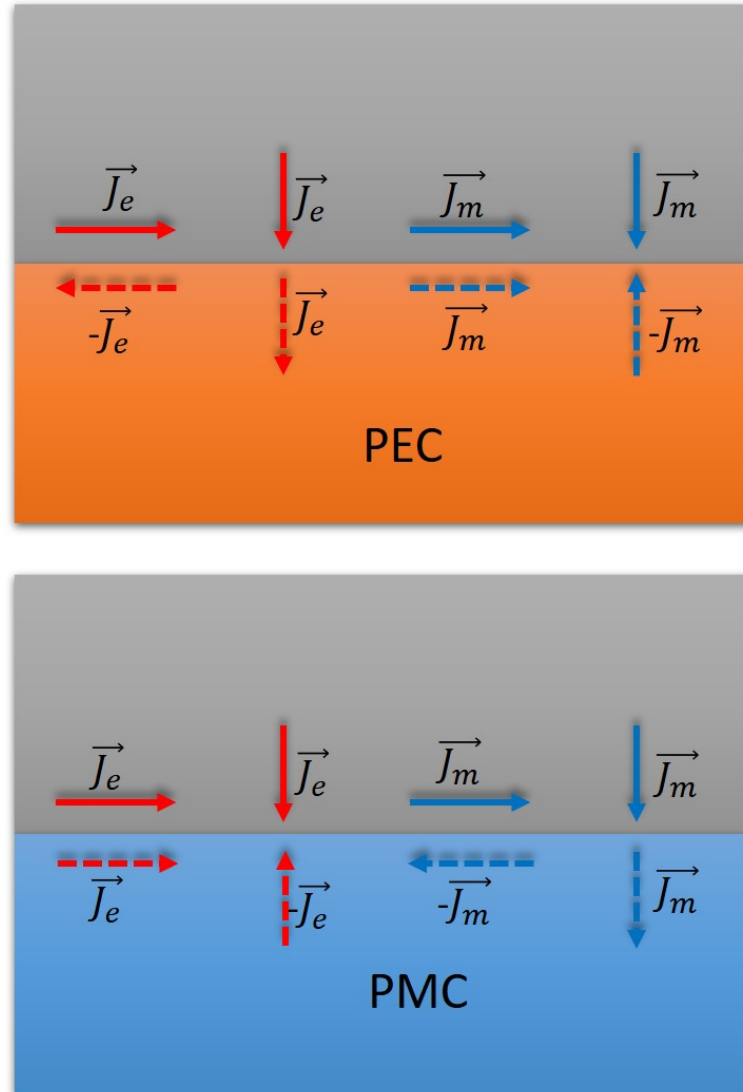


Figure 2.9: Image Currents associated with infinite planar boundaries with perfect electric conductors (PEC) and perfect magnetic conductors (PMC)

2.3 Boundary Conditions

The differential form of Maxwell's equations discussed in the previous sections are used to solve the single-valued, bounded, and possess continuously distributed fields.[11] However, in the real world, not all the materials are uniform, and the electromagnetic wave usually propagates through different materials. From Maxwell's equation above, it can be concluded that the permittivity and permeability have an influence on the fields derived from the solution of Maxwell's equations. As a result,

those equations may not be directly applied along the boundaries of different materials or inside an ununiform material. In other words, some boundaries need to be defined as the limit of the application of Maxwell's equations.

A boundary is defined as a surface where the permittivity and/or permeability of the materials are different on the two sides of it. Along the boundaries, the media involved is discontinued in electrical properties. In those cases, the field vectors are also not continuous. The behaviors of those field vectors across these boundaries are governed by the Boundary Conditions. The modified integral form of Maxwell's equations is not the most convenient method to derive the boundary conditions, and we need to figure out some more effective forms for this case.

2.3.1 Fields in linear materials

Before going into the discussion of the boundary conditions, we need to go over the wave propagation before it hits the boundary. The material is called linear material. Therefore, we can say that Maxwell's equation of fields in linear materials is the basis of all boundary conditions discussions.

In linear materials, where ϵ, μ are not \bar{E} or \bar{H} dependent. Therefore we use the Maxwell's equations in phasor form, which becomes,

$$\nabla \times \bar{H} = j\omega\epsilon\bar{E} + \bar{J}_e \quad \text{Faraday's Law}$$

$$\nabla \times \bar{E} = -j\omega\mu\bar{H} - \bar{J}_m \quad \text{Ampere's Law}$$

$$\nabla \cdot \bar{B} = 0 \quad \text{Gauss's Law}$$

$$\nabla \cdot \bar{D} = \rho \quad \text{Columb's Law}$$

Where,

$$\vec{B} = \mu \vec{H}$$

$$\vec{D} = \epsilon \vec{E}$$

2.3.2 Fields at a material interface

There are many reasons why we're digging into the boundary conditions, and two of great importance are,

1. We want to know how an electromagnetic wave performs at an interface.
2. We need to know how to control the boundary condition in order to create a propagation we want.

Field vectors can be dissolved into normal elements and tangential elements, as shown in Figure 2.10. In the Figure 2.10 and the following discussion in this chapter,

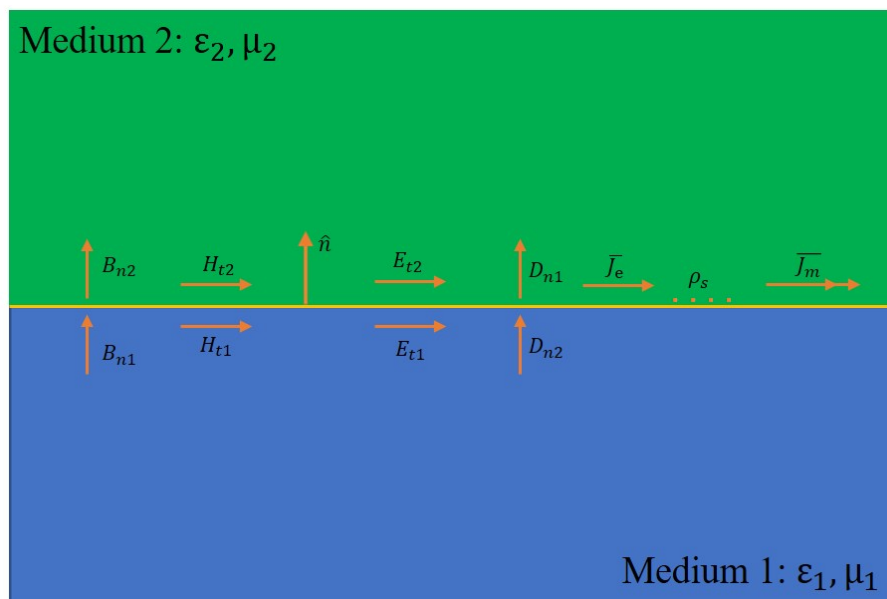


Figure 2.10: Field Vectors at an Interface Between Two Media

the subscripts n represents normal, and t represents tangential. \hat{n} represents the normal unit vector of the interface pointing to medium 2.

General Material Interface

At a general material interface,

$$\bar{D}_{n2} - \bar{D}_{n1} = \rho_s$$

So, we have

$$\begin{aligned}\hat{n} \cdot (\bar{D}_2 - \bar{D}_1) &= \rho_s \\ \hat{n} \cdot \bar{B}_2 &= \hat{n} \cdot \bar{B}_1\end{aligned}$$

Similarly,

$$\bar{E}_{t1} - \bar{E}_{t2} = -\bar{J}_m$$

Then we have,

$$\begin{aligned}(\bar{E}_2 - \bar{E}_1) \times \hat{n} &= \bar{J}_m \\ \hat{n} \times (\bar{H}_2 - \bar{H}_1) &= \bar{J}_e\end{aligned}$$

The example discussed above is a general case for the interface between two media, those equations are subject to change when the media change. Those different cases are discussed in the following sections.

Dielectric Interface

In this case, the media are two lossless dielectric materials, per the definition of dielectric material, here charge or current densities will not exist.[9] No electric/magnetic conductor allows the electric/magnetic current to form in this case

on the interface.

$$\hat{J}_e = 0$$

$$\hat{J}_m = 0$$

Therefore, we have the boundary conditions become,

$$\hat{n} \cdot \bar{D}_1 = \hat{n} \cdot \bar{D}_2$$

$$\hat{n} \cdot \bar{B}_1 = \hat{n} \cdot \bar{B}_2$$

$$\hat{n} \times \bar{E}_1 = \hat{n} \times \bar{E}_2$$

$$\hat{n} \times \bar{H}_1 = \hat{n} \times \bar{H}_2$$

Interface with a perfect electric conductor

In this case, a perfect conductor is filled all the space on one side of the boundary, and now the boundary is called as an “electric wall”.[9] By definition, an electric wall allows no magnetic current to form on its surface (the interface). And no tangential electric field can be formed along the electric conductive interface, no normal magnetic field can be found perpendicular to the interface. We have,

$$\bar{J}_m = 0$$

$$\hat{n} \cdot \bar{D}_1 = \rho_s$$

$$\hat{n} \cdot \bar{B}_1 = 0$$

$$\hat{n} \times \bar{E}_1 = 0$$

$$\hat{n} \times \bar{H}_1 = \bar{J}_e$$

Interface with a perfect magnetic conductor

Fields at the interface with a perfect magnetic conductor is also called a “magnetic wall” boundary condition. The characteristics of the magnetic wall boundary condition are derived based on those of the perfect electric boundaries. As a result, here the tangential components of \bar{H} should vanish as the tangential \bar{E} at a perfect electric boundary. Meanwhile, this time, no electric current forms along the interface. Therefore, we have the boundary conditions,

$$\bar{J}_e = 0$$

$$\hat{n} \cdot \bar{D}_1 = 0$$

$$\hat{n} \cdot \bar{B}_1 = 0$$

$$\hat{n} \times \bar{E}_1 = -\bar{J}_m$$

$$\hat{n} \times \bar{H}_1 = 0$$

Ideal Radiation Condition

When at least one of the two media on two sides of the interface is infinite [9], the boundary condition is different from all the cases discussed in previous sections.

This boundary condition describes a region that has an infinite distance from a source. In this case, the fields should be vanishingly small or propagating in an outward direction. In other words, all field vectors are considered to vanish when hitting the interface.

CHAPTER 3: Background: Antennas

3.1 Antenna Theory

Definition

By definition according to a combination of Webster's Dictionary and IEEE Standard Definition of Terms, an antenna is a means/device which is usually metallic radiating and receiving the radio wave. [31]To specific in a professional way, an antenna is a device used to convert guided waves on a transmission structure into free space waves, or reversely. [31][32][12] An antenna that transfers a signal/guided wave into free space wave is named as a transmitting antenna, and the one convert free space wave into a signal/guided wave is defined as a receiving antenna.

There are numerous antennas that have been applied in all field nowadays, 3.1

Causes of Antenna Radiation

a. Time varies current on a wire

Antennas come in varieties of shapes and structures, however, when we're discussing the radiation mechanism, the wire antenna can be used as an example.[31][12]. According to "Antenna's Theory and Design", radiation is a disturbance in the electromagnetic fields that propagates away from the source.[12]. In order to create radiation, we need to have a time-varying current or an acceleration/deceleration of electric charge. [31]

Now, we can look into a thin wire arranged in a linear configuration. Assume that the current is distributed with a reasonable degree of accuracy, and the wire is placed along the Z-axis, as shown in Figure 3.2.

Then the equations for the electric and magnetic fields are shown as in the equations

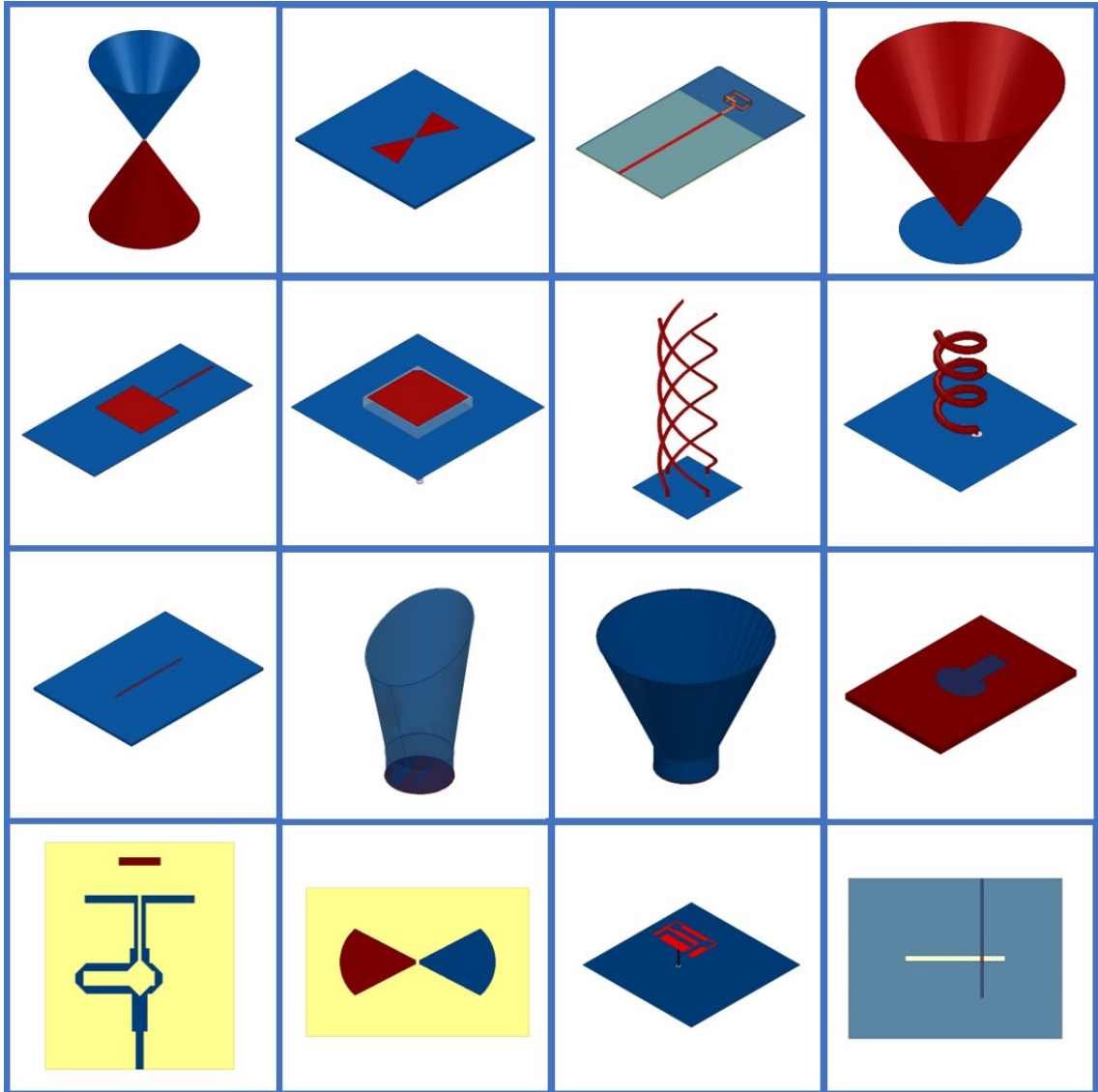


Figure 3.1: Different Kinds of Antennas

below. [12]

$$E_r = 60\beta^2 Idz \left[\frac{1}{(\beta r)^2} - \frac{j}{(\beta r)^3} \right]$$

$$E_\theta = j30\beta^2 Idz \left[\frac{1}{\beta r} - \frac{j}{(\beta r)^2} - \frac{1}{(\beta r)^3} \right]$$

$$H_\phi = j30\beta^2 Idz \left[\frac{1}{\beta r} - \frac{j}{(\beta r)^2} \right] \sin\theta e^{-j\beta r}$$

$$E_\phi = H_r = H_\theta = 0$$

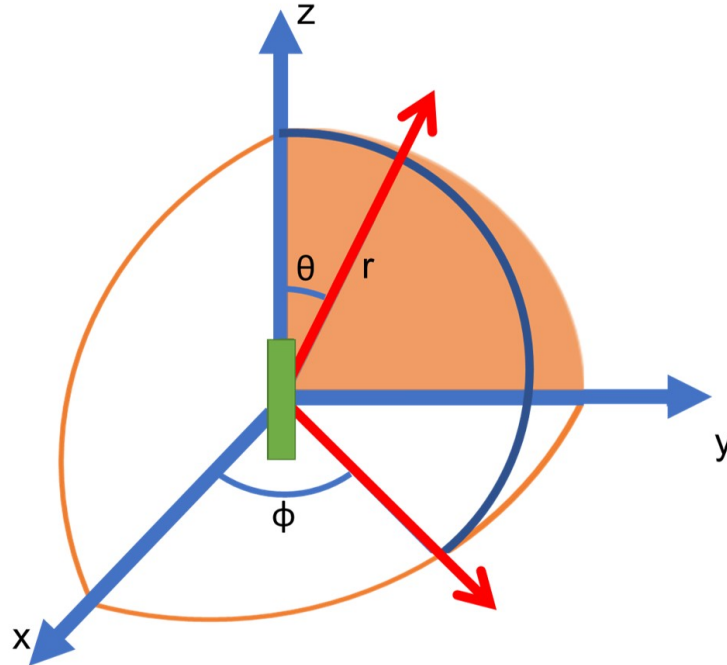


Figure 3.2: Wire in a Spherical Coordinate System

In these equations, r is the distance to the observation point. The current input is assumed to be a time-varying sin wave with a fixed frequency. The time-vary electric field and the time-vary magnetic field generate each other by taking turns, and the energy propagates in this way. The propagation of the energy through the time-varying electromagnetic fields is radiation.

b. Near-fields and far-field

[31]

The radiation of an antenna divides the entire space around it into three parts, the reactive near-field region, the radiating near-field/Fresnel region and the far-field/Fraunhofer region, [31], and they are referred to in the following discussion as Re-NFR, Rd-NFR, and FFR, respectively.

The Re-NFR is said as in [31]

“that portion of the near-field region immediately surrounding the antenna wherein

the reactive field predominates”,

and the equation for it is $r < 0.62\sqrt{D^3/\lambda}$, where r is the distance from the antenna surface, D is the largest dimension of the antenna, whatever that is.

Fresnel Region or the Rd-NFR is said as in [31]

“that region of the field of an antenna between the reactive near-field region and the far-field region wherein radiation fields predominate and wherein the angular field distribution is dependent upon the distance from the antenna. If the antenna has a maximum dimension that is not large compared to the wavelength, this region may not exist. For an antenna focused at infinity, the radiating near-field region is sometimes referred to as the Fresnel region on the basis of analogy to optical terminology.”

, and the equation now is $0.62\sqrt{D^3/\lambda} \leq r < 2D^2/\lambda$, and we can see that when $0.62\sqrt{D^3/\lambda} \geq 2D^2/\lambda$, or $D \leq 0.096\lambda$, this solution set of r is null. That is to say when the overall dimension of the antenna is much smaller than the wavelength, say 1/10, there is no Fresnel region exist.

The FFR or Fraunhofer region is thereby defined as,

“that region of the field of an antenna where the angular field distribution is essentially independent of the distance from the antenna”,

the equation of the inner boundary of the FFR is $r \geq 2D^2/\lambda$ for the general cases.

c. Return Loss

[9]

Wherever the time vary current exists in an antenna, radiation will be generated, and at the same time, a certain portion of the electric energy will be turned into heat or lost in other forms due to the mismatch of impedance. The return loss of an antenna is therefore defined, as the loss when the power delivered by the generator is radiated.

The antenna's reflection coefficient is

$$\Gamma = \frac{Z_L - Z_A}{Z_L + Z_A}$$

Where the Z_L is the load impedance, Z_A is the input impedance of the antenna, and both of them are impedance dependent. And then the return loss in dB is,

$$RL = 10\log_{10}|\Gamma|^2$$

When $|\Gamma|^2 = 0.1$, 10% of the incident power is lost, 90% is radiated. This ration is accepted as the standard of determining whether an antenna is effective. And since $RL_{10\%} = 10\log_{10}0.1 = -10dB$, we define any frequency where $RL \leq -10dB$ as the frequency at which the antenna can operate.

Different Antenna Types

There are different classification methods for the antenna, for example, by shape. There are wire antennas, aperture antennas, microstrip antennas, reflector antennas, array antennas, lens antennas an so on.

a. Radiation Classification[12]

By the details of radiation principles, there are electrically small antennas, resonant antennas, aperture antennas, broadband antennas, and so on. The broadband antennas are also called frequency independent antennas, on which our research is conducted.

Electrically small antennas are named for the extent of their structure is much less than the wavelength of the frequency they work at. Their directivity is low, and they have an input impedance with the small real part but a big imaginary part. As a result, the efficiency of radiation is low.

Resonant antennas are operated at a single or narrow frequency band selected, the

frequencies at which they resonant. This kind of antennas has a low to moderate gain. Since they work at or near their resonance frequency, the input impedance is considered as real, since the definition of resonance is where the imaginary part of impedance crosses 0. Meanwhile, a resonant antenna's working bandwidth narrow resulted from the narrow bandwidth where the resonance occurs.

An Aperture antenna is named for the aperture it has, through which the wave flows. This kind of antenna can have a relatively high gain which increases with frequency on its moderate bandwidth.

The Broadband or frequency independent antenna on which our research is conducted is discussed in the following section.

b. Radiation Bandwidth Classification

By looking into the radiation band of antennas, there are single frequency/very narrow band antennas, narrow band antennas, multiple band/multiple frequency antennas, and broadband/frequency independent antennas.

Every antenna has a continuous series of frequencies. In other words, we have a working band for any antenna. Per previously discussed, the working band is defined by the frequencies where the Return Loss, or $|\text{dB}(S_{11})| \geq 10\text{dB}$, and for the antennas operate at the resonant frequency, the percentage bandwidth is defined as,

$$BW(\%) = (F_H - F_L)/F_R \times 100\%$$

Where F_H , F_L , and F_R represent the high frequency in the working band, low frequency of working band, and the resonant frequency, respectively.

A single frequency antenna is a resonant antenna ideally operates at the resonant frequency with a bandwidth much smaller compared with the frequency of operation, the percentage bandwidth can be 5%, 3% or even narrower. A patch antenna is a typical model of single frequency antennas. The model of a patch antenna is shown

as in Figure 3.3. As observed from the Return loss plot Figure 3.4, the percentage bandwidth is approximately 1.6%, so this patch antenna is a single frequency antenna, or to be more precise, a very narrow band antenna.

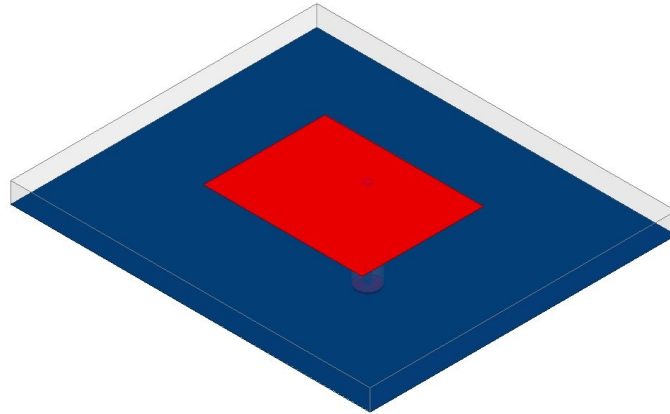


Figure 3.3: Patch Antenna Model

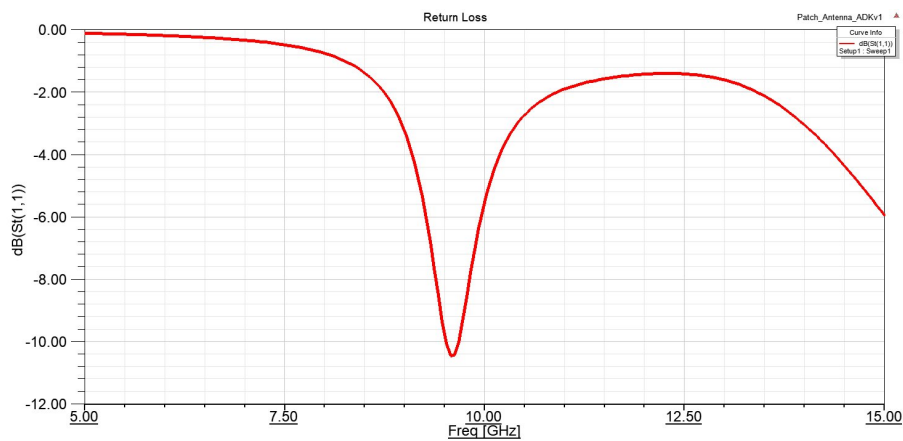


Figure 3.4: Patch Antenna Return Loss

Narrowband antennas are regarded as a type of antenna which works on a narrow band, but much wider than that of the single frequency antenna, the percentage bandwidth is defined to be 5% - 20%. Ideal monopoles and ideal dipoles are good examples of this type, whose structures are shown in Figure 3.5.

Therefore, as observed from the working bandwidth observed from Figures 3.12 and 3.13. By definition, the percentage bandwidth of the monopole plotted is approxi-

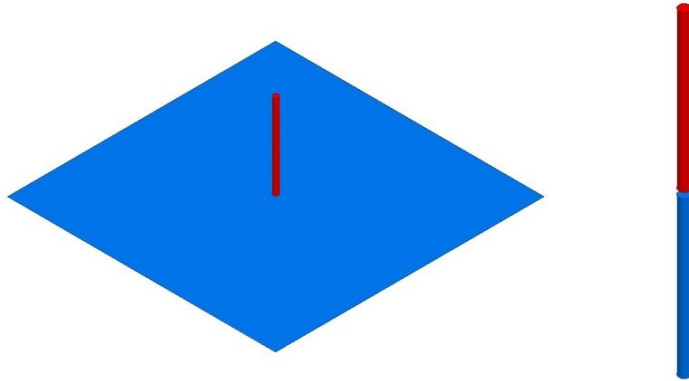


Figure 3.5: Monopole and Dipole Antenna Models

mately 11%, the percentage bandwidth of the dipole is 12%, both are slightly bigger than 10%, in other words, they both have a narrow band.

In some applications, we need one antenna to work with the different band to save space. Hence, researchers came up with antennas which have more than one resonance frequency in the band of interest. Those antennas are named as multi-resonant frequency or multi-band antennas. A Dual Band WLAN antenna is a good example for a multi-band antenna, which operates at both 2.4GHz and 5GHz. 3.6 3.7. It is observed that the bandwidth at 2.4GHz is 1.6% while that of 5GHz is 9.7%, hence, this antenna is a combination of a signal frequency antenna and a narrow band antenna.

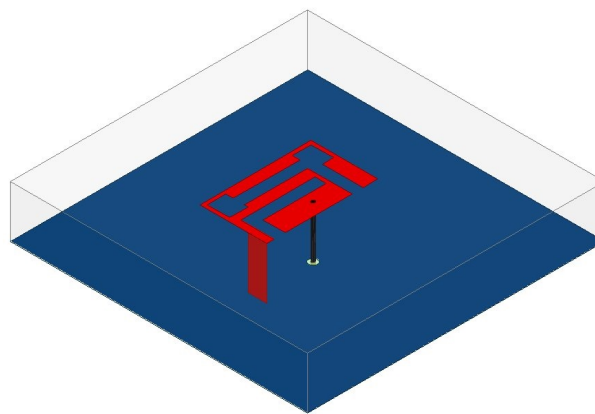


Figure 3.6: Dual Band WLAN Antenna

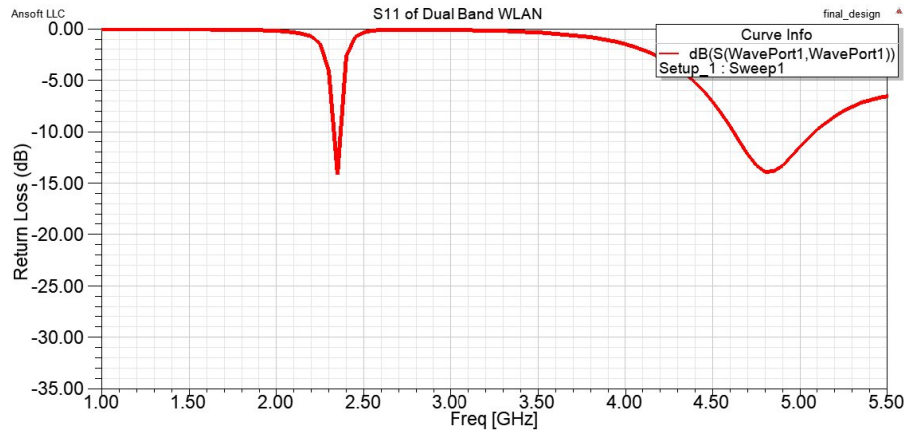


Figure 3.7: Dual Band WLAN Antenna Return Loss

When the antenna percentage bandwidth is discussed, we assume that a clear resonant frequency is able to be found. However, this is not always true, a narrow band comes with a sharp angle around the resonant frequency. But we also need to consider what will happen if the percentage bandwidth becomes increasingly bigger, or even larger than 100%(in theory). In fact, it is understandable that the wider the percentage band is, the flatter the angle around the resonant frequency will become. And meanwhile, the shape of $\text{dB}(S_{11})$ itself turns “smoother”, and the point where resonance takes place will be a blur, and finally becomes undetectable. That is to say, we may still be able to find some frequency point with a return loss slightly bigger than others in magnitude, but we may not simply define it as the frequency of resonance. In fact, even when we look into the impedance plot, we may still not be able to see some sudden change of impedance as expected. Some figures of the zoomed-in return loss focused on the region around the resonance frequency are plotted here to clarify this viewpoint. 3.83.9 we can see that the return loss plot becomes flattered when the percentage bandwidth increase. Besides, there are also some antennas don't operate at their resonant frequency or doesn't even have a resonant frequency at all, for example. a waveguide antenna. None of the frequencies associated with regional minimum values can be described as a resonance. Figures3.10 3.11

As a result, for those antennas discussed above which have no significant frequency

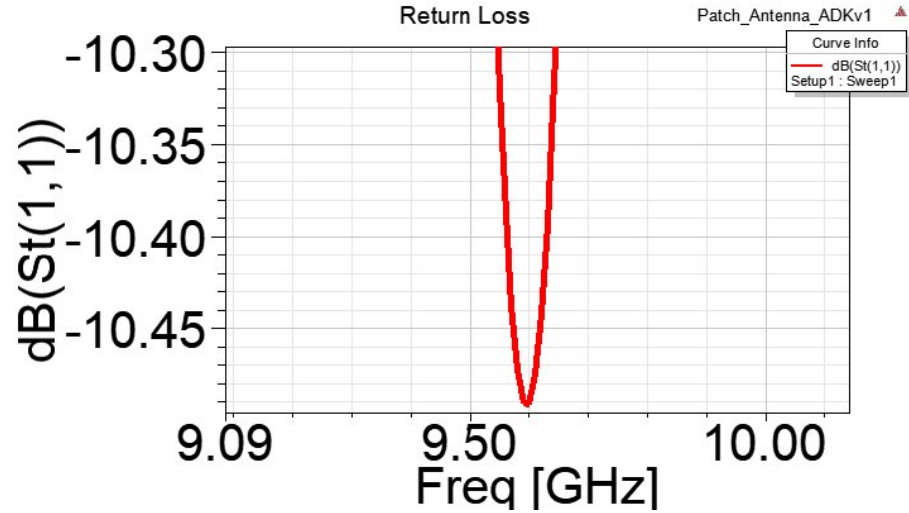


Figure 3.8: Single Frequency Antenna Return Loss Resonance Zoomed in

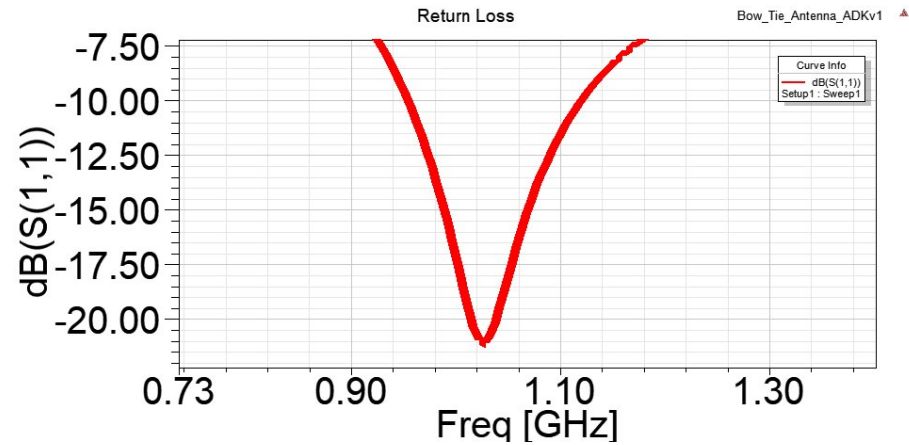


Figure 3.9: Narrow Band Antenna Return Loss Resonance Zoomed in

of resonance, or the antennas don't even have a resonant frequency, the bandwidth is defined in some different way. For example, we may use the ratio of the highest frequency over the lowest frequency. In fact, this method can also be applied in the description of those narrowband antennas, but the number will then be too close to one and not able to significantly show the difference.

$$BW = F_H/F_L$$

A single antenna operates at its resonant frequency is not likely to be a wideband

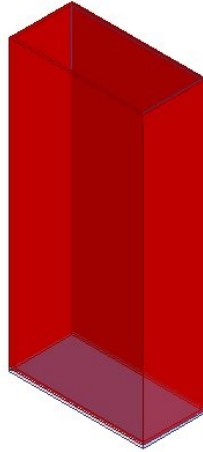


Figure 3.10: Waveguide Antenna Structure

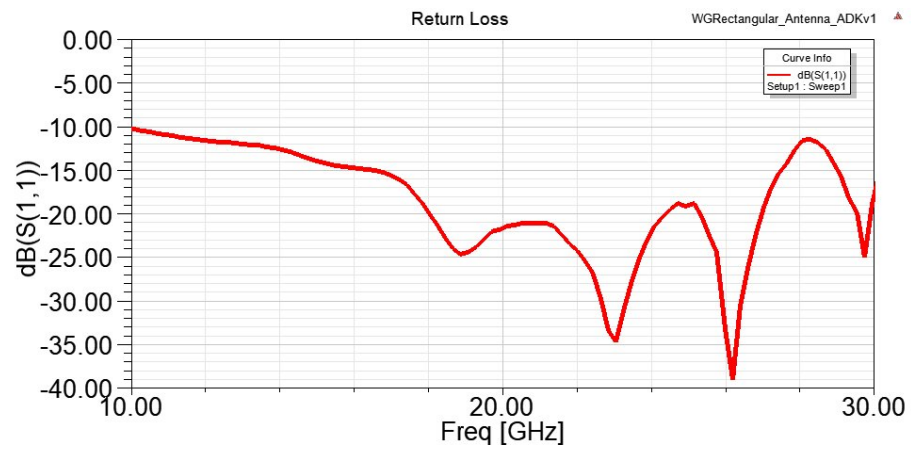


Figure 3.11: Waveguide Antenna Return Loss

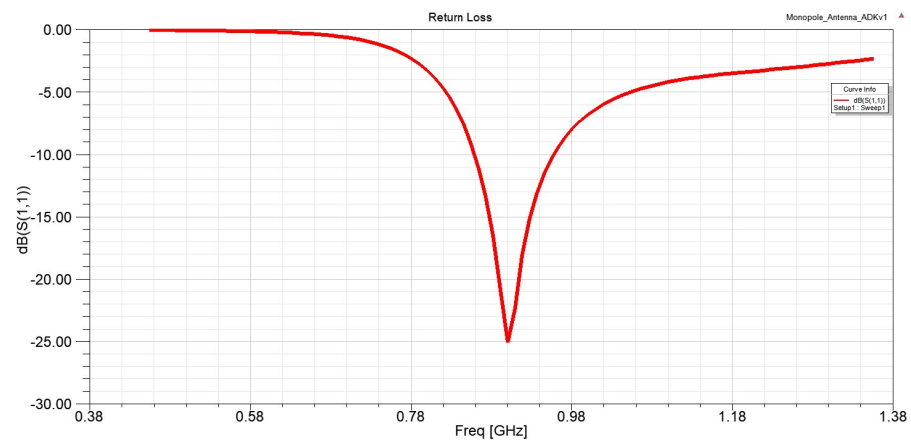


Figure 3.12: Monopole Antenna Return Loss

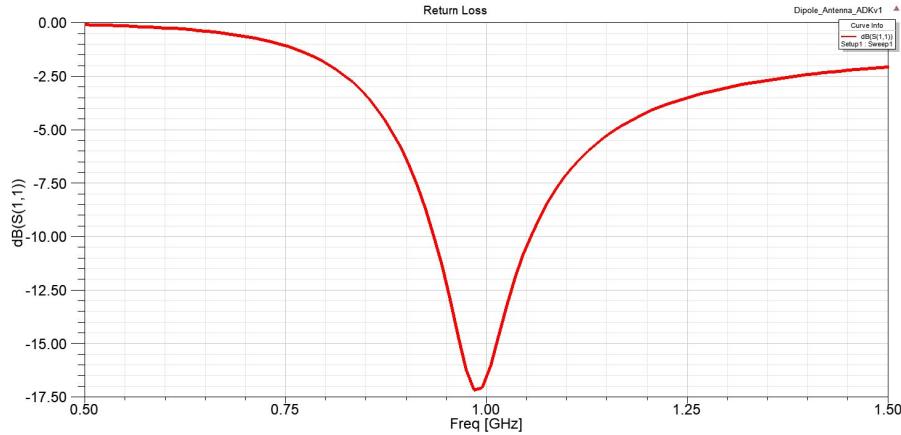


Figure 3.13: Dipole Antenna Return Loss

antenna, unless when a series of these antennas are built to form an “array”. To achieve a broadband antenna performance, researchers have come up with varieties of ideas. The basic principle of these ideas is to combine several dipole antennas in a certain order to ensure the operation across a wide bandwidth. There are many types of broadband/frequency independent antennas. Since the frequency independent antenna in the prototype the antenna applied in our research is based on, it is discussed in details in the following section.

3.2 Frequency Independent Antenna

Frequency independent antennas are a type of antenna that has radiation patterns and gains remain acceptable and are nearly constant within a relatively wide bandwidth, sometimes the relative bandwidth, which is determined by the high frequency over the lowest frequency can be as high as 10 times or even higher[5], therefore, those antennas are regarded as not frequency independent, or frequency independent.

Frequency independent antennas typically have a low to moderate gain, which is considered as a drawback. However, an advantage is that a frequency independent antenna usually has a constant gain over the entire bandwidth, in other words, signals with all frequencies within the working bandwidth are treated more or less equally. Meanwhile, as mentioned in the last paragraph, frequency independent antennas have

a wide working bandwidth. Impedance matching is always a factor of great importance to consider the antenna design procedures. Freq-Ind antennas are generally easy to feed since they have real input impedance, which means the imaginary part of impedance is relatively small. [12]

Broadband/frequency independent antennas are applied in many fields. Generation after generation researchers has come up with many different designs. Most frequency independent antennas we found in open literature have some type of periodic structure, the repeated element can be a “dipole”, a slot or an angle. They are shown as in Table below. The structures are shown as in Figure3.14, the order in the figure is the same as that on the table.

Table 3.1: Different Types of Frequency Independent Antenna

Planar Sinous Spiral	Planar Archimedean Spiral	Planar Log-Spiral
Conical Sinous Spiral	Conical Archimedean Spiral	Conical Log-Spiral
Continuous Vivaldi	Stepped Vivaldi	Linear Taper Slot
Toothed Log Periodic	Trapezoidal Log Periodic	Rectangular Spiral Antenna

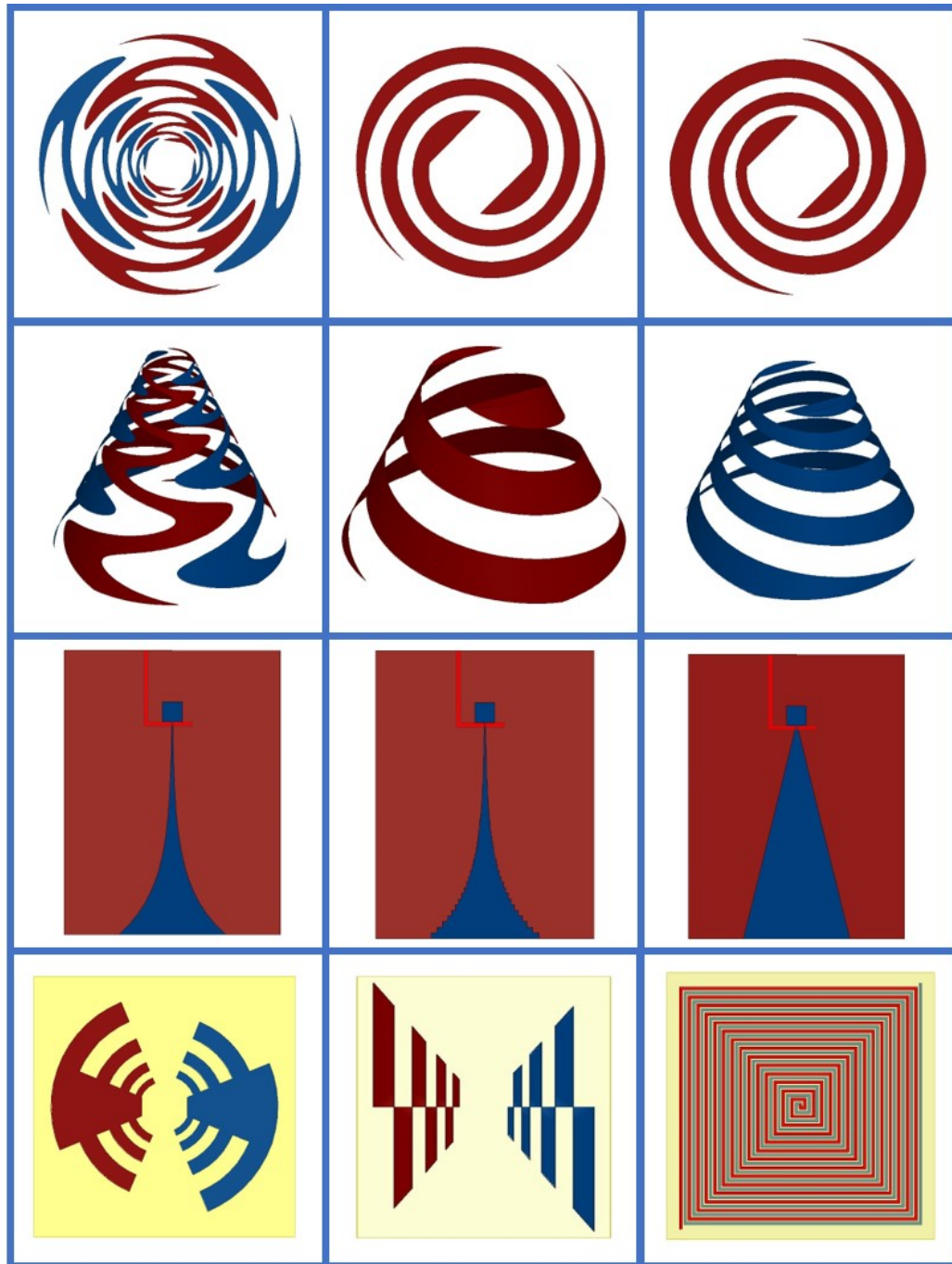


Figure 3.14: Frequency Independent Antenna Structures

CHAPTER 4: Literature Review: on Metamaterials Development

4.1 Introduction of Metamaterials

The project proposed and presented in this document is based on the researches related to the application of metamaterials. As discussed in the previous chapter, a metamaterial is a “material” or “structure” which has an unusual combination of permittivity and permeability.

The term *Meta* is a Greek word means beyond or after. By definition, the metamaterials are a series of artificially fabricated materials which have unusual electromagnetic properties. In other words, properties that are beyond the materials can be found in nature. In the field of electromagnetism, the word “beyond” or “meta” means that the interactions between this very material and electromagnetic waves/fields are different from that of the common materials.

4.2 The prehistory of metamaterials

Researches on metamaterials become increasingly popular in these couple of decades. However, it is really not something brand new, in fact, the first researches on those artificial materials that can manipulate electromagnetic waves were conducted at the end of the 19th century. Sir Jagadish Chandra Bose, a British Indian scientist is considered as one of the earliest founders of the metamaterial researches. He conducted researches on the chiral properties of some substances. [13]. Here chirality is a term first introduced by Lord Kelvin (William Thomson) in 1893, and in his publication in 1894, he said, “I call any geometrical figure, or group of points, ‘chiral’, and say that it has chirality if its image in a plane mirror, ideally realized, cannot be brought to coincide with itself.” [14]

Researches on metamaterials then had a long period of blank for approximately 40 years before achievements on artificial dielectric materials were reported in the late 1940s. These researches lasted for about 20 years, from the 1940s to 1960s. Artificial dielectric, although quite different from the metamaterials referred to today's researchers, the research on it are still considered as the very foundations of the modern metamaterial research and development. The bandwidth of this kind of researches focused on was the microwave, which happens to be the bandwidth our proposed research project is focused on. Important names to be mentioned for this period include W. E. Kock, W. Rotman, and Sergei Schelkunoff. Their contributions on the artificial dielectric include, but not limited to the discovery of tunable permittivity and permeability, permittivity can be negative under some circumstances, artificial particles may be applied to mimic a new material in the scale of electromagnetism, and periodic structures are needed for realizing the special performance of them. [13] Those are still the basic ideas in today's the development of metamaterials, even the original purpose of them is not for this.

4.3 Founders of Metamaterial Techniques

Sir Issac Newton once cited a metaphor of dwarfs “standing on the shoulders of giants” to describe his own contributions to physics, and he himself is certainly another giant whose shoulder now we're standing on. In the field of metamaterials, we also have some “giants standing on the shoulders of other previous giants”. Among those giants, an English scientist named Jonh Pendry is considered as the first literally inventor of metamaterials. The invention came to being as a saying goes, “practice is when everything works but nobody knows why” when a technology company hires Pendry a condensed matter physics expert. The company some novel material named radiation-absorbing carbon for military purpose, it works fantastically, however, the company couldn't explain the reason. Pendry conducted researches on it and finally, he came up with some historical discoveries.

Pendry had some exciting findings in his research, he proved that the radiation absorption is not from the molecular or chemical structure, in other words, not from the microscopic particles. The absorption is generated by the carbon fibers' long and thin physical shape. Mr. Pendry didn't stop when he found the answer, he began to think of something big, he realized that to change the behaviors of a material when interacting with electromagnetic fields/waves, alternating the chemical structure is not necessary, people can simply alter the internal structure on a "very fine scale" instead (but still much bigger than the atomic or molecular scales). Pendry explains here that the "very fine scale" is determined based on the wavelengths of the electromagnetic waves interact with the structure.[16]. Again, reasearches have been conducted on all kinds of different electromagnetic waves, and what is focused on in our proposed research is the microwave. Pendry work is later recognized as the birth of metamaterials, but the open literature we found doesn't point out who is the first person came up with the term of "metamaterial", while we do know that "meta" is a greek originated word with the meaning of "beyond", and therefore, metamaterial is named as it is a material that is beyond the conventional material. It is said, "The discovery/invention of metamaterials will be engraved as the second greatest event in the technology history of human beings, right next to the discovery and usage of metallic materials."

Pendry's work continued after the discovery of metamaterials with unusual permittivities. Later he expanded his idea of metamaterial design to the alterable permeability materials, he came up with a prototype pe magnetic resonant switch, a periodic structure of copper loops with gaps fabricated on fiberglass substrate (e.g FR4). Pendry is honored as the most important founder for his contributions cover both the permittivity alternate materials and permeability alternate materials, and we have some schematic figures as following to show the overall picture of the structures he has been working on.

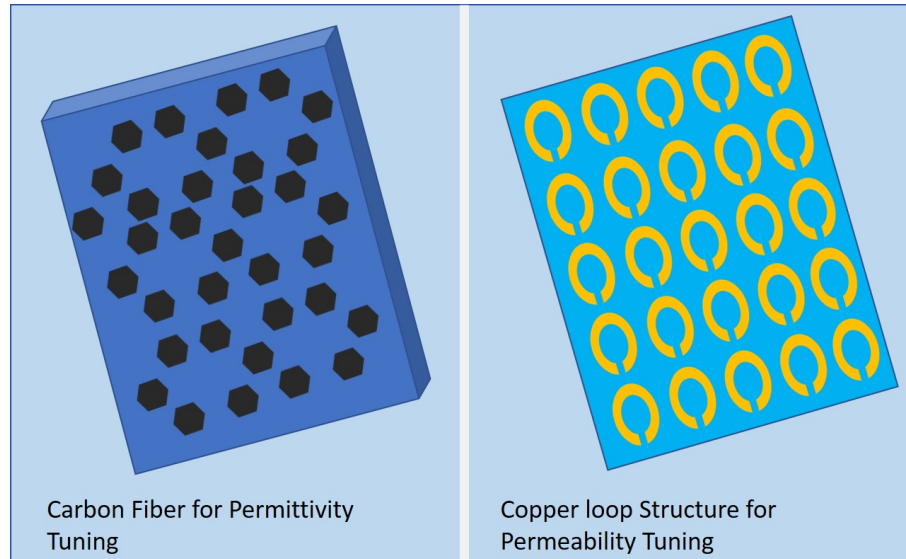


Figure 4.1: Pendry's Metamaterials Schematic Figures

Pendry didn't realize what breakthrough he had made when he first published his summarized work in 1999, he just regarded as a novel method of manipulating the propagation of electromagnetic waves[17]. However, researchers all over the world did. And an increasing number of researches projected started to be conducted since then.

Pendry's carbon fiber research proved that permittivity which was thought to be a molecular property can indeed, be altered by changing the material structure in wavelength scale, which is usually much bigger. His gapped copper loop research showed that a non-magnetic material can have magnetic properties by simple changes of the structure is applied. In other words, permeability can be alternated with structure re-shaping. And the next question is, how far we can go on this way. Can we "create" materials that have permittivities and/or permeabilities that are rare or even do not exist in nature. In fact, the positive answer was given in theory about 30 years before researchers really began to work on engineering them.

The person who came up with the answer is a Ukrainian scientist(when he was born and published his work, the former USSR), Victor Veselago, he published his

historical paper [18] named “The electrodynamics of substances with simultaneously negative values of ϵ and μ ” in 1968, and proved in theory that negative refractive index can exist. In this paper, he introduced the theory of reverting Snell’s was, an extraordinary lens or a superlens. He also came up with theoretical proof of the existence of other “exceptional phenomena” is not against the basic laws of physics.

Veselago’s work was ahead of time, as mentioned above, for about 30 years, before the negative refractive index engineering structures finally occurred. Periodic thin wire structures were introduced in the 1990s by Pendry successfully extended the value range of the permittivity, he also developed permeability tunable structures interact with microwave frequencies. Further research achievements on negative refractive index metamaterials were then presented on “Conference on Quantum Electronics and Laser Science” then published by a group of UC-San Diego lead by Sheldon Schultz [19].

4.4 Progress of Metamaterials

Invisibility Cloak

In the fantasy series and comics, an invisibility cloak often acts as a prop of great importance. Characters use the invisibility cloak to hide from the view of others, light incident to the cloak goes through directly without revealing the cloak itself or the people covered underneath. The invisibility cloak has been regarded as a romantic fantasy until some researchers in the field of metamaterials analyzed it’s working principles in the last decade of the 20th century and the first decade of the 21st century. [20]

An invisibility cloak is made of a material that allows the light to “go through” it as if nothing is there, which looks to be impossible at the first glance. However, the application of metamaterials has made that possible. In 1999, a German scientist living in Scotland named Ulf Leonhardt did the theoretical analysis of the invisibility cloak. His research was focused on a real invisibility cloak or in other words, one

operates at the spectrum of visible light, and therefore, named in his article “Optical Conformal Mapping”. In this document, he referred his idea of the invisibility cloak, or invisibility device using his own words is a device which “should guide light around an object as if nothing is there”, which sounds like an abstract concept. We have plotted some figures here to concrete it. 4.2 We see things because of the light incidents to our eyes, either directly or by reflection or scattering. So an object is invisible to us if no light comes from it goes into our eyes. In the figure, the red arrows represent the light, and the white dashed box in the middle represents the region in which interaction takes place, it’s not a real medium or anything else.

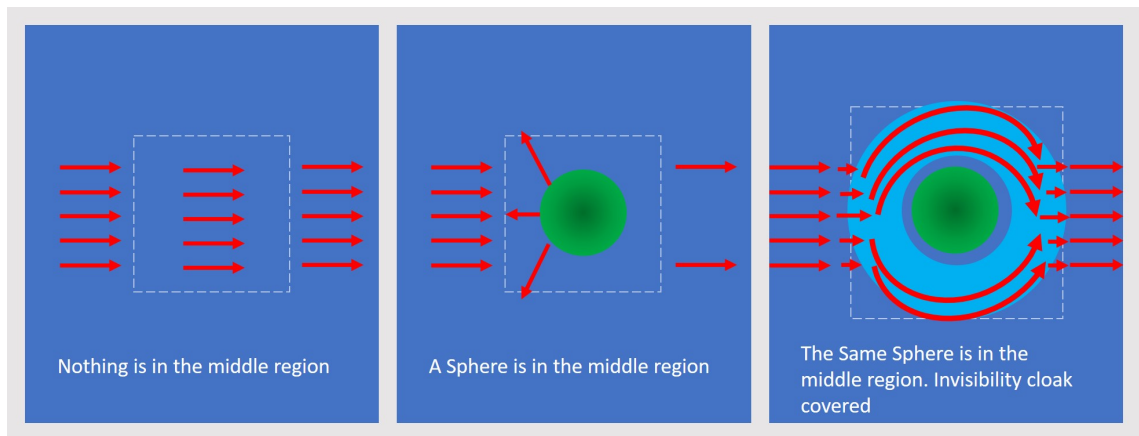


Figure 4.2: Leonhardt’s Ideal Model of an Invisibility Cloak

In this figure 4.2, for the first case, it can be observed that the light enters the region of interaction, and since nothing is there, the light goes through directly, until they are reflected, scattered by some other object or enter our eyes. As a result, we can see what’s behind the region of interaction and know that nothing is in the region.

For the second case, a sphere (and to simplify the discussion, a non-transparent one, say a basketball) is placed in the region of interaction, and this time, light is separated by the sphere, some part still goes through the interaction region for the path is not blocked by the sphere. However, the other part is reflected by the sphere (ignore the scattered and absorbed light which has nothing to do with the discussion), and caused

two results observed, the first is the reflected light enters our eyes so we can see the sphere is there. The second is that since the path of light is blocked, no light incident in this way may reach the region behind the sphere, and hence, we cannot see what's behind the sphere.

A cloak of invisibility changes everything as shown in the third case, in which the sphere is completely surrounded by it, as Harry Potter did when he was leaving the dormitory sneakily. And this time, the light enters the region of the invisibility cloak and then guided inside the cloak until leaves in the same direction of the incident. The light, seen from the result, travels exactly the same as in case one when it enters and leaves the region of interaction. In other words, no light touches the sphere hidden underneath, and therefore, we cannot see the sphere, and all the light incident leaves the same way as it comes. The interaction between the light and the invisibility cloak achieves the goal to make people think “nothing is there”.

Different types of metamaterials were introduced during the decades of the 1990s and 2000s. Typically, the metamaterials are constructed to exhibit periodic formations, and the period in dimensions is much smaller than the free-space/guided wavelength of frequencies of interest. [11] There are a number of different metamaterials that have been applied in different fields.

Almost the same time when Leonhardt was trying to get his work published, Pendry's group was also working on the project of invisibility cloak creation, and in fact, some other research groups were doing similar things almost simultaneously. Theoretical research and practical engineering are not always walking side by side. This time, the first people who developed the “invisibility cloak” using metamaterial techniques are David Schurig and David Smith of Duke University in North Carolina, USA. They engineered a cloak of invisibility for microwave spectrum instead of visible light as introduced in their paper published in 2006 together with Pendry, and so on. [20] However, this invention is indeed, much more valuable compared with the invis-

bility cloak for the visible light, which might be just for fun or decoration purpose, for the possible usage in national defense of it. According to the open document by the US Department of Commerce, the year 2000. [22], the spectrum assigned to be used by DoD is within the microwave band. In other words, totally invisible battleships and airplanes may be developed based on this discovery, which may change the future battlefield completely, think about a beyond visual range attack from something 100% invisible on the radar screen.

We are reviewing the history of metamaterial development and telling the story of invisibility cloak not just for fun, in fact, we're trying to unfold the brand new future in front of us created by the metamaterials. The possibilities for the metamaterials are literally unlimited. And that's why an increasing number of metamaterials are engineered in this age, as briefly talked about in the following sections.

Artificial Impedance Surface(AIS) Development

The properties of those metamaterials we talked about in the previous section are either absorbing (the negative permittivity absorption carbon fiber), or working by guiding the electromagnetic waves to travel through them (the negative permeability ring resonator and the invisibility cloak). However, the application of metamaterials is not limited in these fields. The theoretic basis of these engineering metamaterials is the tuning of permittivity and permeability. We have some other kind of metamaterials that operate based on its properties of reflection, and this type of metamaterial are also engineered based on the analysis of boundary conditions we discussed in Chapter 1.

The history of which we're going to discuss here is the Artificial Impedance Surface, a type of metamaterials which alternates the impedance of the surfaces they're attached to, with the surface impedance changed, the material will have a different performance during its interaction with the electromagnetic waves.

The oldest "real" AIS we're able to find now is a paper published in 1997 by David

Pozar, etc., named “Design of Millimeter Wave Microstrip Reflectarrays” [10]. In which they successfully change the metal surface by fabricating an array of metallic squares on the substrate. In their paper, they call these squares as “patches”, which I think to be the prototype of the future mushroom structure, but without “stipes”, or in other words, the vias connect the mushroom tops and ground plane together.

The basic idea of artificial impedance surface design is to alternate the impedance by changing the structure of the surface. Later in 2002, the earliest open literature we found with a description of the mushroom surface structure was published by Dan Sievenpiper, etc. The paper didn’t use the terms “mushroom” or “mushroom surface” we found firstly introduced in 1991 [28] in its title “A Tunable Impedance Surface Performing as a Reconfigurable Beam Steering Reflector”[25], but the authors did give a whole picture of a mushroom surface by adding the “stipes” or vias “missing” in [10].

The AIS engineering is a novel field with only a history of twenty years. There are a lot of properties to dig into, and researchers all over the world are coming with more and more new designs.

Progress on Other Types of Metamaterials

As previously talked about, all kinds of metamaterials have been engineered since Pendry introduced in the first permittivity tunable(negative) structure and the first permeability(negative) tunable structure. The metamaterials researchers have come up with can be roughly sorted into the following types, Double Negative Materials, Engineered Textured Surfaces, Artificial Impedance Surfaces, Electromagnetic Band-Gap, Photonic Band-Gap Surfaces, Frequency Selective Surfaces, Artificial Magnetic Conductors. They are initialized as DNG, ETS, AIS, EBG, PBG, and AMC, respectively. Fractals and Chirals are also considered as metamaterials. Some of them are already talked about in the previous section.

This classification method is not precise, there are some metamaterials fulfill defi-

nitions of two or more types at the same times. For example, sometimes, AMCs are also considered as a special type of DNG.

a. Double Negative Materials

Double Negative Materials, or DNG, is not found in nature. DNG is a left-handed material that allows backward-wave propagation, and advanced phase. These materials are named as DNG for it has a negative permittivity and permeability, in other words, $\epsilon < 0$, and $\mu < 0$. Other named used for DNG are, Negative Refractive Index(NRI), Negative Index Material(NIM), Backward Media(BW), and Left-handed Media(LH). Figure 4.3 shows the performance of an ideal liquid style DNG works for visible light. This will be a great achievement. Some people proposed that they engineered the invisibility cloak for the visible light, but as far as I know, no clear clue shows that those “invisibility cloaks” are designed according to the Left-Handed performance we discussed. One possible reason may be the dimensions of the units inside. As we know, the dimensions of a left-handed material element/unit should be comparable to the wavelength of their frequency of operation, and the range of the visible light wavelength is 380 nm to 750 nm. Calculate with the biggest possible value, and assume the unit is a cubic, in order to make a 0.1mm thick and 10 cm by 10 cm, handkerchief-sized cloak, which may be big enough to cover a small mouse, the number of units needed will be 2.37×10^{12} , despite the difficulty of fabrication, the cost alone will very likely to be unaffordable to make one that could hide an average adult underneath.

A DNG structure for microwave frequency spectrum is easy to be realized by a linear combination of a “negative permittivity fiber in I Beam Shape” and a “negative permeability resonant ring”. The 3D structures placed in parallel waveguides and built-in HFSS together with the associated results simulated according to the open literature[17][16] are shown in Figures4.44.5. In 4.4, the resonator allows us to have a negative permittivity from DC to about 4Ghz. Then in 4.5, the ring resonator gives

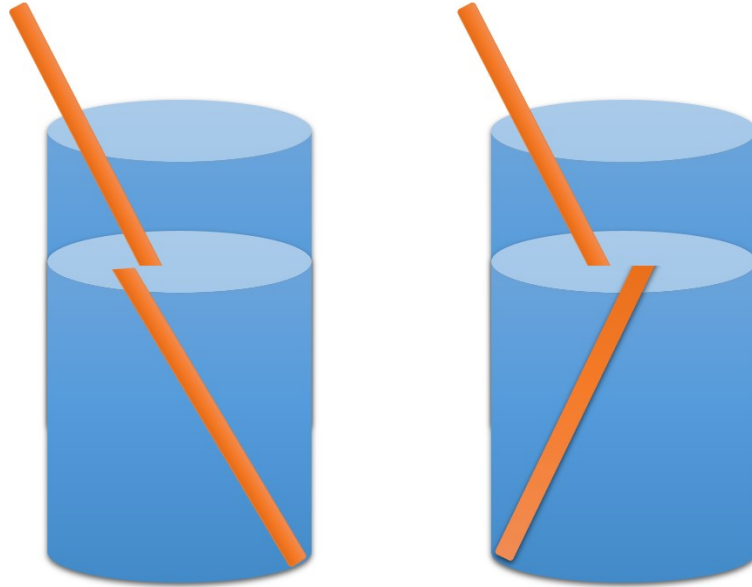


Figure 4.3: Ideal DNG Performance for Visible Light

us a negative permeability from 2.92GHz -3.24GHz.

A simple linear combination of the two components introduced above gives us a unit of a Double Negative Material or a Negative Index Material. As indicated by the name, this kind of material will give us the performance of negative permittivity and permeability. Figure 4.6 shows the structure and associated simulation result.

b. Artificial Impedance Surfaces(AIS)

[11]

Artificial impedance surfaces, or engineered electromagnetic surfaces, have been developed for tens of years. This type of material is applied to change the impedance boundary conditions, (say altering a low impedance surface into a high impedance one).[11] These alterations are used to control the radiation characteristics. If an antenna is placed at or near an AIS, the radiation efficiency and patterns can be altered. An AIS can also change the scattering of the impinging electromagnetic wave. The basic structure of AIS is periodic, just as discussed in [21], artificial impedance surfaces are coatings consisting of periodic structures.

AIS structures include but are not limited to Electromagnetic Band-Gap Structures

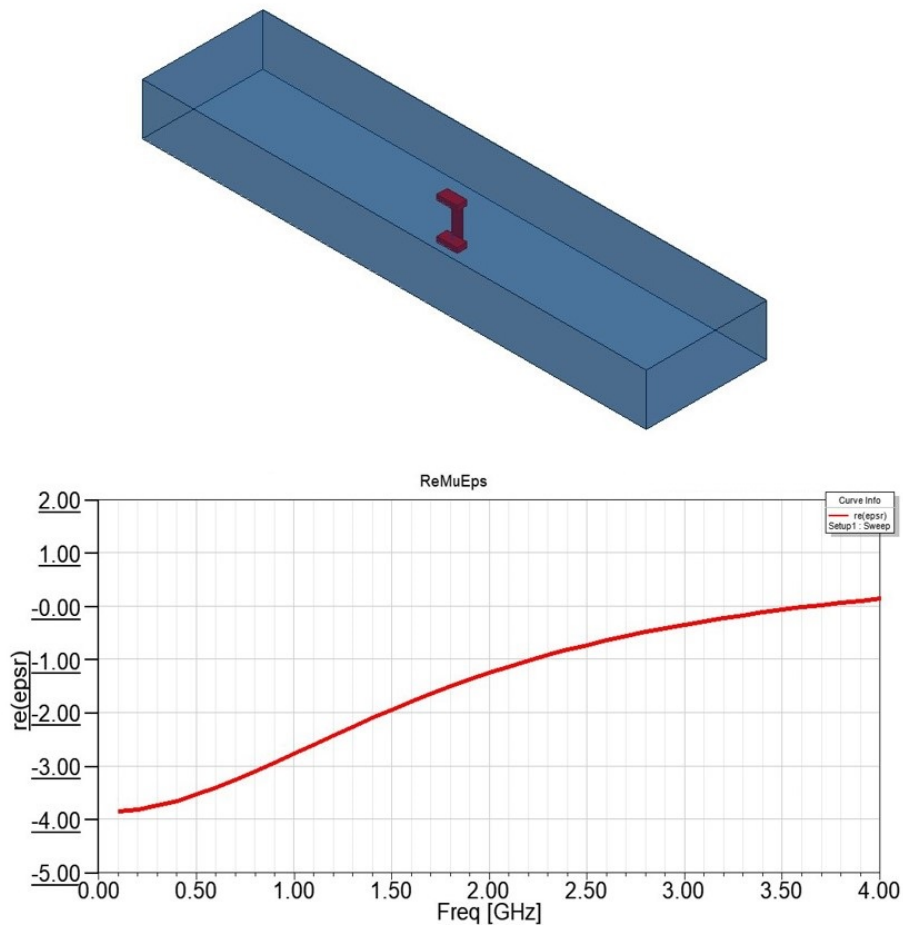


Figure 4.4: Simulation Structure and Result of the Negative Permittivity Ibeam Resonator

(EBG), Frequency Selective Surfaces (FSS), High Impedance Surfaces (HIS), and Artificial Magnetic Conductors (AMC).

Artificial impedance surfaces have been applied to fields like followed, and more are adding to the list. Cited directly from [11].

1. Change the surface impedance
2. Control the phase of the reflection coefficient
3. Manipulate the propagation of surface waves
4. Control the frequency band, such as stop band, passband, and band gaps
5. Control the edge diffractions, especially of horns and reflectors
6. Design new boundary conditions to control the radiation pattern of small an-

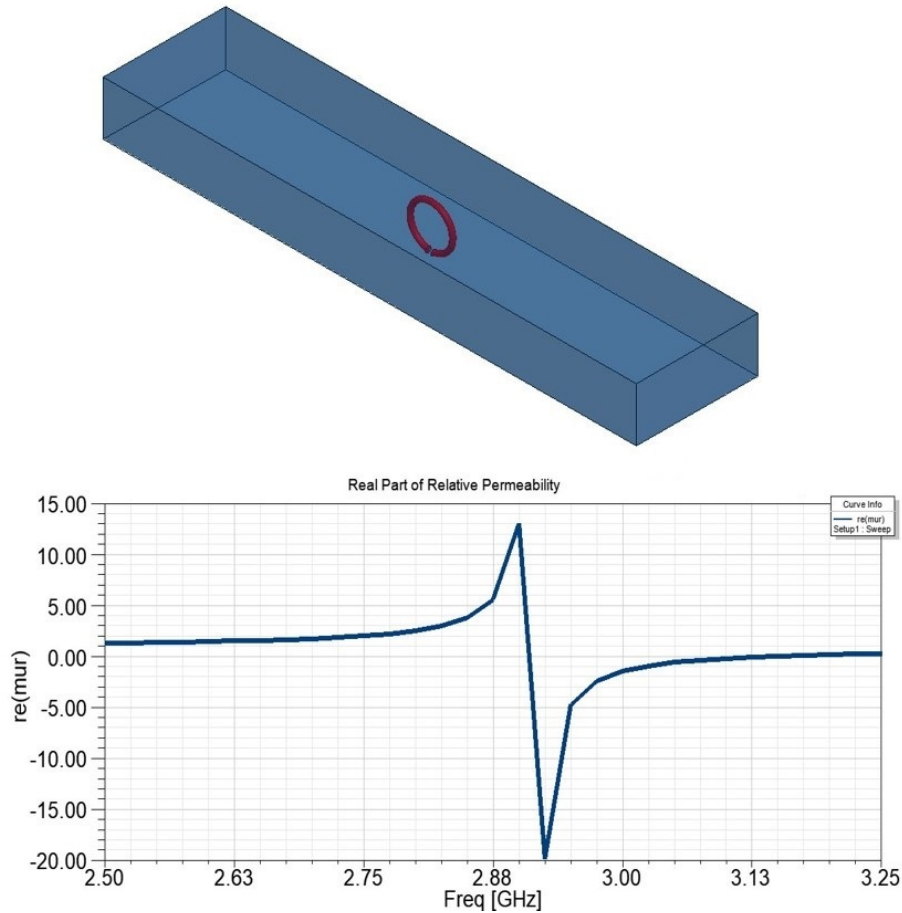


Figure 4.5: Simulation Structure and Result of the Negative Permeability Ring Resonator

tennas

7. Provide detailed control over the scattering properties
8. Design tunable impedance surfaces to be used as:
 - a. Steerable reflectors; b. Steerable leaky-wave antennas
 - c. Frequency Selective Surface

As introduced in the previous section, Frequency Selective Surface, High Impedance Surface, and the Artificial Magnetic Conductor are all Artificial Impedance Surfaces. In fact, there seem to be no real boundaries among the three of them. However, since High Impedance Surface and Artificial Magnetic Conductor are both designed to operate on certain bandwidth, in other words, they both have properties of frequency

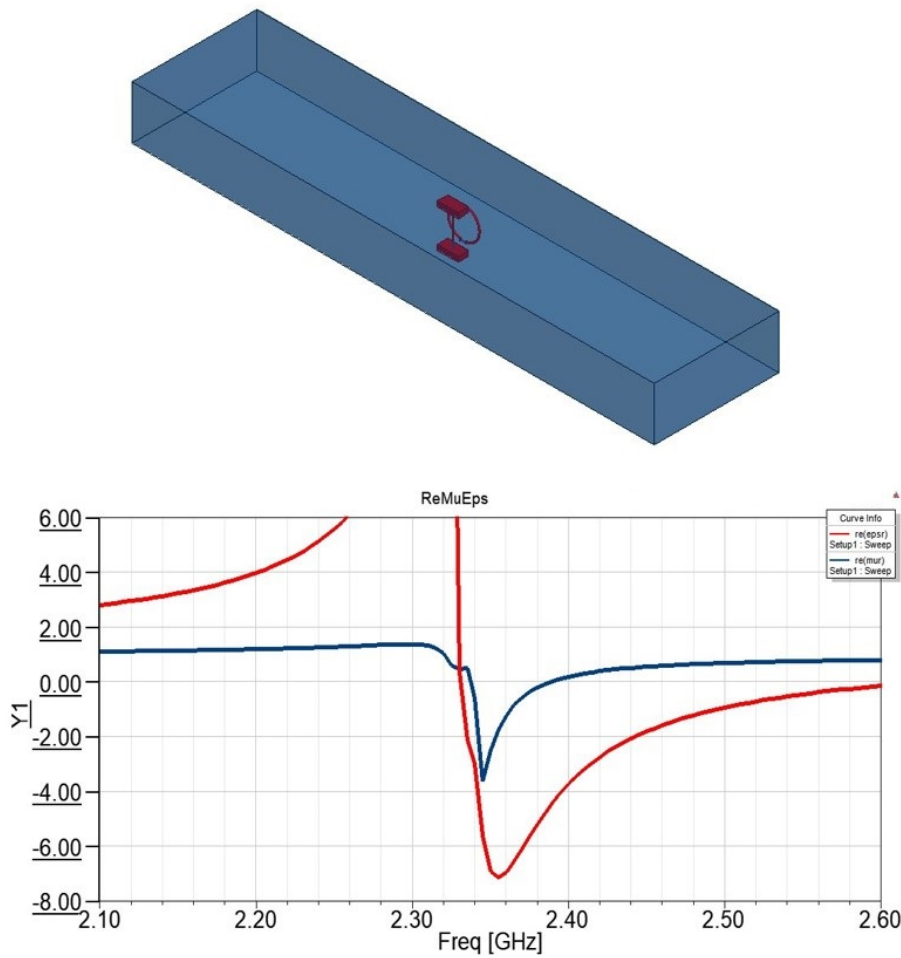


Figure 4.6: Simulation Structure and Result of the DNG Resonator

selection, hence, they are treated as the branches of Frequency Selective Surface. FSS typically has two types, “Band-Pass” and “Band-Stop”.

FFS is a metamaterial the oldest open literature we can find is papers wrote by G. H. Shennum, published in 1973 and 1975, named “Frequency Selective Surface For Multiband Antennas”, “Design of Frequency Selective Surface Using A Waveguide Simulator Technique”, respectively. In the 1973’s paper, Shennum came up with the idea of using FSS as a tool for antenna performance altering. Then In the 1975’s Paper, they presented a device called Frequency Selective Subreflector interacted with an array of dipole antennas. Something else to be mentioned here is that the “waveguide simulator technique”, based on analysis of that paper with taking the

civilian use computers' performance back then, the "simulator" was actually a small testing measurement system from today's viewpoint. However, this technique did inspire the later computer-based simulation software such as HFSS. Our previous discussed simulations for DNG materials are all based on this technique. [27] Later in 1975, A. G. Cha, etc furthered the theory of FSS design [26] based on Schennum's paper in 1973[26], in that paper, they defined FSS as a surface consists of an array of passive resonant elements conformally.

4.5 Artificial Magnetic Conductor

Frequency Selective Surface acts as a reflector when interacts with antennas at the frequencies they're designed to operate.[26], and that's what our research is based on. A reflector is a structure used to enhance the performance of antennas by reflecting the radiation towards the unwanted directions and alter that to the directions we need. In theory, the best performance can be achieved is the performance of a PMC, which reflects all the E field parallel to the surface.

Despite the charming properties PMC has, does not exist in nature. As a result, the performance of it can only be found by looking into that of a Perfect Electric Conductor, as discussed in Chapter 1. [11] It is concluded that a PMC surface is a surface over which the tangential components of magnetic field vanish. Researchers have found plenty of methods to fabricate artificial magnetic conductors that mimic the performance of PMC for certain frequency bands. In the section of Double Negative Index, we mentioned that an AMC can also be regarded as a DNG, and here is the proof from the HFSS simulation.4.8

Artificial PMC surfaces are being synthesized and fabricated for these recent years, and they are only able to exhibit/mimic the PMC-type properties within certain frequency ranges named as the working bandwidth. As a result, APMC or AMC are referred to as Band-Gap Structures or Band-Limited Surfaces.

The AMC applied in our research is named as the mushroom surface. A mushroom

surface consists of an array of periodic metallic patches of a variety of shapes, typically hexagons or squares, placed on a layer of the substrate, which could be air[11], and it is air in our case, and then the patches are connected to a ground plane by conductive vias. The entire structure looks like a tidy array of mushrooms and hence named.

The physical structure of a mushroom unit is shown in 4.7

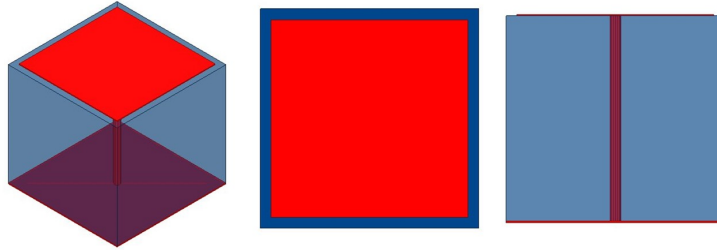


Figure 4.7: Mushroom Unit Cell Physical Structure

In the section of Double Negative Index, we mentioned that an AMC can also be regarded as a DNG, and here is the proof from the HFSS simulation, in which two adjacent unit cells are put together inside a parallel plate waveguide, just as other resonators we simulated.

The mushroom unit cell(s) structure and its equivalent circuit are shown in Figure 4.9[11]

When the wave impinges upon a mushroom unit cell, across the gap, electric fields are generated. And this E field may be described as capacitance C. At the same time, the wave generates currents between adjacent unit cells, and this effect may be described as an effective inductance L. The AMC mushroom structure design are discussed in the following chapters.

Literature Review: on Artificial Magnetic Conductor Design

In this part, the design principles and achievements found in the open literature on which the Frequency Selective Surface Artificial Magnetic Conductor proposed are reviewed and discussed.

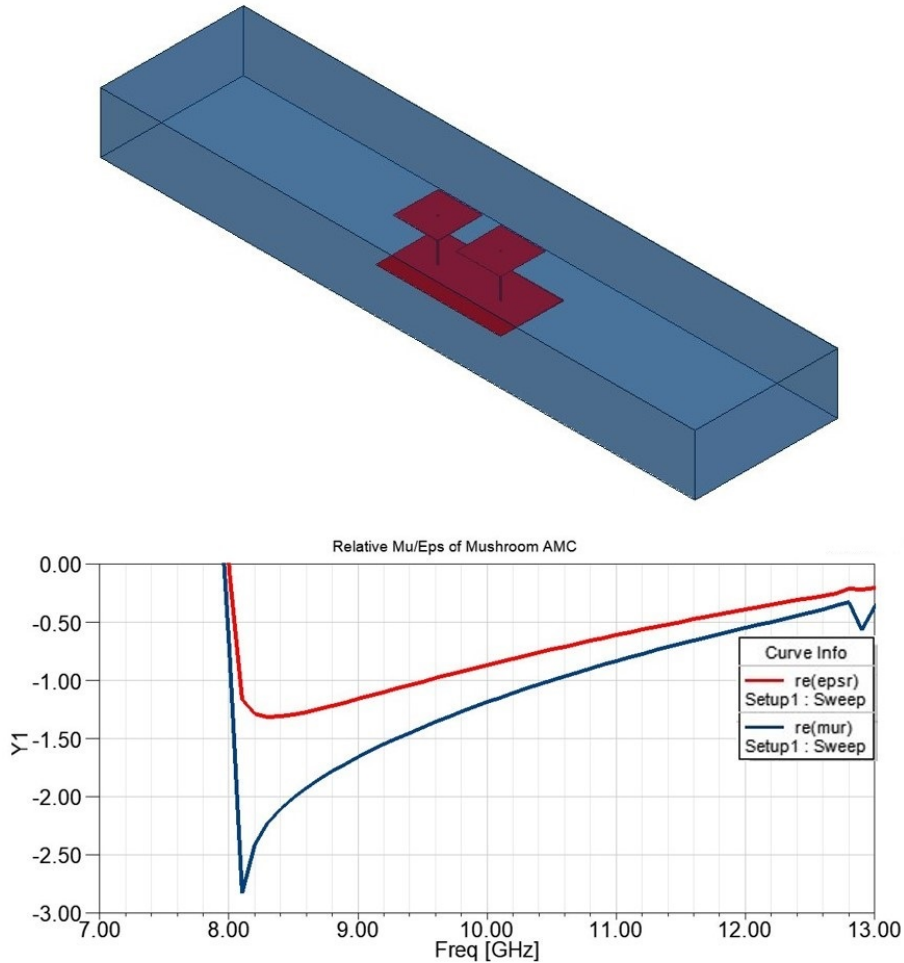


Figure 4.8: Mushroom Unit Cell Acting as DNG Material

As introduced and discussed previously, the FSS AMC is not literally limited to the mushroom structure. However, most of the current FSS AMC designs are mushroom surface structures or their alternative forms. For example, some designs may only come with gapped patched but no vias connection between the surface and the bottom ground plane.

Resultly, the mushroom surface, as a relatively mature type of FSS AMC, compared with others, it a good starting point from which we can start to build basic understandings of the FSS AMC, theoretical models summarized based on them is also a good reference for the proposed work.

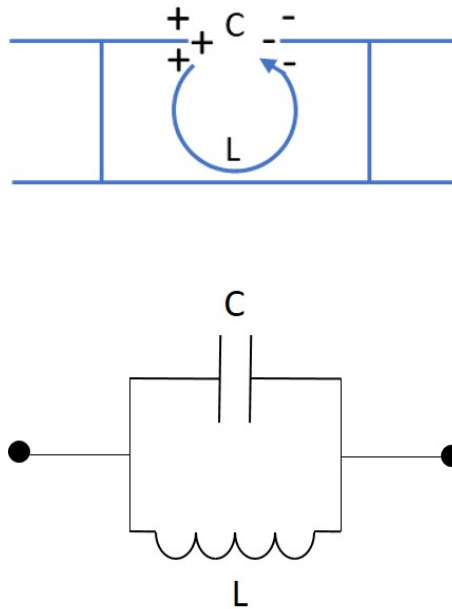


Figure 4.9: Mushroom Unit Cell(s) and Equivalent Circuit

4.6 Mushroom AMC Design Equations

Like most of the other electrical structure, the mushroom surface AMC also has a different abstract model of explaining why and when it can work. Among them, the simplest model seen at this point is what we call the “LC resonant model”, upon which the mushroom AMC design equations have been built and analyzed. Although the discussion seems to start at the surface impedance of the equivalent circuit of the mushroom surface structure.

Theoretically, dimensions of the mushroom AMC are determined by the following equations, cited from [11]

The surface impedance of Mushroom AMC,

$$Z_s = j \frac{\omega L}{1 - \omega^2 LC}$$

The impedance becomes infinity when resonant, we have the resonant frequency

$$\omega_0 = \frac{1}{\sqrt{LC}}$$

Effectively, the mushroom AMC unit has an equivalent circuit represented by the sheet inductance and the sheet capacitance, then, the resonant frequency becomes,

$$\omega_0 = \frac{1}{\sqrt{L_s C_s}}$$

The in-phase band, over which the phase of reflection coefficient is between $\pm 90^\circ$, is expressed as.

$$BW = \frac{\Delta\omega}{\omega_0} = \frac{\sqrt{L_s/C_s}}{\sqrt{\mu_2/\epsilon_2}} \quad (4.1)$$

in which, ϵ_2 and μ_2 are the permittivity and permeability of the material above the mushroom structure (named as an upper layer or superstrate), while ϵ_1 and μ_1 are that of the material inside the mushroom structure (called the dielectric layer or substrate).

Concepts L_s and C_s are introduced in the equation above as the most important determining parameters of the bandwidth as well as the resonant frequency of the mushroom structure. However, although they look to be two simple single values, each of them is indeed, a combination of several different sources of inductance or capacitance. The inductance and capacitance can be abstracted as the sheet inductance and sheet capacitance only when the mushroom surface structure is simple enough. In other words, the LC resonator model is not universal for all FSS AMC and may not even be effective for mushroom surfaces with a more complicated structure. And the universal model of FSS AMC is one of the works proposed by use hereby in this document.

Now we need to figure out how to calculate the sheet inductance and capacitance, for the linear inductor we have,

$$L_s = \mu_1 h$$

h is the height of the mushroom unit, or via height.

When it comes to the sheet capacitance, it is determined by the capacitance between each two adjacent parallel edges of mushroom units. Capacitance C of each unit cell is related to the sheet capacitance C_s ,

$$C_s = C \times F$$

in which F is a factor related to the number of edges of each mushroom unit, and $F=1$ for square mushroom units.

$$C = C_s = \frac{s(\epsilon_1 + \epsilon_2)}{\pi} \cosh^{-1}\left(\frac{s+g}{g}\right)$$

[11] in this equation, s is the side length of the mushroom unit, and g is the gap width between adjacent mushroom units.

From these equations above, the factors that influence the percentage bandwidth and resonant frequency can be found.

4.7 Restrictive Conditions of Mushroom AMC Design

The AMC Mushroom structure discussed here is a reflector for antennas, therefore, limitation conditions are mostly from the requirement of its interactions with the antenna. Limitation conditions for the mushroom structure observed at the first glance are listed as followed,

1. h is the via or mushroom structure height. For this mushroom AMC is designed for antenna enhancement, h cannot be longer than the quarter-wavelength of the operation frequency, at least cannot be longer than the $\lambda/4$ of the lowest operation frequency to avoid unwanted resonance, and to be a properly working mushroom

surface, it is best to be shorter than $\lambda/10$ for the entire working bandwidth.

2. s is the side length of the mushroom top square which is supported by the via a wire connected to the ground plane, therefore, the side length s cannot be smaller than the diameter of via, d_{via} . Else, the via itself will become the “mushroom top” itself.

3. g is the gap width between adjacent mushroom units, which needs to have a reasonable value, the minimum value is limited by the fabrication techniques, claimed to be 0.1mm by Balanis[11], while the maximum value is determined by the following conditions.

a. The side length of the mushroom unit(not the mushroom top or patch side length) is $a = s + g$, and the mushroom surface is a periodic structure. Hence, if we have a g which is too big, then the entire mushroom surface would be unreasonably large in area.

b. When g is comparable to $\lambda/4$ of the antenna’s operating frequencies, the mushroom surface may act more like a finite ground plane rather than a mushroom AMC surface unit which has completely different electromagnetic properties.

The equations on which our mushroom surface structure is based on have a built-in requirement, and we can find it when looking back into 4.9, where theoretic model of the mushroom structure is regarded as an LC resonator. In this model, the main source of capacitance is considered to come from the parallel capacitor formed by two adjacent square mushroom tops. When the thickness of the mushroom top is defined as t , we have $C = \epsilon A/d = \epsilon_2 st/g$ in this case.

It is observed that when the ratio of g/s becomes bigger and bigger, the bandwidth doesn’t always increase, and this phenomenon indicates the existence of another limitation, which makes the conclusion from the equation saying an infinite gap width will give us an infinite bandwidth” not valid. The possible reason could be the equivalent circuit is no longer the same as in 4.9 when g/s goes infinite, or s/g goes 0.

And in this case, the capacitance of the gap between adjacent mushroom tops is no longer dominating. In fact, that model will become more like a PEC reflector placed approximately a quarter wavelength away from the antenna. Figure 4.10 shows the new equivalent circuit, formed by a resonator consists of two parallel capacitors and one inductor, one of the capacitors is the capacitance of the gap between the adjacent mushroom tops(C_g), while the other is the capacitance between the mushroom top and ground plane(C_p).

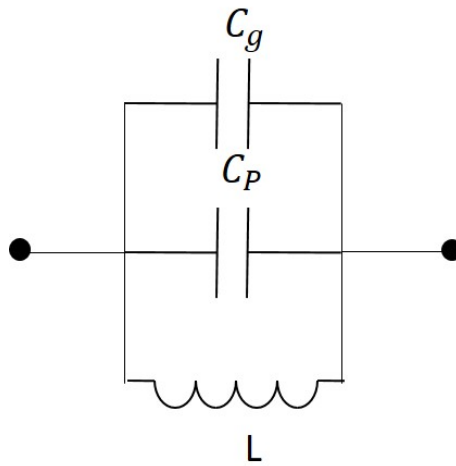


Figure 4.10: New Equivalent Circuit of Mushroom Surface When g gets bigger

Now the capacitance of the resonant circuit becomes, $C = C_g + C_p$, and by applying the parameters of the mushroom surface. We have the equations for the capacitance,

$$\begin{aligned}
 C_g &= \epsilon_2 st/g \\
 C_p &= \epsilon_1 A_m/h = \epsilon_1 s^2/h \\
 C &= \frac{\epsilon_2 st}{g} + \frac{\epsilon_1 s^2}{h}
 \end{aligned}
 \tag{4.2}$$

Where A_m stands for the area of the mushroom top,

The New percentage bandwidth can therefore, be determined per the Dan Sieven-

piper's work [30]

$$BW = \frac{Z_0}{\eta_2}$$

$$Z_0 = \sqrt{L/C}$$

$$\eta_2 = \frac{\mu_2}{\epsilon_2}$$

1. In order to maintain the physical structure of a mushroom surface, the minimum value of s should be defined as d_{Via} as discussed previously.

2. h , the height limitation is $\lambda/4$ as discussed previously (and the shorter the better, if possible).

3. The equation also seems to be suggesting to reduce the thickness of mushroom top as much as possible, however, it is limited by the current techniques, and in fact, there will not be really big charge even if we can use an ideal PEC with 0 thickness.

Go back the point where we decided whether the C_p can be ignored, we can figure out the relationship should be set up between g and other dimensions. We decide C_p to be not ignorable when $C_p \geq 0.1C_g$

Equite C_p with $0.1C_g$, in which case the C_g is no longer dominating, then we have the relationship between g and s ,

$$g = \frac{\epsilon_2 th}{10\epsilon_1 s}$$

In fact, when the gap gets even bigger, there is no longer C_g anymore, and the mushroom structure falls apart, as a result, it cannot be analyzed using the principles of the mushroom surface structure.

CHAPTER 5: Artificial Magnetic Conductor Design

5.1 Design Analysis

A perfect magnetic material(PMC), as discussed previously, only exists in theory till now[11]. PMC is named for it is a type of material that allows a magnetic current to flow on its surface freely, comparable to what a perfect electric conductor does to an electric current. Meanwhile, the PMC reflects the perpendicular incident wave onto its surface back completely towards the opposite direction. However, as previously mentioned, such PMC is not found in nature yet, despite the fantastic natures it possesses.

In order to solve this problem, researchers came up with a series of metamaterials named artificial magnetic materials(AMCs) to mimic the PMC, as introduced in Chapter 2. Each AMC only mimic the performance of an ideal PMC across a certain frequency band. This band is named as AMC's working band. Among those AMCs, Mushroom Surface[11] is one type which has been applied as reflectors in different antenna systems. Characteristics of the mushroom surface structure are relatively clear. Thus, our designs presented in this chapter and the entire document are mushroom surface AMC materials based on. to simplify the discussion and fabrication, the square-shaped mushroom unit is selected as the basic unit element of the AMC proposed.

Per the mushroom AMC (or mushroom surface) design theory summarized in Chapter 2, a mushroom surface is defined as a periodic structure with each element/mushroom called a unit. The equivalent circuit of the unit cell formed by every two adjacent units is a pair of parallel capacitor and inductor. Mushroom units come with different shapes, to simplify the discussion and fabrication, the square-shaped

mushroom unit is selected as the basic unit element of the AMC proposed.

In the common cases we discuss, the “superstrate” of the mushroom surface is air, or free-space, in other words, $\mu_2 = \mu_0, \epsilon_2 = \epsilon_0$

We now have the design parameters of the mushroom surface structure prototype. In order to expand the bandwidth of the mushroom surface, and when the superstrate is the free-space. What we need to do is reducing the average dielectric constant of the space “inside” the mushroom surface structure, or the “equivalent substrate”(any materials occur between the mushroom top and bottom/ground layers). Since air has the dielectric constant closest to the free-space, and generally it is the material with smallest possible permittivity (unless other mater materials are applied), we need to have as much as possible air to play the role of the “equivalent substrate”.

In theory, the best case is to fabricate the mushroom ground on one PCB board and fabricate the mushroom tops on another and then connected them together with metallic wires. In this case, the entire space between the top and bottom of the mushroom surface is filled with air except that occupied by the substrate layers.

However, this structure is not possible to fabricate as it is since the wires are usually not strong enough to support the mushroom top layer. Hence, a supporter is needed to fulfill these requirements for fabrication.

1. Strong enough to support the mushroom top layer.
2. Must be able to maintain its shape while strong surface tension is applied.
3. Must have a reasonable low dielectric constant.
4. Easy to fabricate.

Several different materials are on the list of selection, and finally, a plastic material named as Acrylonitrile Butadiene Styrene(ABS) is selected to make the supporter. And the fabrication tool is decided to be a 3D printer, which can freely make the ABS filaments it uses into any shape.

5.2 Artificial Magnetic Conductor Design

The Artificial Magnetic Conductor is used to mimic the Perfect Magnetic Conductor over a certain bandwidth, which is called the in-phase band, where the phase of reflection is $\pm 90^\circ$. In the previous chapter, a theoretical model of AMC is discussed, and since the structure is described using the inductance and capacitance of the AMC units, it is named as the LC model. A number of different mushroom unit AMCs have to be introduced by different researchers using the LC model, and it is proved that this model is effective. This model can be effective in a number of applications. For example, according to what is predicted by the LC model, the bandwidth will increase when the inductance is getting bigger. As shown in 5.1, when the via of the AMC mushroom is straight, the bandwidth is 2.30GHz - 5.28GHz, and the percentage bandwidth is 78.63 %. And when the via of the AMC mushroom is twisted, the bandwidth becomes 1.70GHz - 4.56GHz, and percentage bandwidth is 91.37%.

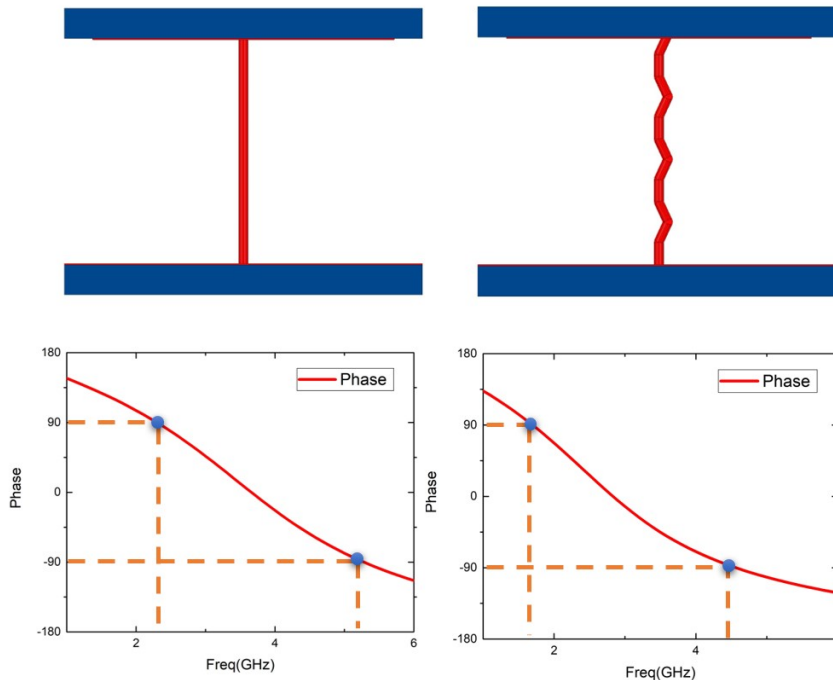


Figure 5.1: Twisted Mushroom

However, the LC model is not always precise, and not even always correct. In

practice, it is only effective for simple artificial magnetic conductor structures, which can be abstracted into a linear combination of sheet inductance and sheet capacitance. In order to better describe the performance of other types of AMCs more universally, it is necessary to look into the models that are more elemental and essential.

5.3 The Artificial Atom Model

The Artificial Atom Model, the AA model, is a model in which the metamaterials are view in a way that is similar to which the bulk materials are looked. The model is deeply rooted in the principle of physics, which says every item in the universe is consist of particles. The modern physicians haven't yet found the limitation of the minimal size of the particles, however, it is not a problem for the discussion hereby presented. A particle in practice typically means a structure or an item which is not dividable or this is no necessity of dividing it in the scale the research is conducted.

The spectrum of electromagnetic wave is very, very huge, and as a result, in the field of electromagnetism, we define the "particles" in a flexible way, we call that every "element" or "structure" which has physical dimensions small enough compared with the wavelength of the electromagnetic wave of interest is a "particle", else we say it is not, despite the meaning in physics or chemistry.

For example, a piece of sand which has a volume of $1mm^3$ is not considered as a particle when the electromagnetic wave is a visible light, which has a wavelength of hundreds of nm s, and it will definitely be defined as a particle when we are discussing the wave of a WiFi signal, whose wavelength is $125 mm$ s and the diameter of the sand is less than one hundredth of it. The concept of a particle is of great importance in the research presented hereby, for it is the solid theoretical basis of an Artificial Atom. In other words, when the size of a structure is small enough compared with the wavelength of the electromagnetic wave on which the research focuses, the internal structure will be "neglected" by the wave, just like the visible lights "neglect" the internal structure of a real atom by God.

The real atoms form the bulk materials in a periodic way, therefore, the Artificial Atoms also need to be distributed in that way. Furthermore, when it comes to our Artificial Magnetic Conductor, it is a must to realize that although an AMC is named as "conductor", it is indeed trying to mimic the interface layer between a bulk material and a metamaterial only. Consequently, we don't have to worry about how an artificial atom will repeat itself along the Z-axis in the space, what we need to do is to repeat the artificial atoms along the X and Y axes.

From the discussion of the AA model, our thoughts are liberated from the frame of mushroom surface structure AMC. However, on the other hand, it brings another problem, it doesn't show a guide for us to build one that will fulfill our requirements, although it does give a clear limitation of the design, any dimension of the artificial atom or unit must be viewed as small enough compared with the wavelength, typically, this limitation is $\lambda/8$ or $\lambda/10$.

5.4 The Intrinsic Impedance Model

Metamaterials, as a young research field which only has a history of about 30 years, it is reasonable to have a lot of unclear things to look into. The research on AMCs are even shorter, people haven't even come to an agreement for which name should be used. However, although no one can tell what exactly should the AMCs be, it is still possible to throw a light upon the question of what an effective AMC should look like. The Intrinsic Impedance Model is, therefore, raised to answer this question.

The Intrinsic Impedance Model, or the IM model, is a model which developed based on the AA model. The AA model tells us, a periodic artificial atom unit can be regarded as a real particle such as an atom in the spectrum of interest. In other words, a piece of metamaterial, here the AMC, can be looked into in exactly the same way as a bulk material, for which we have much more theory resources to rely on.

Now it is time to look back into the reason of which the intrinsic impedance is generated. A general material has two built-in physical quantities, the permittivity ϵ

and the permeability μ . They define the intrinsic impedance as in the equation,

$$Z_{material} = \sqrt{\frac{\mu_{material}}{\epsilon_{material}}} \quad (5.1)$$

To design an AMC, what we need to do is to make the impedance of the AMC to have a proper value for Γ . The AMC applied here as a reflector is considered as "effective" when $\Gamma_{real} > 0$, and we can simply say that $\Gamma > 0$ to simplify the discussion. In other words, the impedance of the AMC should be bigger than that of the space from which the wave comes from, to be clear here, space does not necessarily be the free-space, and in fact, sometimes we intentionally make it be some other dielectrics to have better results. To express in equations, we say that a successful AMC should be: $Z_{AMC} > Z_{Space}$. Therefore,

$$\Gamma = \frac{Z_{AMC} - Z_{Space}}{Z_{AMC} + Z_{Space}} > 0 \quad (5.2)$$

In the viewpoint of real permittivity and real permeability, we have.

$$\sqrt{\frac{\mu_{AMC}}{\epsilon_{AMC}}} > \sqrt{\frac{\mu_{Space}}{\epsilon_{Space}}} \quad (5.3)$$

From this equation, it can be observed that there are several methods to make $\Gamma > 0$, 1. Increase μ_{AMC} , 2. Decrease ϵ_{Space} , 3. Increase ϵ_{AMC} , 2. Decrease μ_{Space} .

These four methods can be applied separately, or together. However, the difficulties are not equal. Generally speaking, ϵ and easy to tune for both the "space" and the AMC, however, tuning the μ of AMC is a little more difficult, while the μ of the space is even not possible or too costly to tune. Meanwhile, the AMC is used to enhance the performance of certain components, such as the antennas, so it is not very reasonable to change the component itself other than the dielectric material. The IM model is a good guide for us to determine which direction an AMC design needs to go when it doesn't meet our initial design purpose.

To summarize, the design of an AMC can be abstracted into ANY method which can equivalently change the permittivity and permeability of the AMC.

5.5 Artificial Magnetic Conductor Design Examples

The theoretical models of AMC discussed above can all guide the design of AMCs in some aspects, using these principles, we come up with a series of different new AMC designs, some are totally new structures, while others are based on previous designs and the bandwidths are greatly improved. All the comparison is based on the most commonly applied mushroom surface structure in the lab nowadays. The standard of determining the bandwidth is any frequency whose wavelength is 8 times or bigger than that of the largest dimension of the mushroom unit.

The standard structure has a dimension of solid ground, 4.7mm top patch side-length, 0.1mm gap width, and a height of 4.8mm. The "Space" material is free-space, and AMC substrate is FR4 with a dielectric constant of 3.82, and bandwidth is 1.77GHz - 2.16GHz, only 19%. 5.2

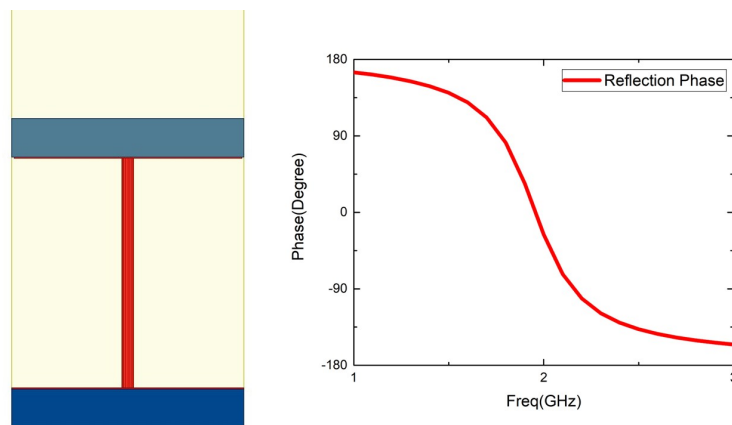


Figure 5.2: Mushroom AMC Unit for Reference

By replacing the solid ground plane with a cross structure (a net-like structure when viewed as a whole), the bandwidth can be increased to wider than 21%, and the 0 crossing point can be shifted by 10%. 5.3

By replacing the mushroom top patch with a cross structure, the bandwidth can

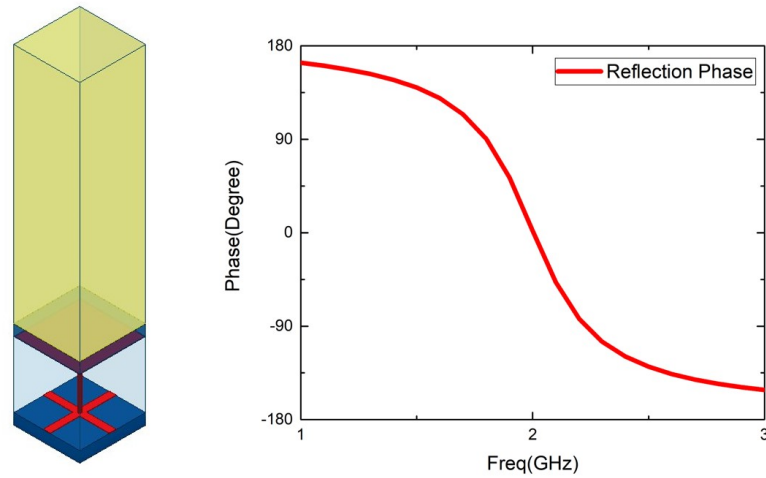


Figure 5.3: Mushroom AMC Unit With Crossed Ground

be increased to 29%, 2.57GHz - 3.43GHz, 5.4

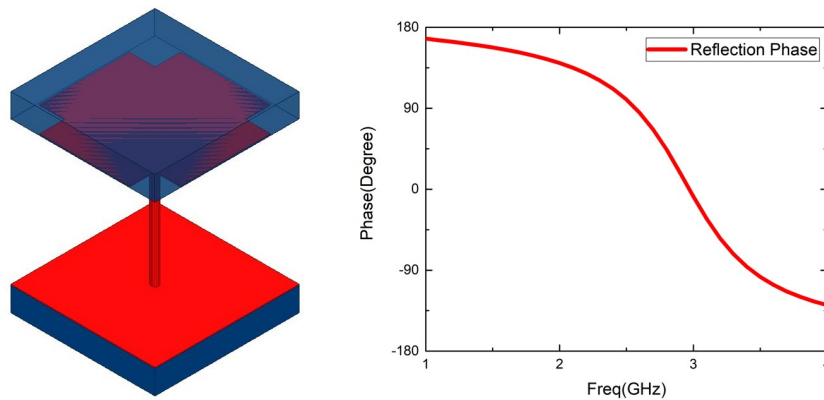


Figure 5.4: Mushroom AMC Unit With Crossed Mushroom Top Patch

By replacing the Space material with RO4350 by Rogers, and the AMC substrate with air, the bandwidth becomes 1.28GHz - 2.99GHz, in percentage is 80%, we have an increase of 4 times. 5.5

The LC model indicates that the mushroom patch doesn't have to be solid, as a result, we designed the hollowed mushroom surface structures. The basic structure is still based on the mushroom surface structure AMC with a square patch of 4.7mm sidelength and 0.1mm gap width. Reducing the area of metallic part viewed from

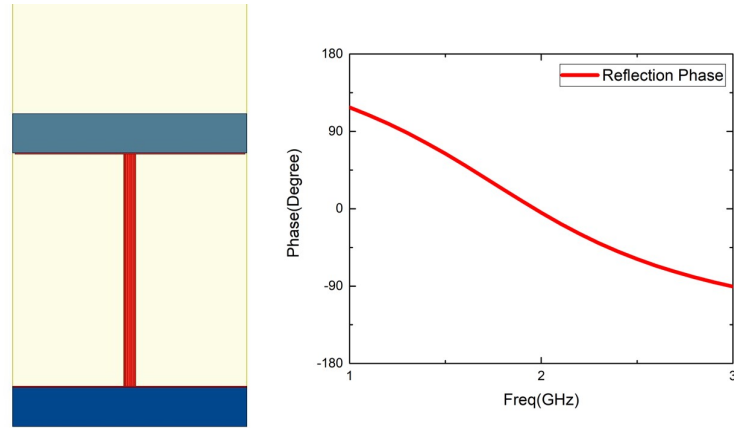


Figure 5.5: Mushroom AMC Unit With Air Substrate and RO4350 Superstrate

the top is an effective way to decrease the loss caused by the interaction between the antenna and the AMC, which will be discussed in the following chapters.

The first idea is to replace the N/Regular cross with a curved one, for example, a Malta Cross, the result is shown below. The bandwidth is 3.16GHz - 4.53GHz, a 36%, to compare, the N/Regular cross with the same edge width has a 24% bandwidth of 2.19GHz - 2.79GHz. 5.6

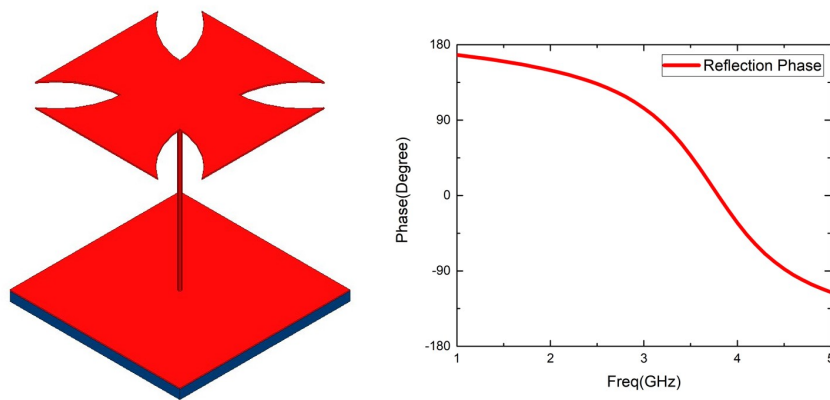


Figure 5.6: Malta Cross Mushroom AMC Unit

To further reduce the "contact" area of the metallic patch, we "punch" holes on the Malta Cross surface, and got a new bandwidth of 35% of 3.11GHz - 4.43GHz^{5.7},

Reducing the contact area of metallic parts are reducing the surface current formed on the patches. Therefore, we make the holes to further divide the patch, the band-

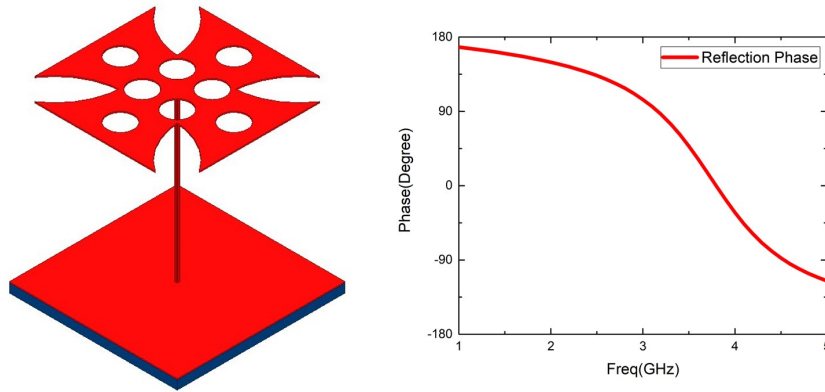


Figure 5.7: Malta Cross With Holes Mushroom AMC Unit

width associate becomes 34% of 3.28GHz - 4.61GHz. 5.8

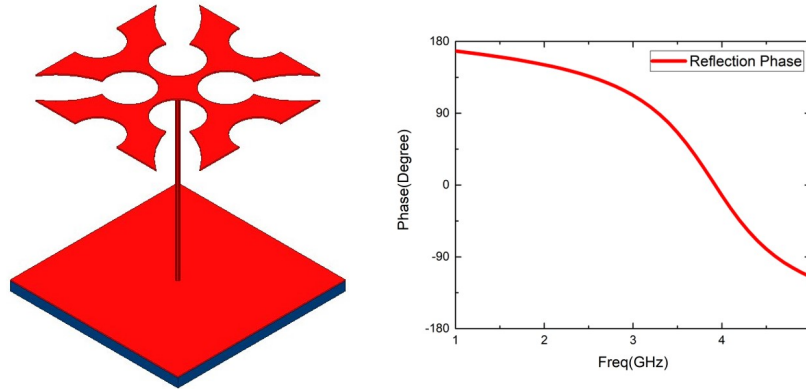


Figure 5.8: Disconnected Malta Cross With Holes Mushroom AMC Unit

Another way of expanding the bandwidth is to combine the Malta cross and an ordinary mushroom patch. Through this way, the bandwidth can be expanded to 53% of 4.46GHz - 7.66GHz. 5.9

Or another method that removes less of the Malta Cross, bandwidth 53% of 4.49GHz - 7.75GHz, 5.10

As indicated by the LC model, and the bandwidth is shown by the "hollowed mushroom" AMCs, it is concluded that we may reduce the amount of metal usage even further, for example, we can use wire structures to build the mushroom AMCs.

A wired structure with a hollowed exponential shape has a bandwidth of 71%, 3.79GHz - 8GHz. 5.11

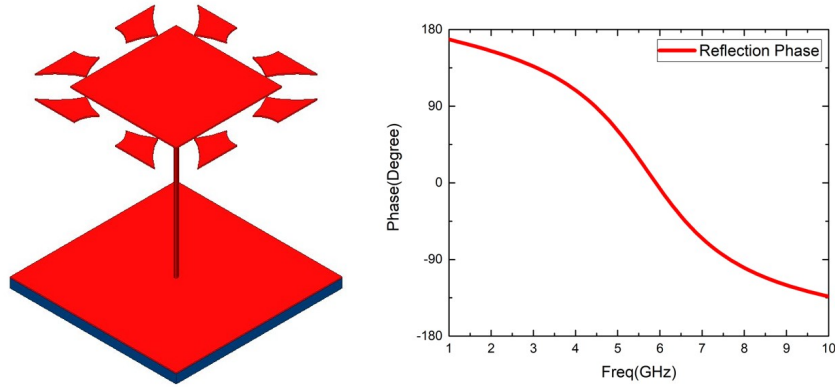


Figure 5.9: Malta Cross With Holes Mushroom and Middle Patch AMC Unit

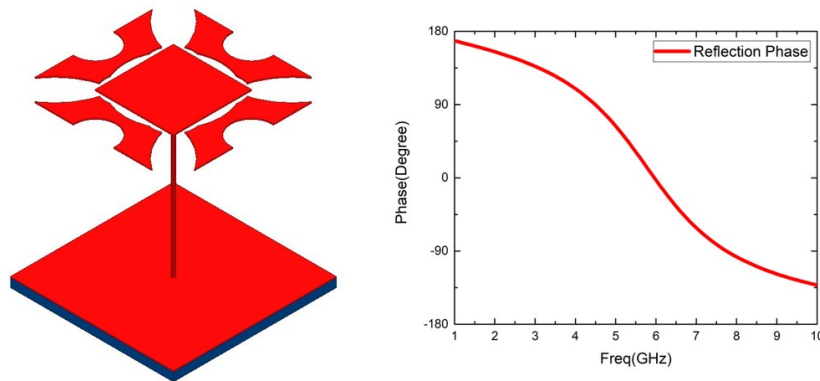


Figure 5.10: Less Removed Malta Cross With Holes Mushroom and Middle Patch AMC Unit

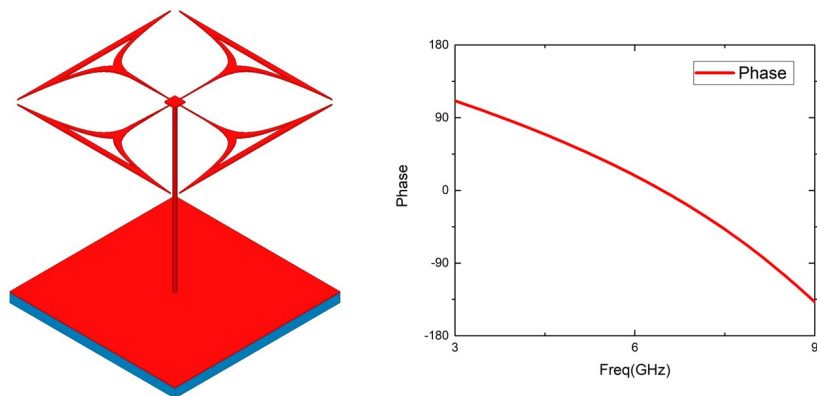


Figure 5.11: Hollowed Exponential Wire Structure AMC Unit

A wired structure with a cruciferous shape has a bandwidth of 61%, 3.19GHz - 5.99GHz. 5.12

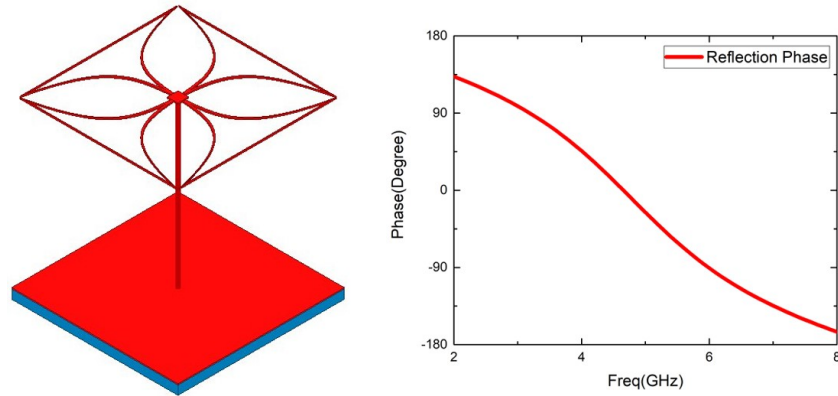


Figure 5.12: Cruciferous Wire Structure AMC Unit

A wired structure with a doji/Shuriken shape has a bandwidth of 51%, 3.12GHz - 5.17GHz. 5.13

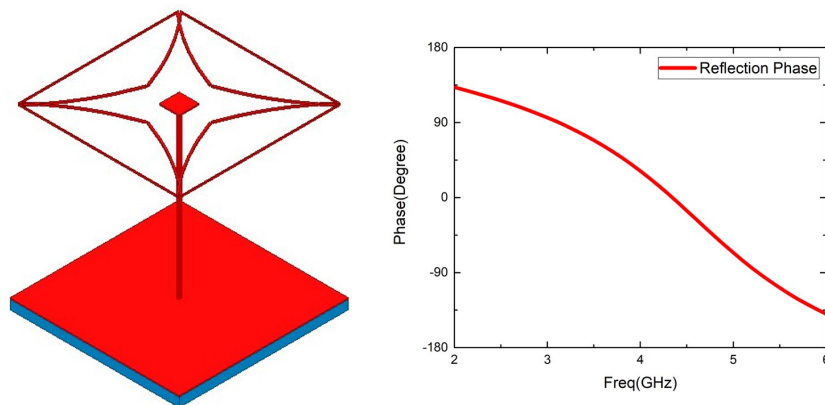


Figure 5.13: Wire Doji/Shuriken Structure AMC Unit

A wired structure for the Melta Cross has a bandwidth of 67%, 3.24GHz - 6.53GHz. 5.14

A wired net structure based on the previous models is built to have a bandwidth of 77%, 3.29GHz - 7.40GHz. 5.15

To summarize, the models shown above are just a small portion of all mushroom surface AMCs we design, and any combination of a via and a patch or patch-like mushroom top structure can form a mushroom AMC unit, as long as they can be abstracted to be described as a linear combination of inductors and capacitors, per the

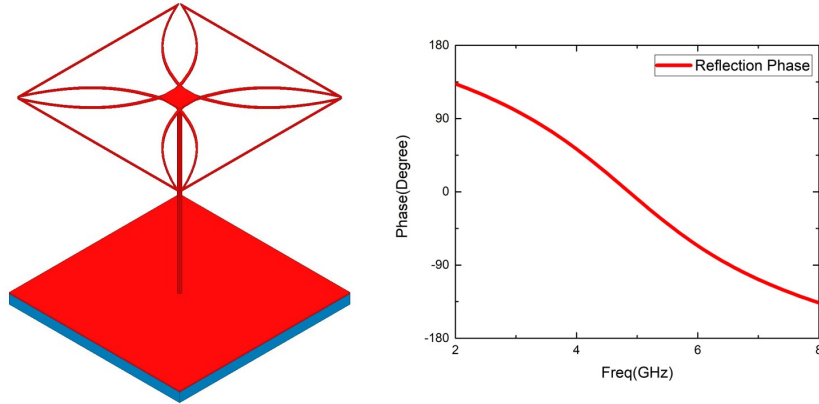


Figure 5.14: Hollowed Malta Cross Wire Structure AMC Unit

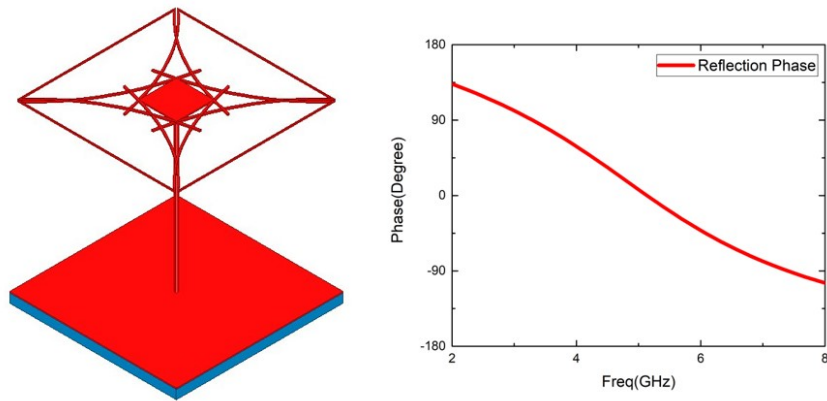


Figure 5.15: Hollowed Wire Net Structure AMC Unit

indication of the LC model, meanwhile, the 0° cross point can be tuned by changing the solid ground into a net structure and tuning the width of the "wires". Another thing to be emphasized that when the mushroom unit structure becomes more complicated, the via itself will no longer be considered as the only major source of inductance.

5.5.1 Non-Mushroom AMCs

As we can see, the mushroom surface structure AMC unit tuning shown above is mostly based on the LC model. However, in those models, a via is still a must for every model, during the fabrication procedure, this is difficult to automatically attach to the mushroom structure. As a result, we may want to have some structure

that can be fabricated automatically without manual work or just need a very small portion of manual work. Also, the LC model limits the tuning methods of the AMC.

In order to better tune the AMC unit, we come up with other structures that are more tunable. The basis of Non-mushroom AMCs is to remove the vias connecting the mushroom top patch and the ground plane.

The first idea we come up with is a patch to patch structure AMC, which is not a mushroom structure but looks very similar to it. There are two major differences between a patch to patch AMC and a mushroom AMC, 5.16

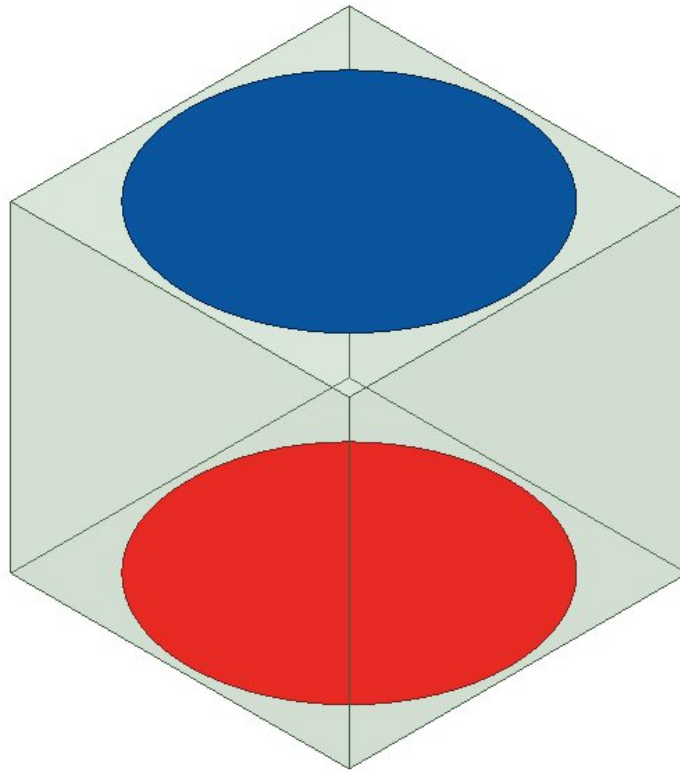


Figure 5.16: Patch to Patch AMC Unit

1. A mushroom AMC has a wire to connect the mushroom top patch and the ground plane, but the patch to patch structure has not.

2. A mushroom AMC has a connected/united ground plane/common ground, while the ground of the patch to patch AMC is a combination of discontinuous patches.

Inspired by the passive metamaterials, or DNG, we came up with the idea of us-

ing non-mushroom structures, which tune the permittivity and permeability through resonance.

The patch to patch structure has an ultrawideband performance, 94% of 1.57GHz - 4.38GHz. 5.17

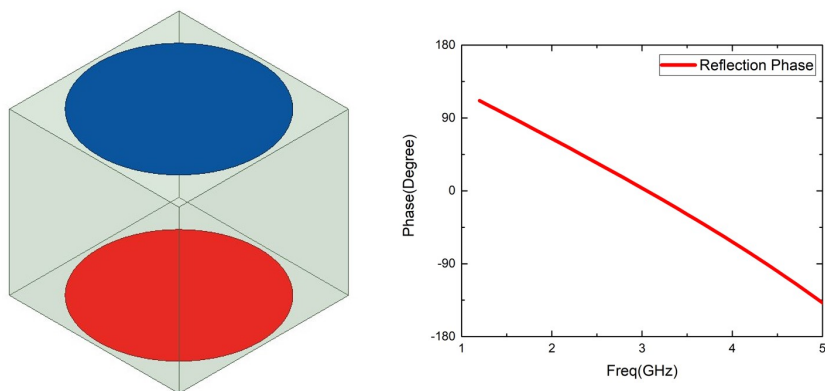


Figure 5.17: Patch to Patch Structure AMC with Reflection Phase

Nesting Rectangular Ring Structure is. the structure and the Phase of reflection are shown as in 5.18, the bandwidth is 73%, 3.74GHz - 8GHz.

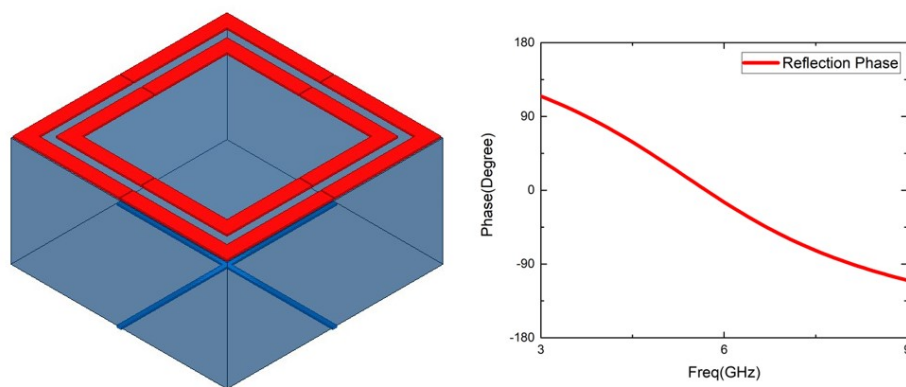


Figure 5.18: Nesting Rectangular Ring Structure AMC

The reason for building the resonance structures that are vertically placed is shown in the following discussion, the examples for those resonance structures are:

The Structures of three rings, 5.19, 4.31GHz - 6.38GHz, a bandwidth of 38%.

The Structures of crossed circular rings, 5.20, 4.69GHz - 7.36GHz, a bandwidth of 44%.

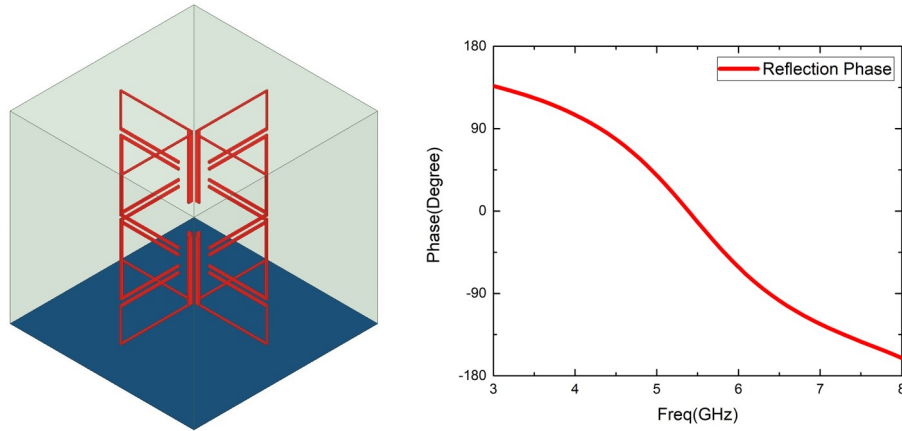


Figure 5.19: Three Rings Structure AMC

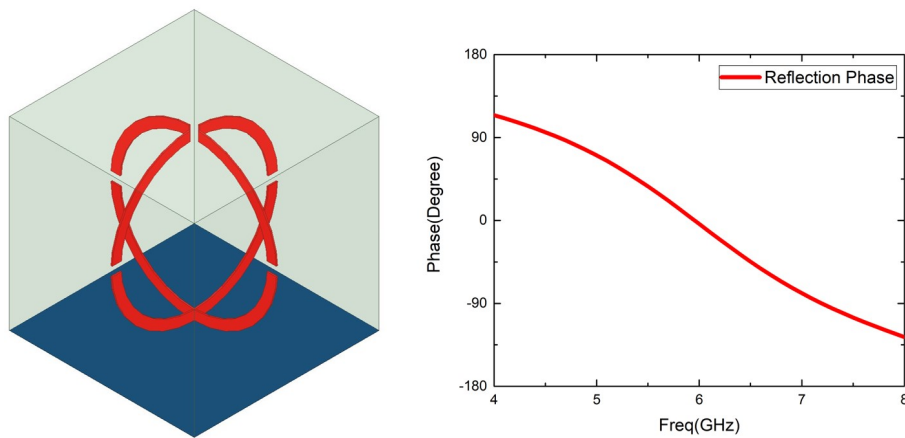


Figure 5.20: Crossed Circular Rings Structure AMC

To have higher equivalent permeability and reasonable permittivity, the three rings structure AMC is modified into eight wings four rings structure AMC. 5.21, the bandwidth is 3.75GHz - 8GHz, or 72%.

The non-mushroom AMC structure designs shown above are just a few examples. In practice, any periodic metallic structures that resonant and therefore can be used to tune the permeability and permittivity. This basic principle can be used to apply to the design of any spectrum and expand or narrow the bandwidth when necessary.

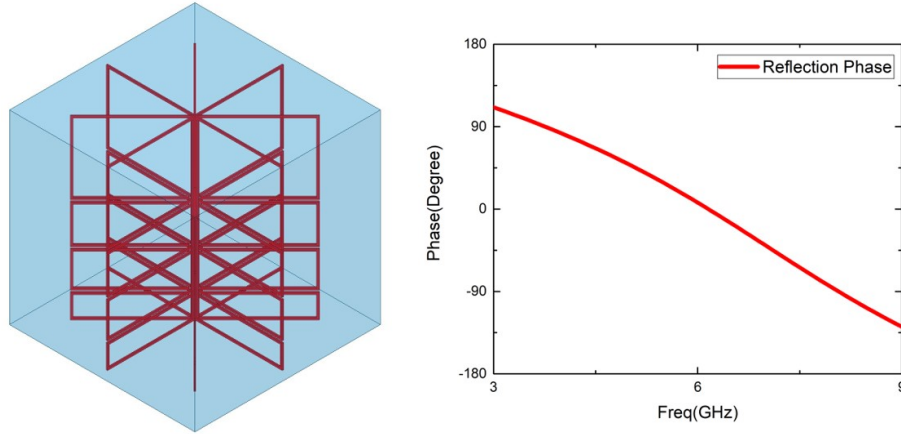


Figure 5.21: Four Rings Eight Wings Structure AMC

5.5.2 Millimeter Wave AMCs for 5G Applications

As discussed in the introduction part, the 5G wireless communications push the spectrum into millimeter waves, our AMC can be used to enhance the performance of the 5G antennas.

Generally speaking, all kinds of AMCs mentioned in the previous section can be scaled to fit the 5G applications. Meanwhile, to reduce the heat generated, we make the millimeter wave AMCs with crossed resonant rings.

In order to change the working bandwidth to the millimeter wave which will be applied in 5G, it is necessary to look back into the theoretic basis why the AMC works with antennas placed very near to it as reflectors.

A big difference between the tests of the mushroom surface AMC unit and the entire mushroom interacted with an antenna. When the incident wave is a plane wave, the mechanics of reflection is simple as described in the ideal model. However, when the radiation is from the antennas, the story is totally different. Theory pinpoints that when the antenna is placed infinite close to a PMC surface, the current on the antenna which is parallel to the interface will generate an image current with the same magnitude, direction, and phase. But this is not our case, unlike an ideal case in which PMC is regarded as a uniform material just as FR4 or ABS, our AMC mushroom

structure is mimicking the performance of the PMC using some metallic components. The truth here is that the fringing field, near field effects, or the interactions between the conductive antenna and conductive surface of the AMC are not avoidable. The antenna sees the AMC in two ways, a component which interacts with it in the near field, and a medium which influences the far field radiation pattern.

The interaction between the antenna and AMC in the near field will undoubtedly add extra impedance to the antenna, mostly capacitive reactance, since the small sections of antenna traces and the mushroom top beneath can be treated as capacitors. However, the antenna still can be described as an effective one as long as the return loss remains under -10dB, this return loss value also indicates that the energy lost in this kind of interactions is just a small portion.

When the radiation comes out from the antenna, the antenna begins to see the mushroom surface structure AMC beneath it as a uniform medium, and the reflection can be calculated using the equations mentioned above, with the effective μ and ϵ . In the real cases, the radiation of the antenna is not in the form of a plane wave, but more like a spherical one, although not perfect, either. All the electric fields contained in the wave propagating downwards has a component parallel to the mushroom surface, except the ones that vertically point down. Within the in-phase band of operation, these E fields are reflected by the AMC with a phase range of $\pm 90^\circ$, in other words, the energy is collected and used to enhance the radiation to the upper half of the space above the antenna. Consequently, the AMC within its in-phase band will work with the antenna placed above it with a reasonably close distance, but not all the energy will be reflected and used to enhance the antenna's performance.

However, when it comes to the discussion of why the AMC tested with a sourceless plane wave can work with antennas in the reactive near field, the previously discussed models may not be used to explain. In this case, it is still needed to be seen as a complicated structure, consists of metal and dielectric.

As known, in order to make the AMC effective, the distance between the antenna and AMC needs to be very close, ideally 0. On the other hand, the distance needs to be reasonably big to reduce the near field interaction happens between the AMC and the antenna. To know what the proper distance may be, we need to refer to the Distance vs. Region equations of the antennas.

When the distance satisfies this inequality, where D is the largest dimension of the antenna, r is the distance, and λ is the wavelength.

$$r < 0.62\sqrt{D^3/\lambda} \quad (5.4)$$

The AMC is in the reactive near field of the antenna.

And when the distance satisfies this,

$$0.62\sqrt{D^3/\lambda} < r < 2D^2/\lambda \quad (5.5)$$

The AMC is in the radiating near field of the antenna.

To calculate the distance, some parameters are introduced into the discussion. First, the D is defined as 10mm, near the average size of the antennas applied of testing purpose. Meanwhile, the frequency range is selected to be 10GHz - 50GHz, to demonstrate the 5G millimeter wave spectrum and the λ is defined as 30mm - 6mm, correspondingly. Therefore, the thresholds are shown as in the table.

Table 5.1: Thresholds of Distance

Frequencyz	10GHz	50GHz
Reactive Distance	0.174mm	0.05mm
Rediating Distance	6.7mm	3.3mm

In the discussion of AMC, we typically define 3% of λ as "very close", so we have the "very close distances" for 10GHz and 50GHz as 0.9mm and 0.2mm. It is clear that

the distance between the AMC and the antenna will be certainly in the reactive near field. Now we can use the reactive near field equations of the antennas for calculation.

Ideally, frequency independent antenna can be regarded as a combination of a series of dipoles, each operates at a narrow bandwidth. To simplify the discussion, the antenna is represented by a simple dipole antenna placed at the origin and along the z-axis. The transformation is shown as in figure 5.22

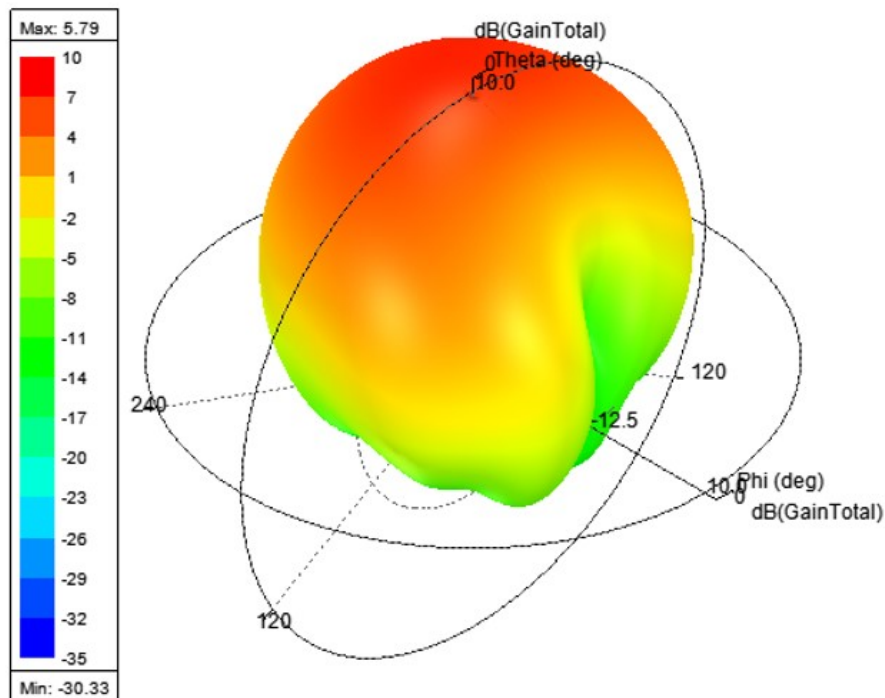


Figure 5.22: Typical 3D Radiation Pattern to Show How AMC Works as a Reflector

Based on the designed structures in the previous section, and modifications necessary for millimeter wave spectrum applied for the 5G techniques in this section. Some examples of the millimeter wave AMCs are shown here. In this part, the AMC is sorted with mushroom and nonmushroom structures. All the AMC units discussed are with a unit sidelength of 0.9mm, and the height of each unit is also 0.9mm, which is the $\lambda/8$ at 41.7GHz. In the purpose of reducing the interaction of reactive near field, the mushroom surface structures used here are not with solid mushroom top patches.

The wired structure of an ax top patch and solid ground, 5.23, has a bandwidth of 72%, 16.63GHz - 34.91GHz.

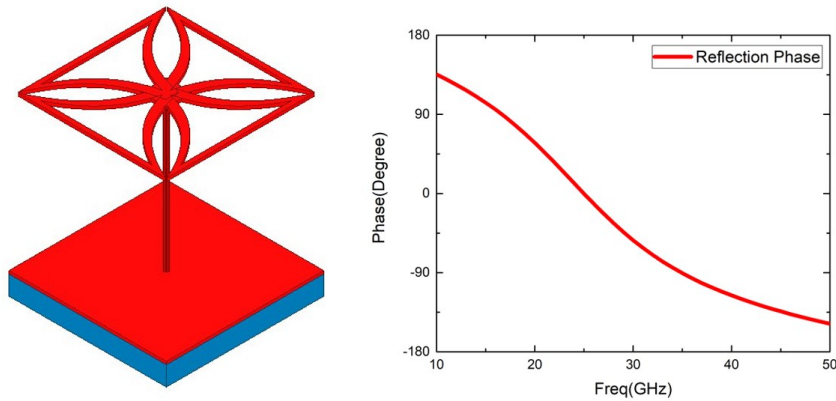


Figure 5.23: Wired Ax Top Millimeter Wave AMC

The wired structure of an axe top patch and a cross ground, 5.24, has a bandwidth of 72%, 16.57GHz - 36.11GHz.

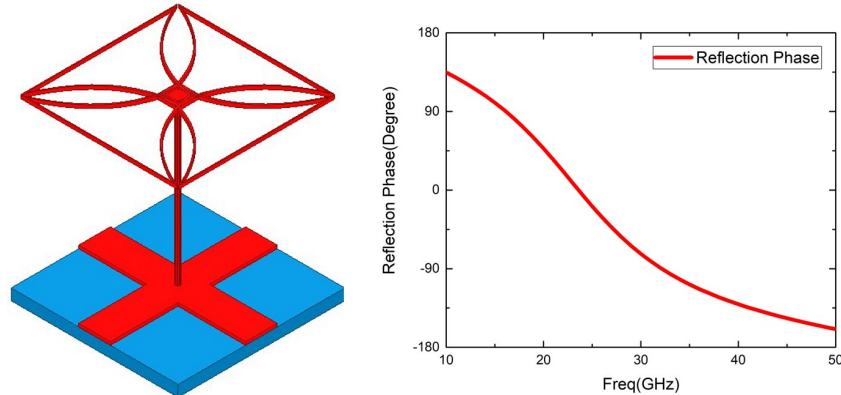


Figure 5.24: Wired Axe Top Cross Ground Millimeter Wave AMC

The wired structure of four spears top patch and a cross ground, 5.25, has a bandwidth of 77%, 18.49GHz - 41.67GHz.

To further reduce the reactive near field interaction and the surface current created by the antenna, and to make the automatic fabrication of the AMC easier, it is best to use nonmushroom surface structure AMC. Meanwhile, when we take the artificial

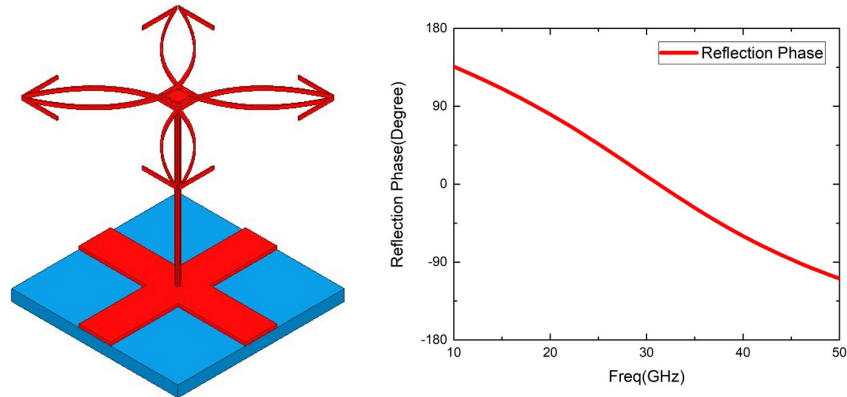


Figure 5.25: Four Spears Top with Cross Ground Millimeter Wave AMC

atom model into consideration, it is realized that this structure is, literally mimics a Bohr model atom, which explains the origin of electric and magnetic moments.

The vertical crossed rectangular rings structure is a good example, 7.15, the octagon/stop sign shaped metallic part in the middle is used to bring the resonance frequency or 0° crossing frequency down, and it is observed that the -90° crossing point is much higher than 41.7GHz. Therefore, it is calculated that the bandwidth is 60%, 22.39GHz - 41.7GHz. In this model, the rings mimic the orbits of electrons, and the crossed stop sign core represents the atom nucleus.

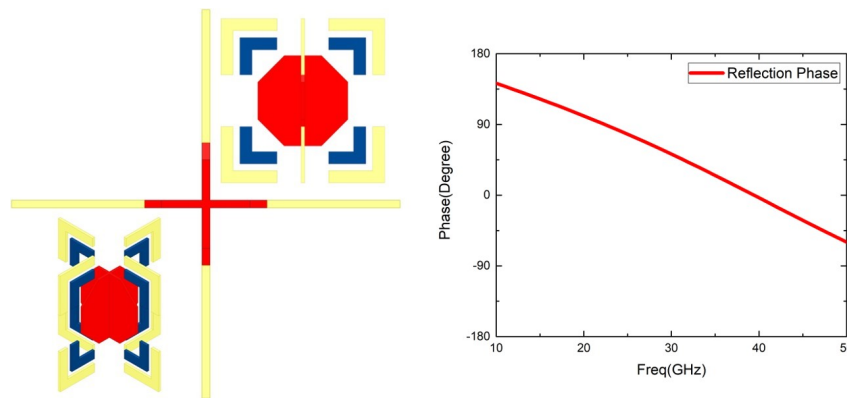


Figure 5.26: Vertical Cross Millimeter Wave AMC

CHAPTER 6: Ultra Wideband Antennas Design and Feeding Methods

6.1 Traditional Rectangular Spiral Antenna

The rectangular frequency independent antennas vary with the bandwidth of operation in our research. However, the principle behind all of them are the same, in this chapter, a prototype [32][31] of rectangular spiral antenna we use is shown as an example, which is a seventeen and a half turns the rectangular planar spiral antenna, as in Figure. 6.2 and Table below[3].

This example spiral antenna works for a wide band of 0.8GH-7GHz and the band needed for later discussion is 1GHz - 5GHz. The Return Loss and E-Plane radiation patterns are shown below. 6.3 6.4

Table 6.1: Parameters for Rectangular Spiral Antenna Prototype

Parameter	Value(unit)
Gap Width	1.8mm
Trace Width	1.2mm
Number of turns	17.5
Substrate Material	FR4
Substrate Dielectric Constant	4.4
Substrate Thickness	1.5875mm

6.2 Varieties of Feeding Method

Theoretically, the simplest way of feeding the rectangular spiral antenna is to solder the outer conductor of a coax cable to one arm of the antenna and inner conductor to the other arm. To simplify the later discussion, we name this feeding method as "Direct Coax". Despite the advantages the Direct Coax method has, it is not that practical for now. It has at least two problems: 1. Impedance matching problem.

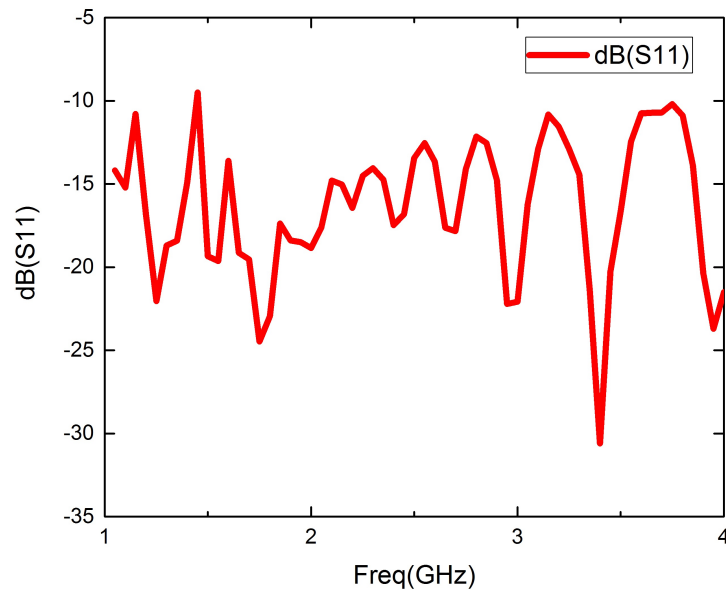


Figure 6.1: Return Loss of the Rectangular Spiral Antenna over the Mushroom Surface

The impedance of typical measurement systems used nowadays is 50Ω . However, the impedance of the Direct Coax is bigger than 100Ω , a very big impedance mismatch will occur. 2. Fabrication problem. If we strictly follow the simulation structure during fabrication, the diameter of the coax needed will be very, very thin, best to be 1.2mm. The inner conductor will be even thinner (about 100um). It is very difficult to solder both the inner and outer conductors to the spiral antenna. As a result, it is necessary to figure out other feeding methods.

Feeding methods presented here are three most promising one, structure and the radiation patterns are shown in figures attached. The feeding methods are named as: A. Vertical Transformer, B. Integrated Transformer, C. Full Add-on Layer.

A. Vertical Transformer

Vertical Transformer is a design in which the antenna is fed with an FR4 Stripline Transformer placed perpendicularly to the plane of the antenna. Figure.(6.5). Radi-

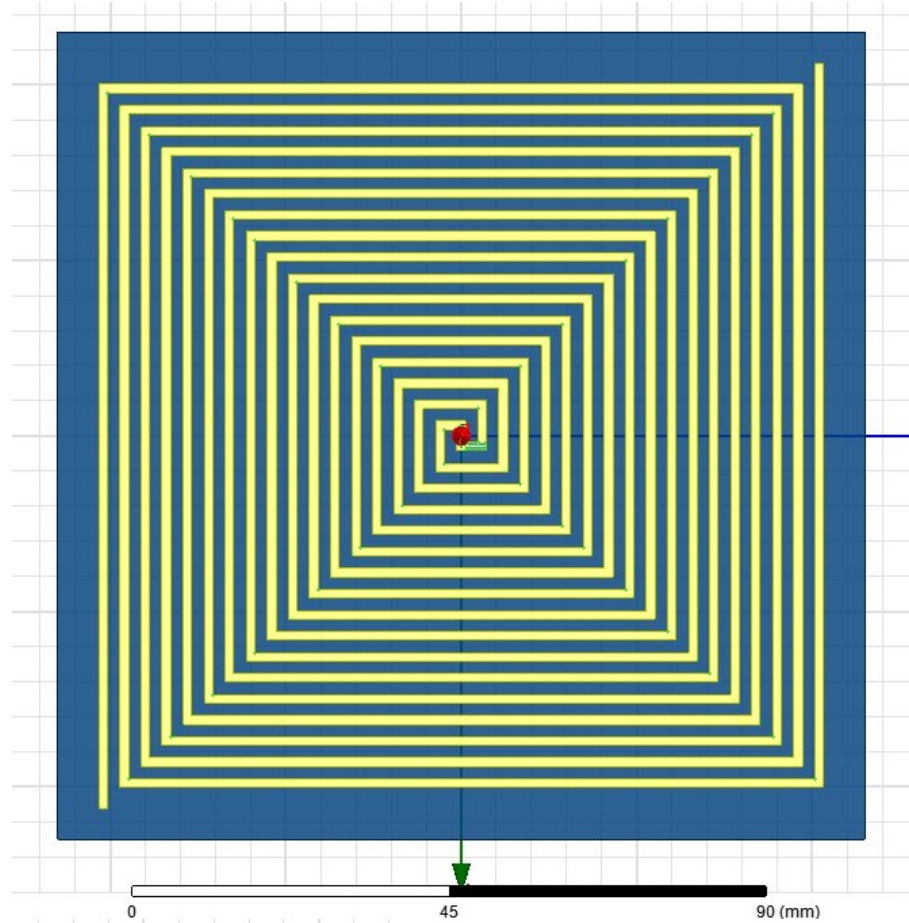


Figure 6.2: Rectangular Planar Spiral Antenna

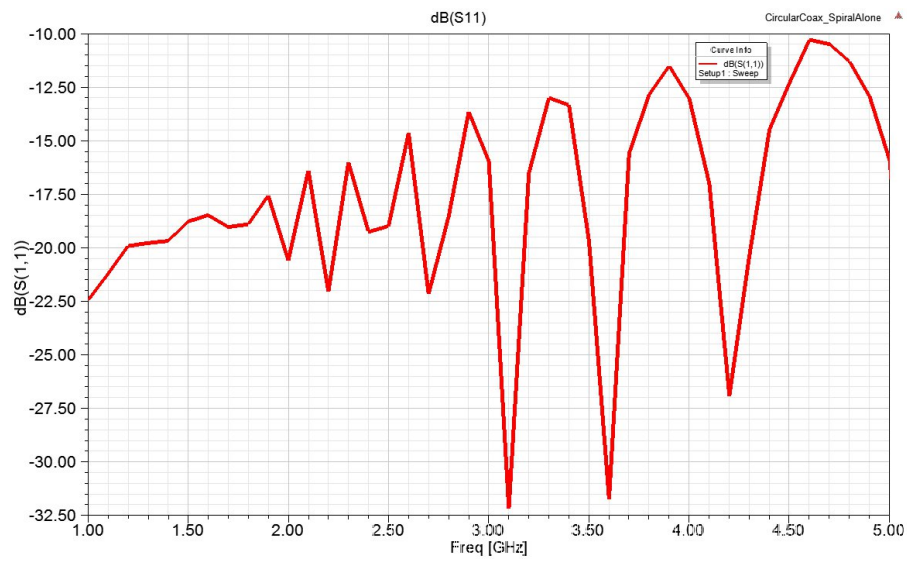


Figure 6.3: Rectangular Planar Spiral Antenna Return Loss

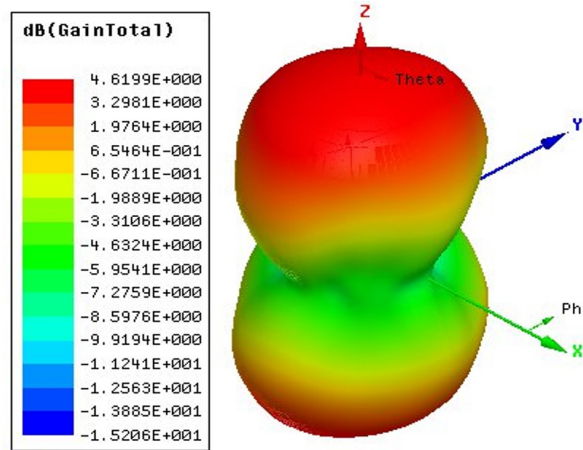


Figure 6.4: 3D Radiation Patterns of 3.5GHz

ation patterns are plotted as Figure. (6.6), with and without the mushroom surface AMC. A serious problem we can observe it that the radiation patterns are not that balanced.

B. Integrated Transformer

Integrated Transformer is a design in which a few turns in the middle of the spiral antenna[37] are removed. The space left is then occupied by a dual layer paired strip[35][36] transformer[43]. In this design, the feed line consists of two parts, the direct connection line, and the paired strip transformer, and they intersect. Figure.(6.7). Radiation patterns are plotted as Figure. (6.8), with and without the AMC mushroom surface. The radiation patterns of this method indicate that on H-Plane, the radiation is much narrower than that of the E-Plane when there is no mushroom surface AMC. Another problem occurs here is a relatively too strong side lobe. Those problems may come from the impedance mismatch, which can be improved in the future.

C. Full Add-on Layer

From the radiation patterns of the Integrated transformer, it can be observed that the radiation is not balanced. As a result, we come up with the Full Layer on Top

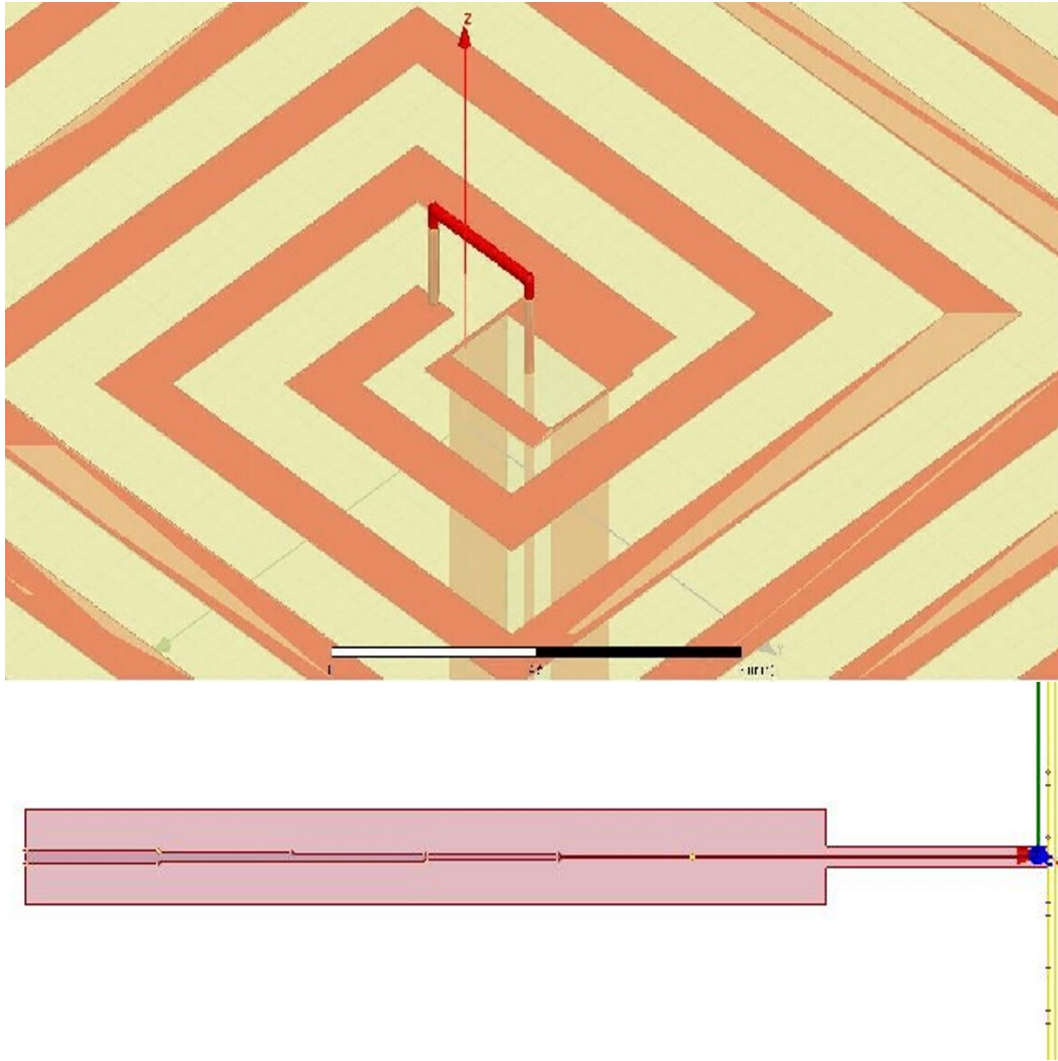


Figure 6.5: Vertical Transformer Design

design.

Full Layer on Top is a design with which we try to preserve the advantages of both the design above and get rid of their disadvantages. The Vertical Transformer design is perfectly balanced. However, the radiation pattern indicates some "leakage" of the input power, this leakage is caused by the radiation of the long transformer. Meanwhile, it's also difficult to fabricate and requires some human labor. The Integrated Transformer Design is easier to fabricate, but the radiation is not balanced.

Therefore, in this design, we add an extra PCB Layer with all the traces turns removed from the spiral antenna. Those removed turns are later connected back to

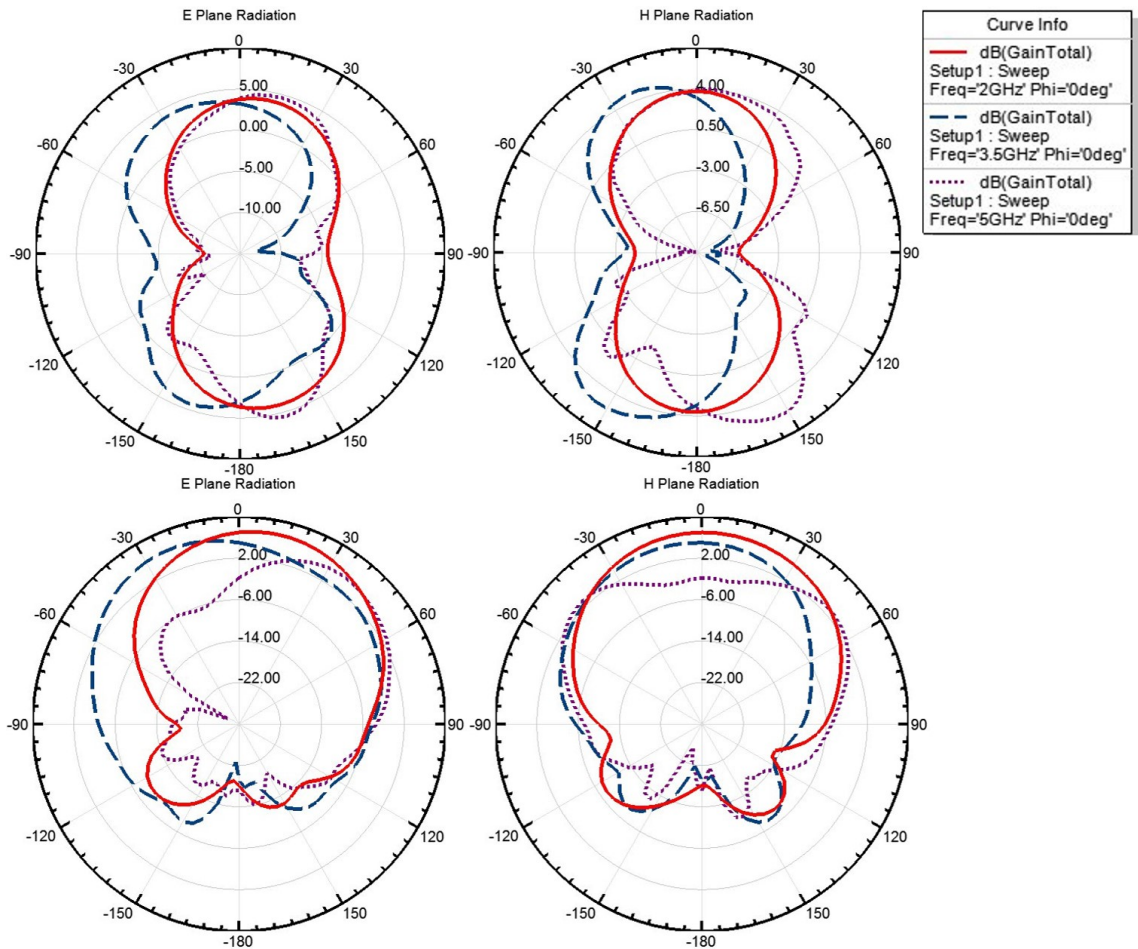


Figure 6.6: Vertical Transformer Radiation Pattern With/Without AMC Mushroom Surface

the bottom layer with the other part of the spiral. The paired strips of this design are almost the same as in the previous design of Integrated Transformer. Figure.(6.9. Radiation patterns are plotted as Figures, with and without the AMC.(6.10)

As predicted by theory, when adding the removed spiral trace turns back using an extra piece of PCB, the radiation patterns become more balanced. Side lobes also decreased, especially when integrated with the mushroom AMC. However, the gains are still not as good as they should be, which is a result of possible impedance mismatch to be improved in future.

6.3 Offset Dual Layer Spiral Antennas

Unfortunately, all of the feeding methods mentioned above have some same issue:

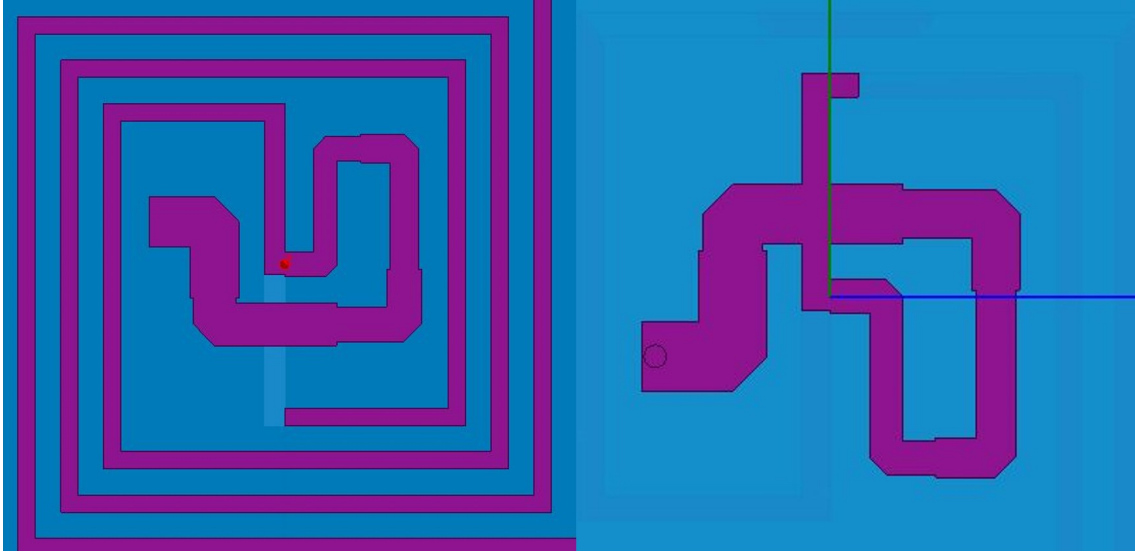


Figure 6.7: Integrated Transformer Design

1. All of them require extra work in the fabrication procedure.
2. All of the feeding methods disturb the field distribution when the AMC is not in present.
3. The feeding methods are not universally transplantable, each application for difference bandwidth will require the design to be repeated all over again.

The conclusion of the discussion above is clear now, that is, the best way of feeding the spiral antenna when it integrates with the AMC structure is to make the impedance of the antenna itself to be 50Ω . Inspired by the Full-Layer-On-Top design and the work of our labmate Dip [5]'s work of "Offset Archimedian Circular Spiral Antennas", we designed the Offset Dual Layer Spiral Antennas, which have the following advantages.

1. Easy to simulate and fabricate, all the work need it to move one entire arm of the spiral antenna into the other side of the substrate.
2. The impedance is tunable, within a reasonable range of the thickness of the substrate, which is the Z-axis distance between the two arms, reducing the thickness reduces the impedance, while increasing the thickness makes the impedance higher.
3. The feeding structure required is only a 50Ω coax cable, which comes in all

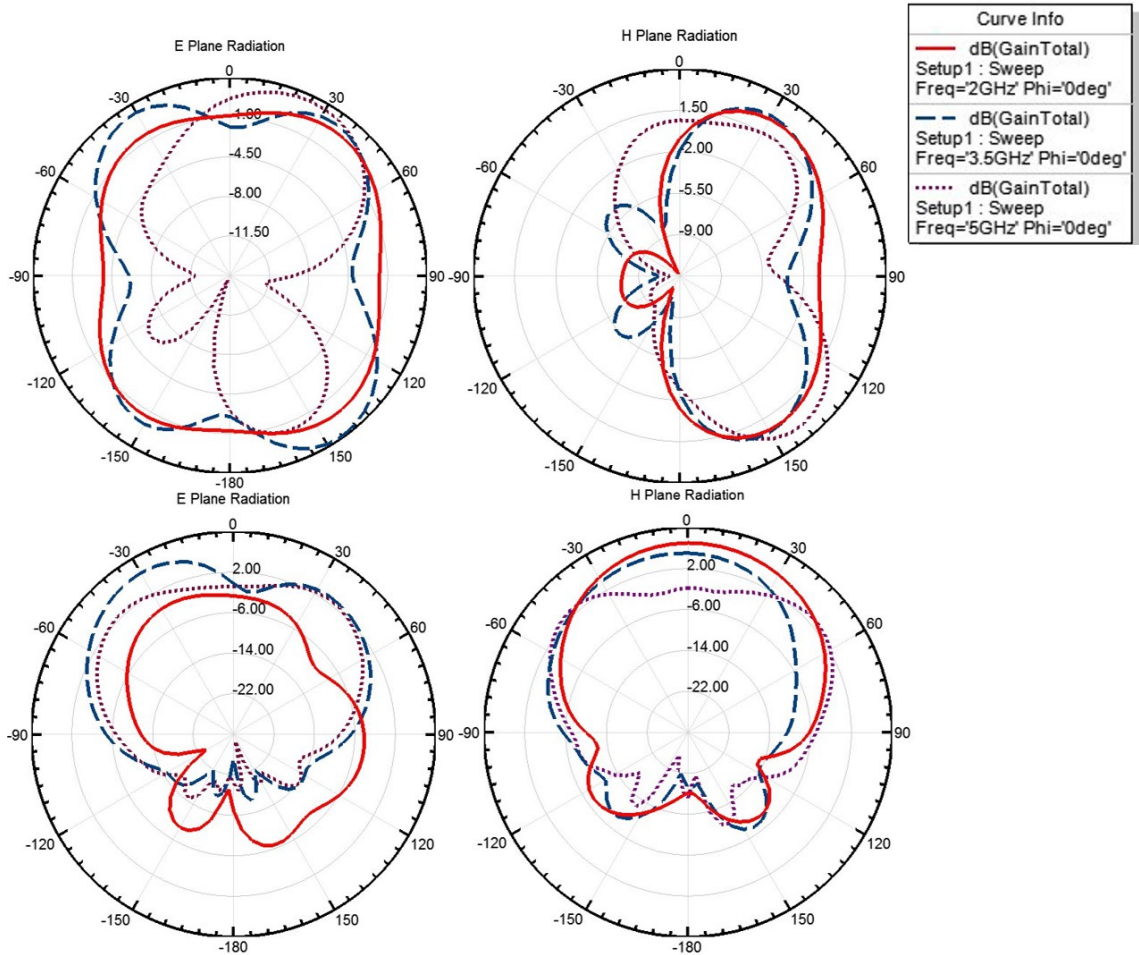


Figure 6.8: Integrated Transformer Radiation Pattern With/Without AMC Mushroom Surface

different sizes and also simple to customize with any desired dimensions.

4. The idea is transplantable, as shown in the following part, we successfully use this idea to feed the rectangular spiral antennas.

6.3.1 Example of Offset Dual Layer Spiral Antennas

Parameters of the offset dual layer circular spiral antennas are listed in the following table. Mark that here the "gap width" means the distance between "adjacent" traces on the XOY plane, though they have different Z coordinates. If we still want to know the distance between adjacent traces on each side, it is calculated by:

$$\text{Single Side Gap Width} = \text{Trace Width} + 2 \times \text{Gap Width}.$$

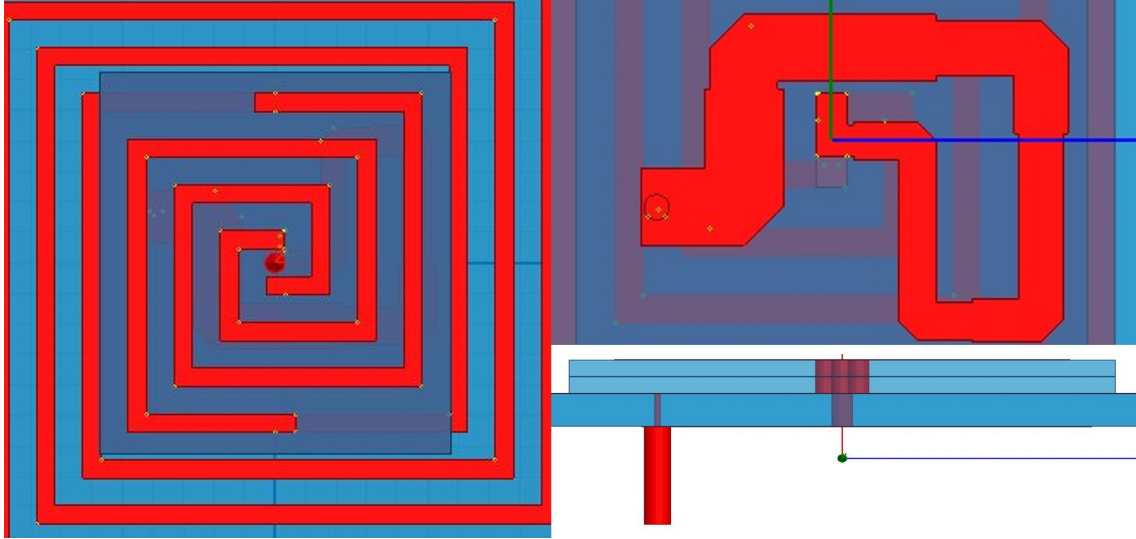


Figure 6.9: Full Layer on Top Transformer Design

Therefore, this gap width can be as small as 0, and can even be set to negative to allow a much wider range of input impedance tuning.

Table 6.2: Parameters for Offset Dual Layer Circular Spiral Antenna

Parameter	Value(unit)
Gap Width	0mm
Trace Width	0.25mm
Number of turns	12.9
Substrate Material	RO4350
Substrate Dielectric Constant	3.66
Substrate Thickness	0.132mm

The structure of the offset dual layer spiral antenna is shown as in 6.2 and, the spiral traces on top are slightly different from those on the bottom in color, the top traces are red, while the bottom traces are blue.

In 6.12, the feeding method is shown with the coax cable highlighted(not necessarily in scale), and since the cable is perpendicularly connected to the offset dual layer spiral antenna, the choice of coax cable is flexible. We select the same ideal coax cable as we used for the rectangular one to demonstrate.

When the offset dual layer circular spiral antenna operates by itself, we have the

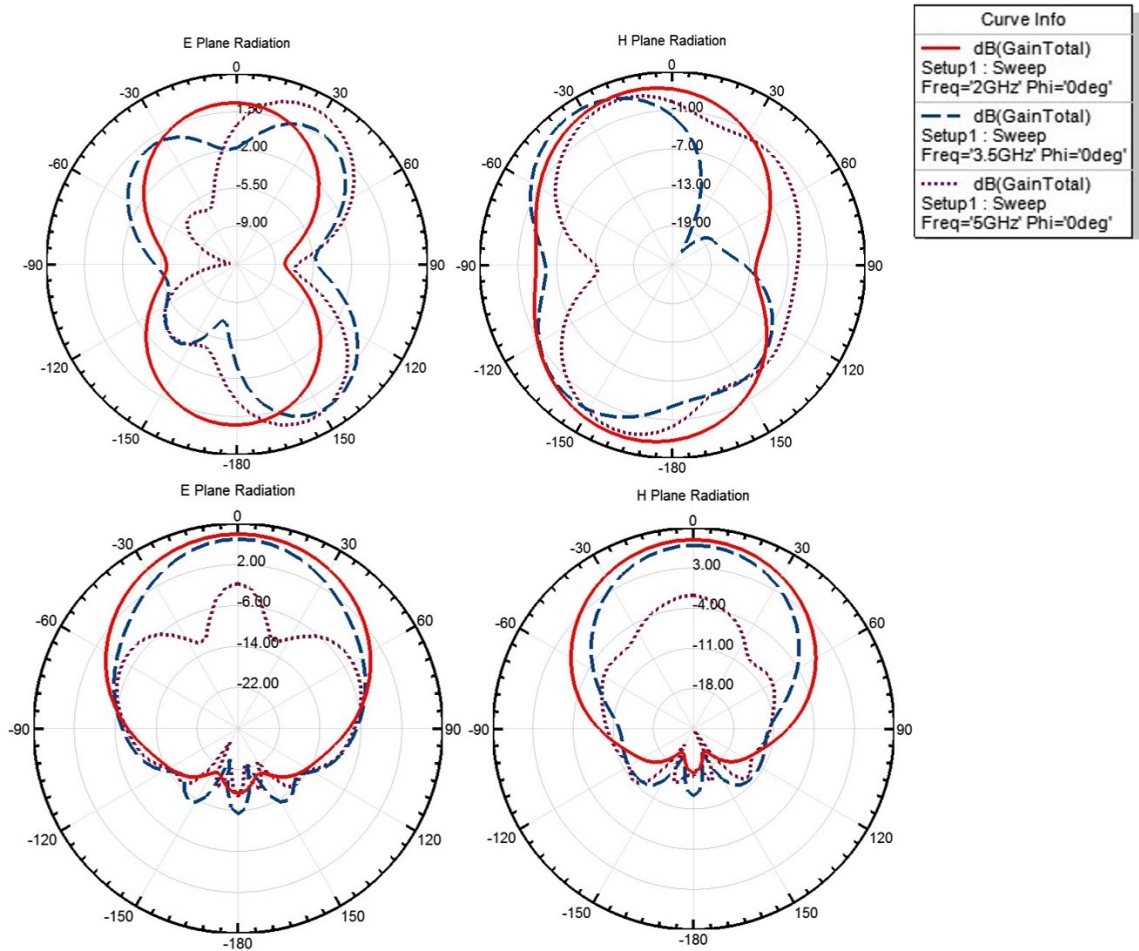


Figure 6.10: Full Addon Layer on Top Radiation Pattern With/Without AMC Mushroom Surface

return loss plotted as in 6.13. The 3D radiation pattern is also plotted as in 6.15 at 30 GHz, to show that the offset dual layer spiral antenna has a relatively balanced radiation pattern when there is no balun used. The return loss figure also shows the bandwidth of 10GHz to 50GHz, which is sufficient for our research.

6.3.2 Offset Dual Layer Rectangular Spiral Antenna

Similarly, the parameters of the rectangular offset dual layer spiral antenna are listed in the following table. Mark that here the "gap width" means the distance between "adjacent" traces on the XOY plane, though they have different Z coordinates. If we still want to know the distance between adjacent traces on each side, it

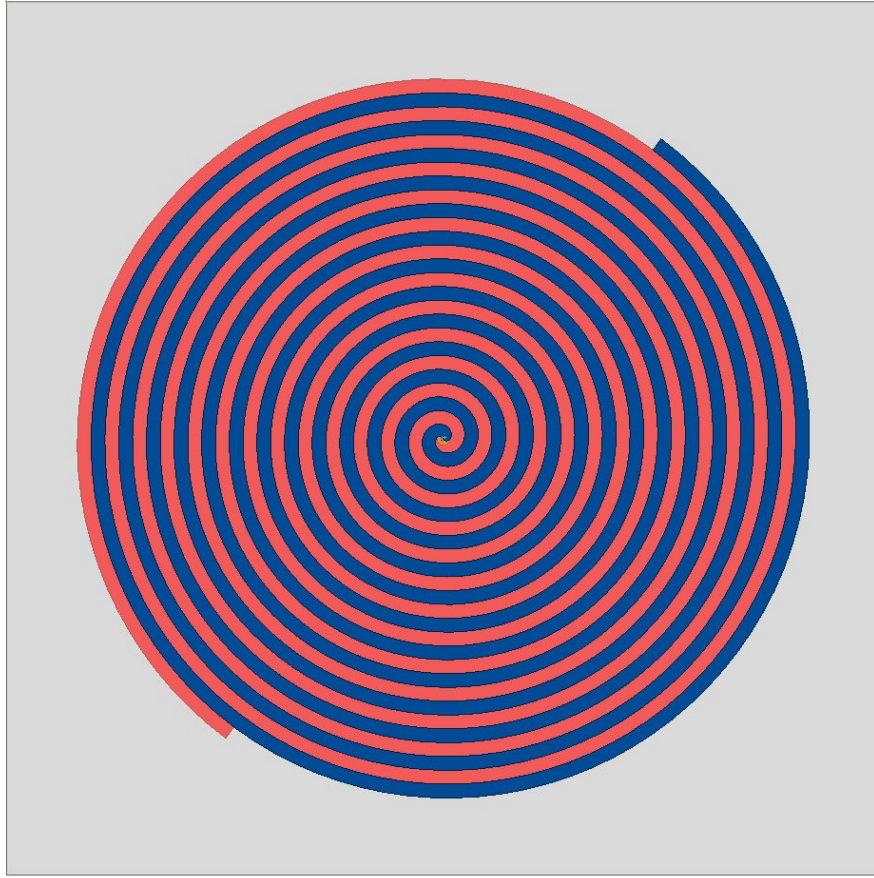


Figure 6.11: Millimeter Wave Offset Dual Layer Circular Spiral Antenna

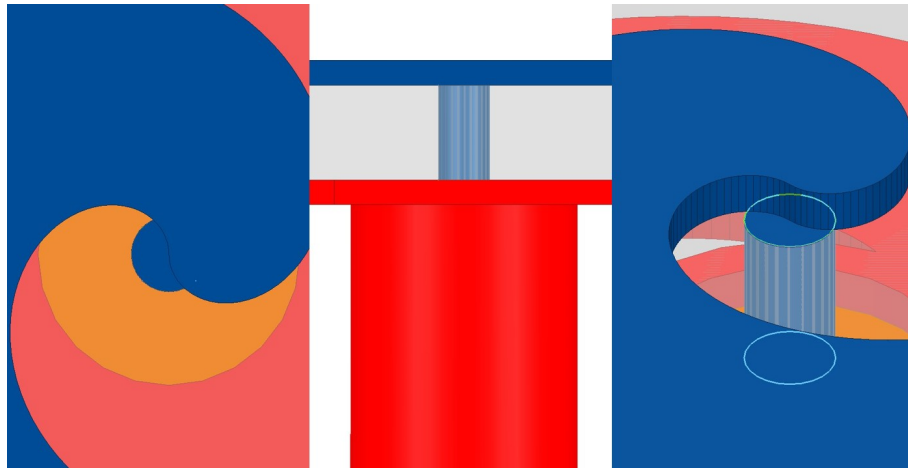


Figure 6.12: Offset Dual Layer Circular Spiral Antenna Fed with Perpendicular Coax Cable

is calculated by:

$$\text{Single Side Gap Width} = \text{Trace Width} + 2 \times \text{Gap Width}.$$

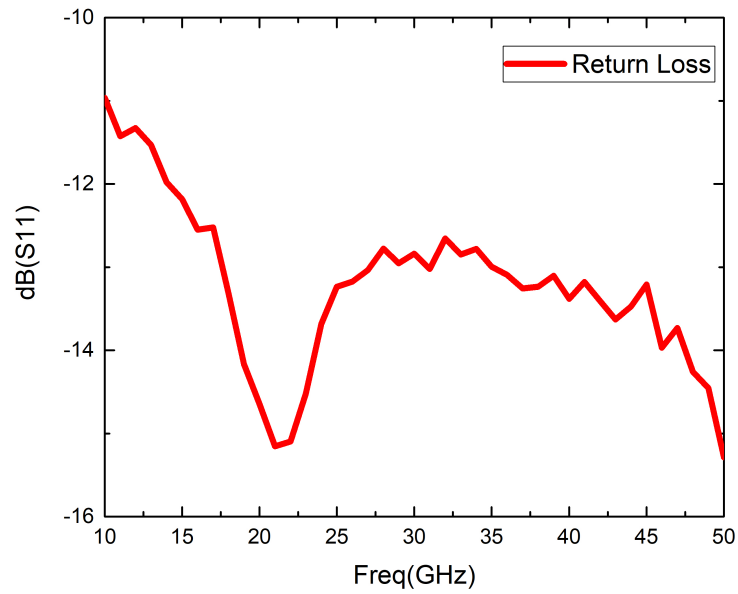


Figure 6.13: Return Loss of the Millimeter Wave Offset Dual Layer Circular Spiral Antenna

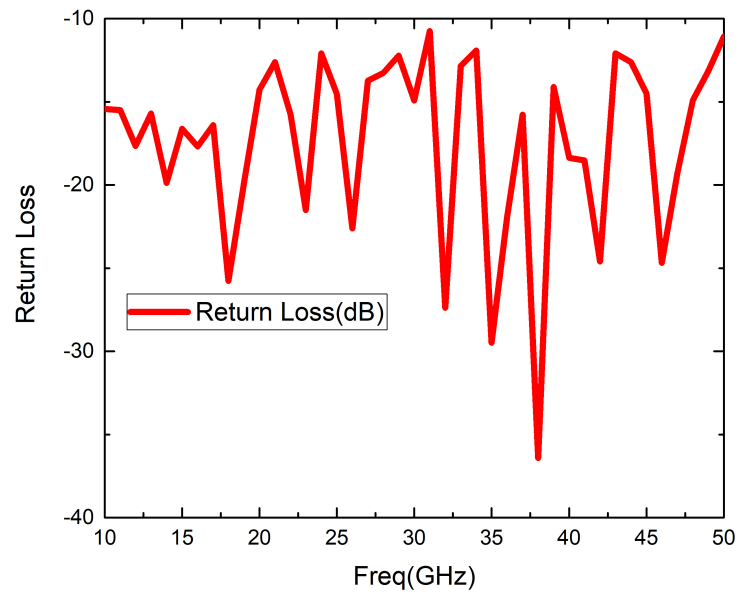


Figure 6.14: Return Loss of the Offset Dual Layer Rectangular Spiral Antenna

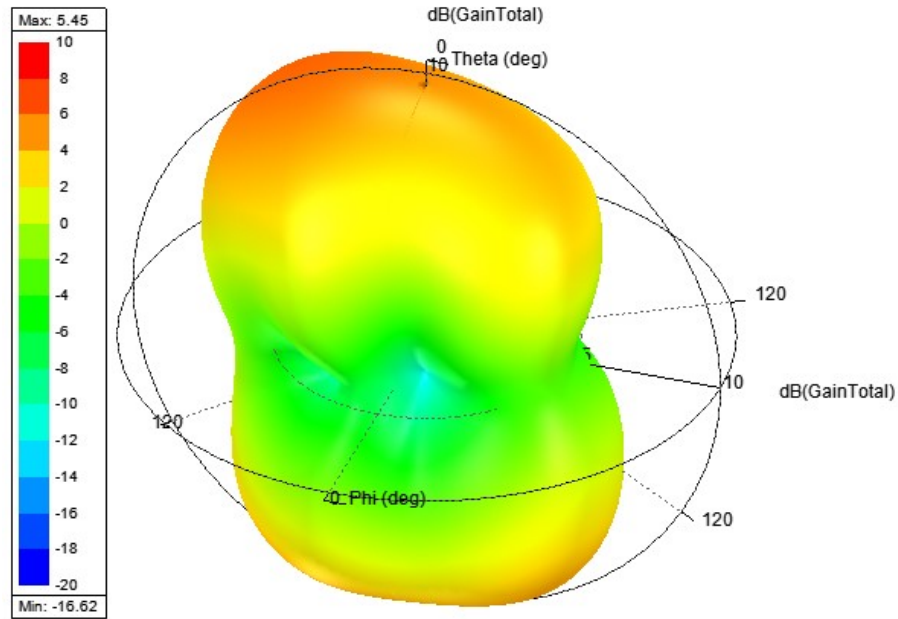


Figure 6.15: Circular 3D Radiation Patterns of the Millimeter Circular Spiral Antenna at 30GHz

Therefore, this gap width can be as small as 0, and can even be set to negative to allow a much wider range of input impedance tuning.

Table 6.3: Parameters for Offset Dual Layer Rectangular Spiral Antenna

Parameter	Value(unit)
Gap Width	0.01mm
Trace Width	0.2mm
Number of turns	17.5
Substrate Material	RO4350
Substrate Dielectric Constant	3.66
Substrate Thickness	0.11mm

The structure of the offset dual layer spiral antenna is shown as in 6.16, the spiral traces on top are slightly different from those on the bottom in color, the top traces are red, while the bottom traces are blue.

In 6.17, the feeding method is shown with the coax cable highlighted(not necessarily in scale), and since the cable is perpendicularly connected to the offset dual layer spiral

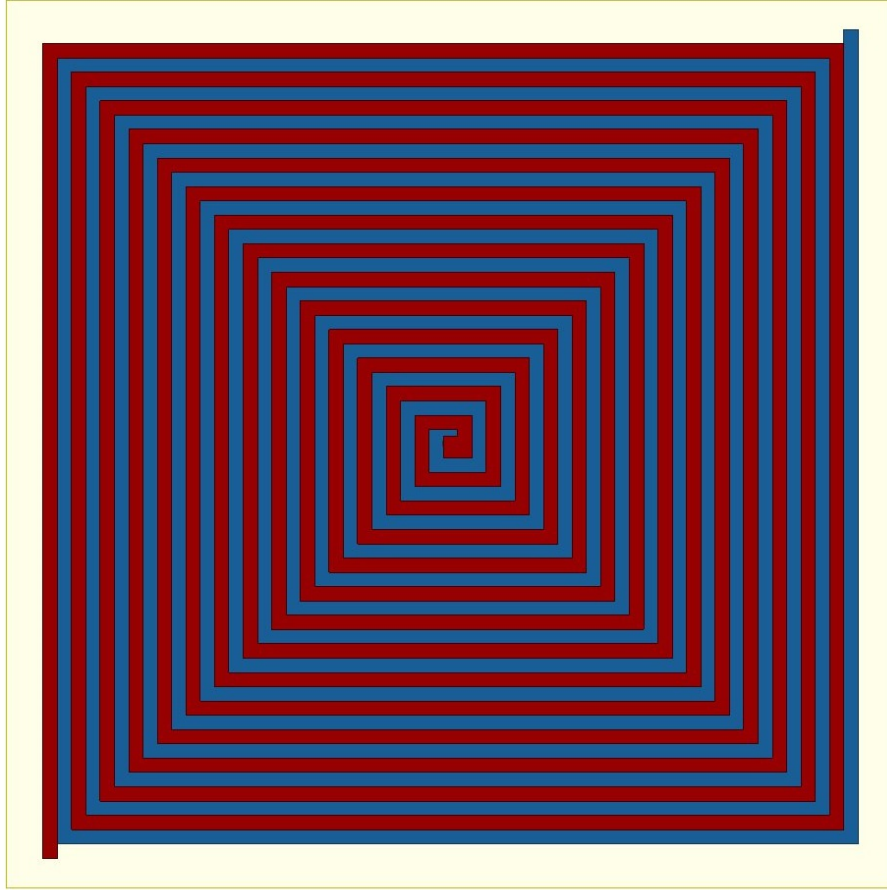


Figure 6.16: Millimeter Wave Offset Dual Layer Rectangular Spiral Antenna

antenna, the choice of coax cable is flexible. We select an ideal coaxial to demonstrate in the simulation.

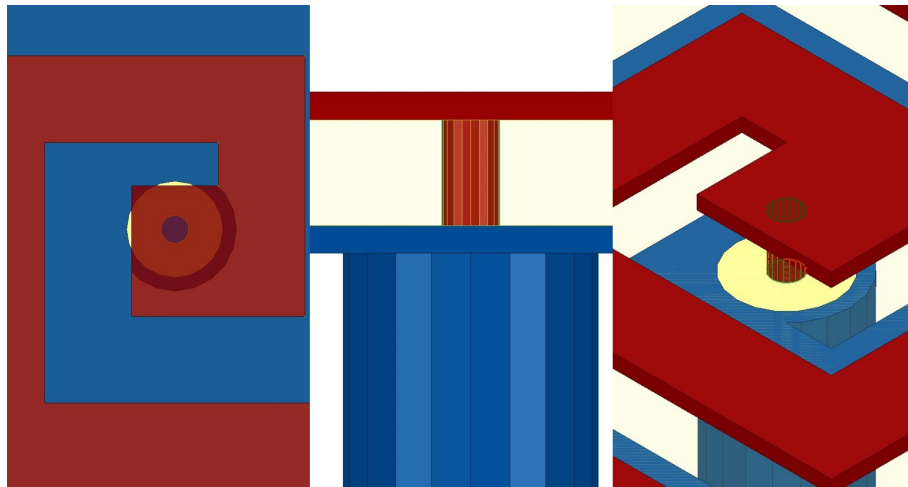


Figure 6.17: Rectangular Spiral Antenna Fed with Perpendicular Coax Cable

When the offset dual layer rectangular spiral antenna operates by itself, we have the return loss plotted as in 6.14. The 3D radiation pattern is also plotted as in 6.18 at 25GHz, from which we can see that the offset rectangular dual layer spiral antenna has a balanced radiation pattern when there is no balun used.

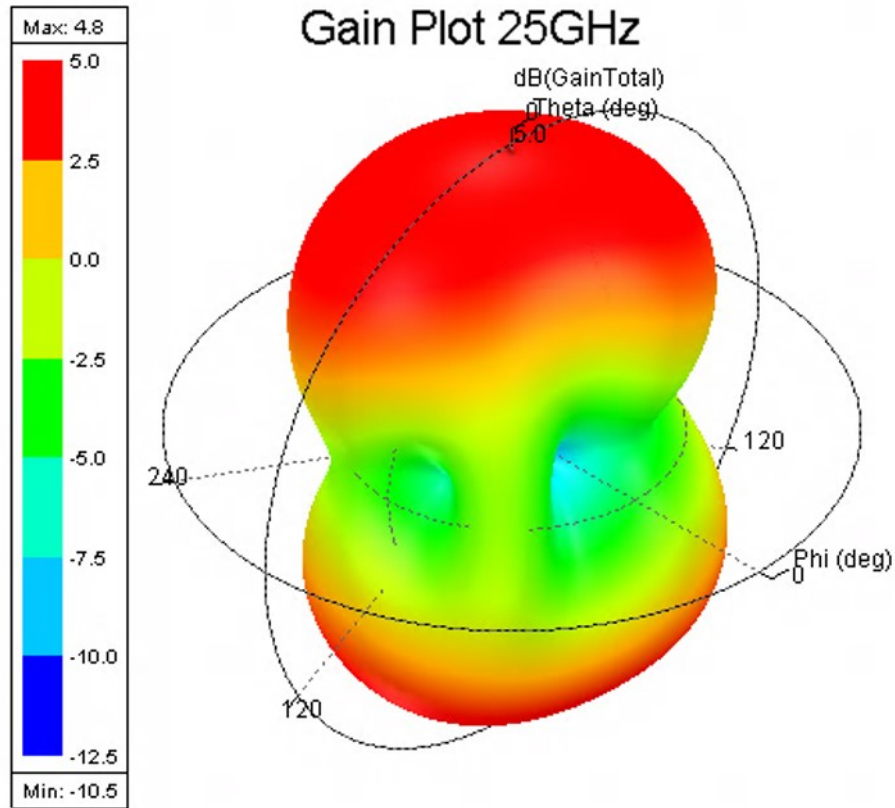


Figure 6.18: 3D Radiation Patterns of The Offset Rectangular Dual Layer Spiral Antenna

6.4 Results and Conclusion

When all the parts discussed previously are combined together, we have the UWB AMC Antenna System (Antenna System) to in figure 6.19 and 6.20

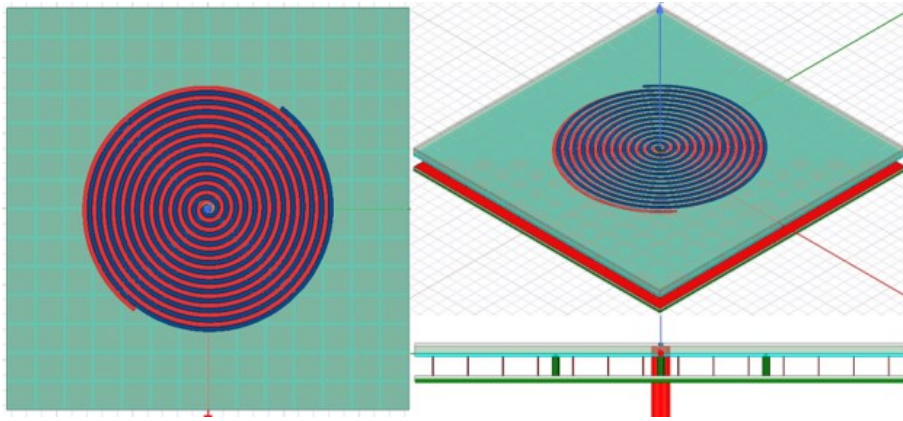


Figure 6.19: Offset Dual Layer Circular Antenna System Three View

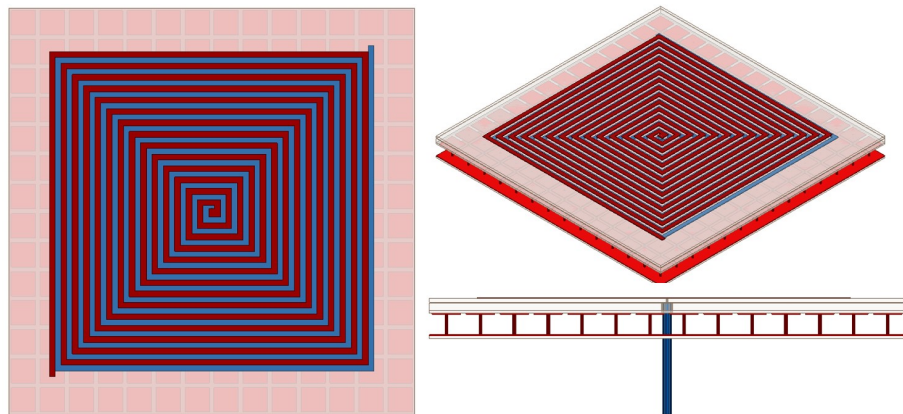


Figure 6.20: Offset Dual Layer Circular Antenna System Three View

CHAPTER 7: Ultra Wideband Antenna for 5G Millimeter Spectrum with AMC

7.1 Ultra Wideband Antenna for 5G Millimeter Spectrum

In this chapter, the ultra wideband antennas are presented base on the antenna discussed in the previous chapter. To design the millimeter wave antennas, the width of antenna traces as well as the thickness of the substrate need to be small, and may not to scale, meanwhile, to work with the 5G millimeter wave AMCs, the distance between the antenna and the AMC also needs to be closely compared that simply scaled, the spiral antennas are assumed to feed with 50Ω coax lines, and they can be easily changed with any other 50Ω feeding method, especially when designed as one single chip. Another very important characteristic of the antennas is the substrate, FR4 cannot running smoothly beyond 10GHz, as a result, the RO4350 by Rogers Company is selected to be the substrate of the antennas. From the data presented below, it is observed that the performance of the circular structure antenna is more stable than that of the rectangular structure. 7.1,7.2

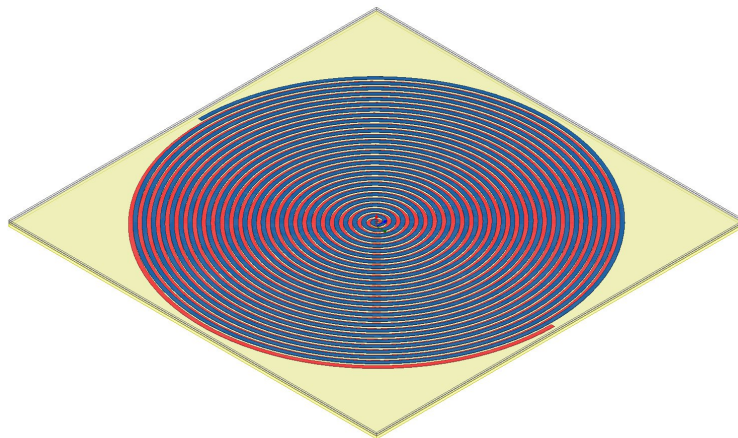


Figure 7.1: 5G Millimeter Wave Circular Spiral Antenna

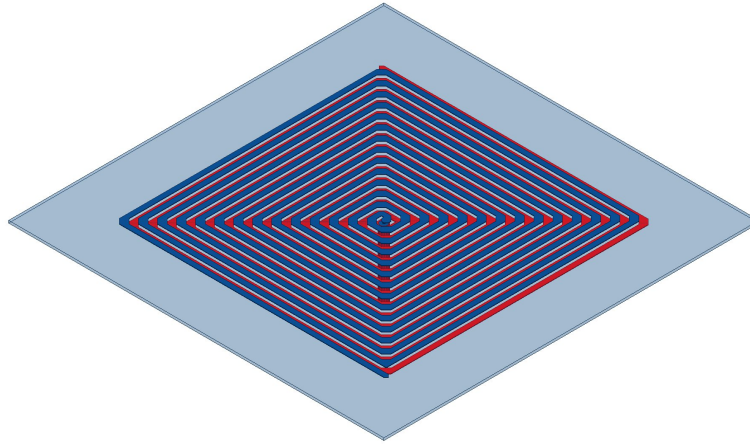


Figure 7.2: 5G Millimeter Wave Rectangular Spiral Antenna

7.1.1 Circular Millimeter Wave Antenna

The design Parameters, the return loss 7.3, and the impedance are shown as below 7.4, as well as the selected gains of 10GHz - 50GHz, with a step length of 10GHz, 7.5.

Table 7.1: Parameters for Offset Dual Layer Rectangular Spiral Antenna

Parameter	Value(unit)
Gap Width	0mm
Trace Width	0.167mm
Number of turns	27
Substrate Material	RO4350
Substrate Dielectric Constant	3.66
Substrate Thickness	0.066mm

7.1.2 Rectangular Millimeter Wave Antenna

The design Parameters, the return loss, and the impedance are shown as below. We encounter a new problem while designing the offset dual layer rectangular millimeter wave spiral antennas. The 90° turning is too sharp for the millimeter waves, and sometime may even cause unwanted resonance. As a result, the corners are chamfered. 7.6 and the impedance are shown as below 7.7, as well as the selected gains of 10GHz - 50GHz, with a step length of 10GHz, 7.8

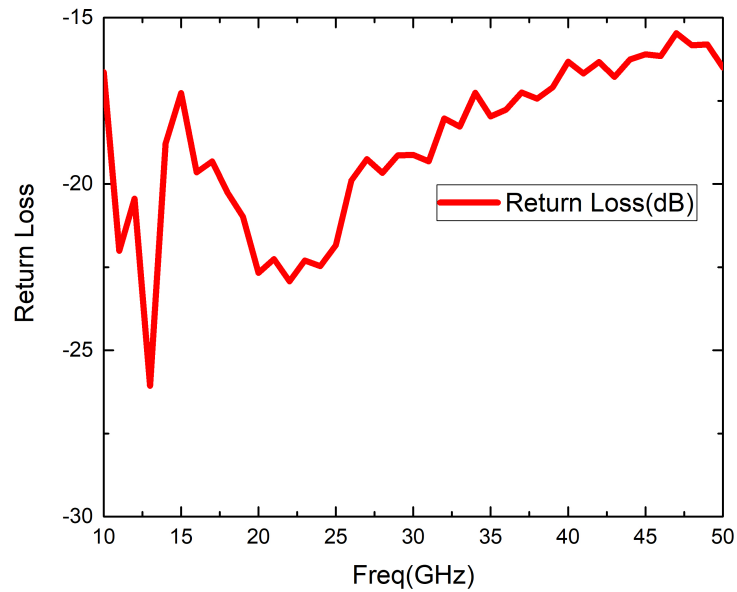


Figure 7.3: Return Loss of Millimeter Wave Circular Spiral Antenna

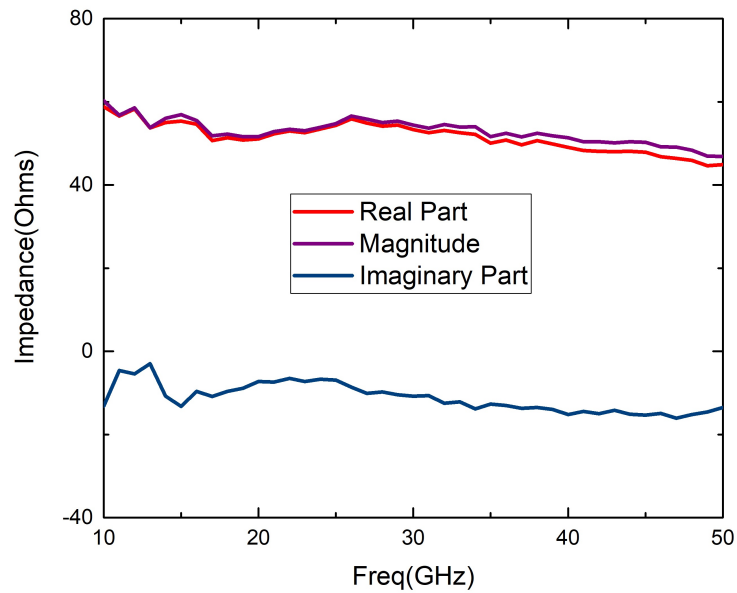


Figure 7.4: Impedance of Millimeter Wave Circular Spiral Antenna

7.1.3 Spiral Antennas with 5G Millimeter Wave AMCs

In this part, each different design of the AMC is presented with the unit view and the phase of reflection. When integrated with the antennas, the return loss and

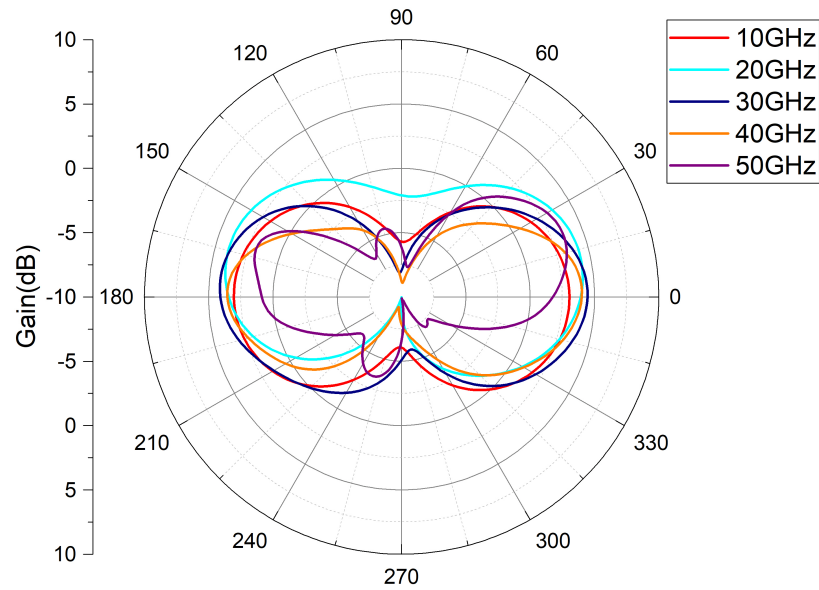


Figure 7.5: Gain of Millimeter Wave Circular Spiral Antenna 10GHz - 50GHz

Table 7.2: Parameters for Offset Dual Layer Rectangular Spiral Antenna

Parameter	Value(unit)
Gap Width	0mm
Trace Width	0.16mm
Chamfered Radius	0.16mm
Substrate Material	RO4350
Substrate Dielectric Constant	3.66
Substrate Thickness	0.08mm

typical radiation patterns are shown, to prove the AMC enhances the gain in given directions.

Previously the AMC units are demonstrated with plane waves, in order to prove that they are still functional when interacted with the antennas. We use a simple antenna model for analyzing purpose.

The electromagnetic fields in this region can be calculated with the equations given below. [32] These equations are applied here to describe how strong the interaction

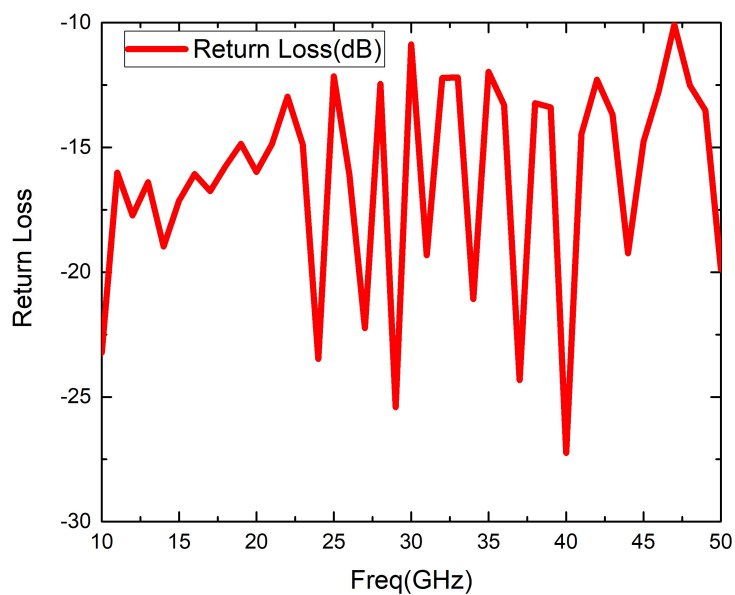


Figure 7.6: Return Loss of Millimeter Wave Chamfered Rectangular Spiral Antenna

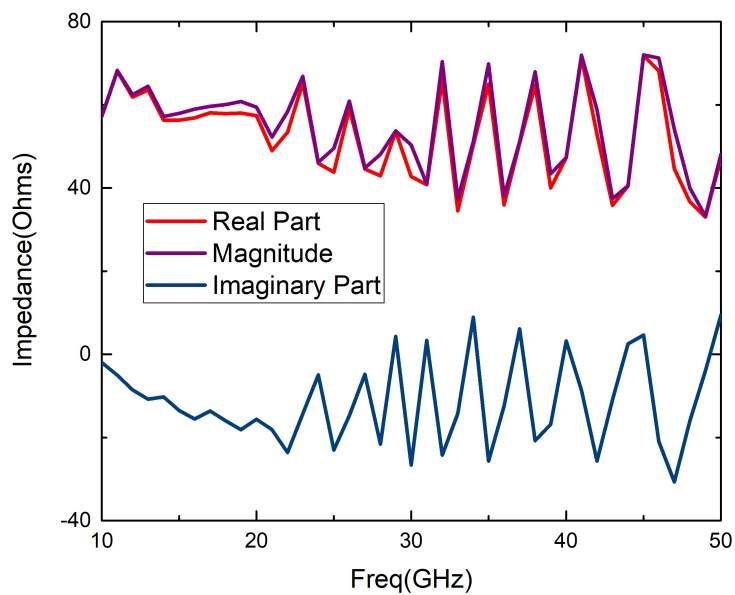


Figure 7.7: Impedance of Millimeter Wave Chamfered Rectangular Spiral Antenna

between the antenna and anything placed near it.

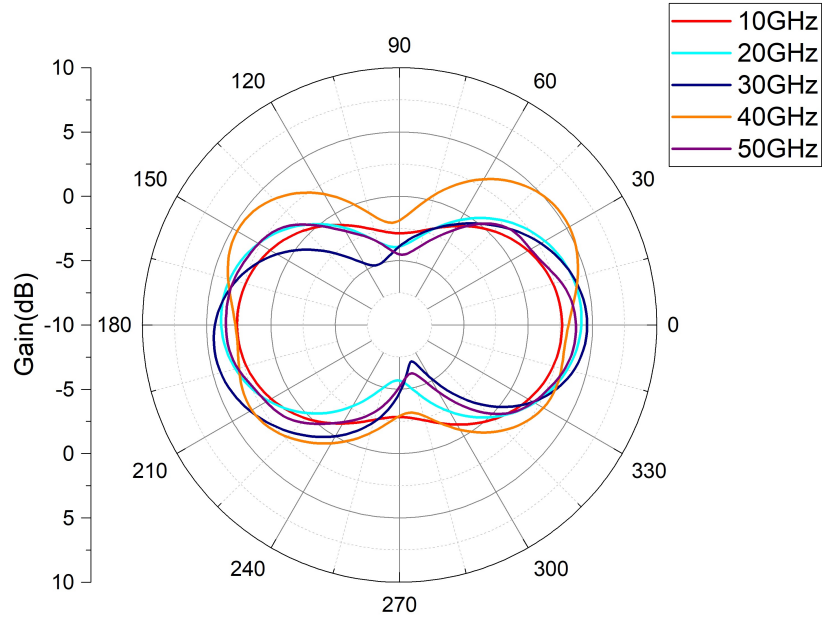


Figure 7.8: Gain of Millimeter Wave Chamfered Rectangular Spiral Antenna 10GHz - 50GHz

$$E_r = 60\beta^2 Idz \left[\frac{1}{(\beta r)^2} - \frac{j}{(\beta r)^3} \right] \quad (7.1)$$

$$E_\theta = j30\beta^2 Idz \left[\frac{1}{\beta r} - \frac{j}{(\beta r)^2} - \frac{1}{(\beta r)^3} \right] \quad (7.2)$$

$$H_\phi = j30\beta^2 Idz \left[\frac{1}{\beta r} - \frac{j}{(\beta r)^2} \right] \sin\theta e^{-j\beta r} \quad (7.3)$$

$$E_\phi = H_r = H_\theta = 0 \quad (7.4)$$

In these equations, r is the distance to the observation point. The current input is assumed to be a time-varying sin wave with a fixed frequency. In the discussion of AMC, now we only need to consider the E fields. The equations for the r and θ become.

$$E_r = 60Idz\left[\frac{1}{r^2} - \frac{j}{\beta r^3}\right] \quad (7.5)$$

$$E_\theta = j30Idz\left[\frac{\beta}{r} - \frac{j}{r^2} - \frac{1}{\beta r^3}\right] \quad (7.6)$$

As shown in the equations above, β is the wave number, which is fixed for a given frequency. Therefore, it is observed that the E fields are dominated by the item with $(1/r^3)$ in the reactive near field of the antenna, and when the distance r increases only a little bit, the field decreases dramatically. For example, when r increases from 0.01λ to 0.02λ and the current is 1 unit. The change of the E fields are shown as (with $\beta = 2\pi/\lambda$)

For $r = 0.01\lambda$

$$E_r(r = 0.01\lambda) = \frac{6 \times 10^5 Idz}{2\pi\lambda^2} (2\pi - 10^2 j) \quad (7.7)$$

$$E_\theta(r = 0.01\lambda) = \frac{j30Idz}{2\pi\lambda^2} (4 \times 10^2 \pi^2 - 10^4 j 2\pi - 10^6) \quad (7.8)$$

For $r = 0.02\lambda$

$$E_r(r = 0.02\lambda) = \frac{6 \times 10^3 Idz}{2\pi\lambda^2} (5\pi - 125j) \quad (7.9)$$

$$E_\theta(r = 0.02\lambda) = \frac{j30Idz}{2\pi\lambda^2} (2 \times 10^2 \pi^2 - 5 \times 10^3 \pi j - 1.25 \times 10^5) \quad (7.10)$$

To make a comparison, we need to drop the items that are not dominating, therefore we have

$$E_r(r = 0.01\lambda) \approx -j6 \times 10^7 Idz / 2\pi^2 \lambda^2$$

$$E_r(r = 0.02\lambda) \approx -j7.5 \times 10^5 Idz / 2\pi^2 \lambda^2,$$

and

$$E_\theta(r = 0.01\lambda) \approx -j3 \times 10^7 Idz / 2\pi \lambda^2$$

$$E_{\theta}(r = 0.02\lambda) \approx -j3.75 \times 10^6 Idz / 2\pi^2 \lambda^2$$

Consequently, the values are,

$$\frac{E_r(r = 0.02\lambda)}{E_r(r = 0.01\lambda)} \approx 0.0125 \quad (7.11)$$

and

$$\frac{E_{\theta}(r = 0.02\lambda)}{E_{\theta}(r = 0.01\lambda)} \approx 0.125 \quad (7.12)$$

This calculation proves that a small increase of the distance between the antenna and AMC can greatly reduce the reactive near field effect between them, and therefore, properly adjust the distance can ensure the AMC performance with the antenna.

Meanwhile, the reactive near-field effect DOES influence the impedance of the antenna and causes a frequency shift. When demonstrated with the narrow band antennas, the effect is more obvious. As shown in 7.9, we demonstrate the frequency shift with a wire structure bowtie antenna, with an without a mushroom AMC.

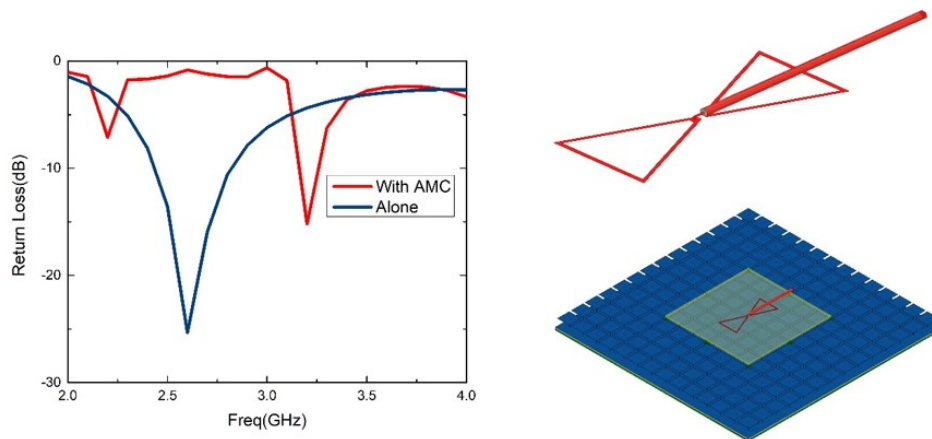


Figure 7.9: Return Loss Comparison for a Wire Bowtie Antenna with and without Mushroom AMC

From this comparison, it is observed that with the reactive near field effect caused by the presence of mushroom AMC, the resonant frequency of the wire bowtie antenna shifts from 2.6GHz to 3.2GHz, which is 23% to the higher end. When the return losses near the resonant frequencies are compared, the impedance of the antenna is worse

matched with the AMC's presence. And at higher frequencies, the difference of return loss with and without the mushroom AMS becomes insignificant. The reason is that the wavelength is shorter for higher frequencies, and the distance between the antenna and AMC are relatively bigger in the aspect of wavelength.

To further understand what happens when the wire bowtie antenna is integrated with mushroom AMC, we also plot the impedance comparison, as shown in 7.10

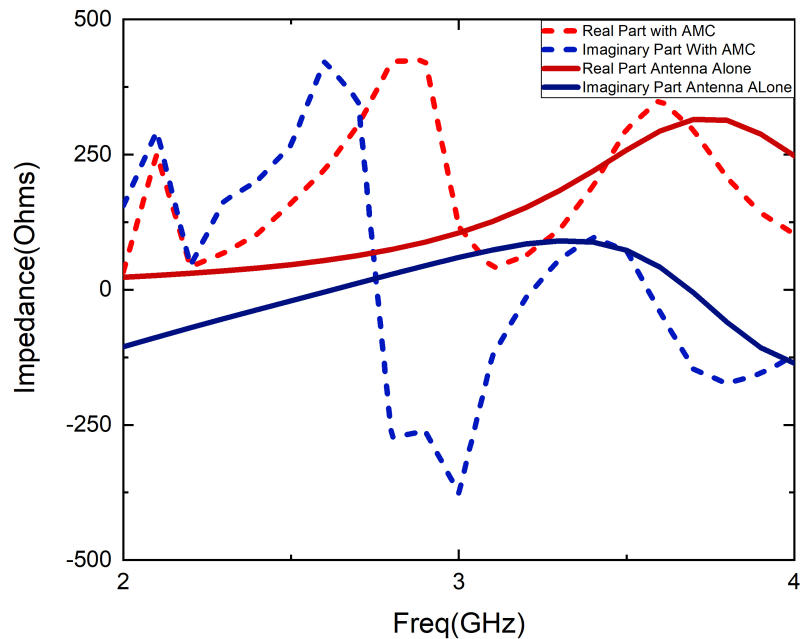


Figure 7.10: Impedance Comparison for a Wire Bowtie Antenna with and without Mushroom AMC

From the impedance comparison, we can see that with the presence of mushroom AMC, both the real and imaginary parts of the impedance change more rapidly with the frequency compared with that when the wire bowtie antenna is by itself. This proves that the reactive near field effect does have big impacts on the impedance of the antenna. Meanwhile, it is also observed that for higher frequencies, the impact becomes smaller as the impedance with and without the mushroom AMC are getting closer to each other. This effect is also a reason for us to choose the frequency

independent antenna for demonstration purpose. Narrowband antennas are typically resonant antennas, whose performance is affected greatly by the reactive near field, and the frequency independent antennas don't have a clear resonant frequency, so this kind of frequency shift has relatively smaller impacts. As shown in 7.11 and 7.12, especially for higher frequencies, the impact of the presence of the AMC is bigger when the frequency is getting closer to the starting point of resonance.

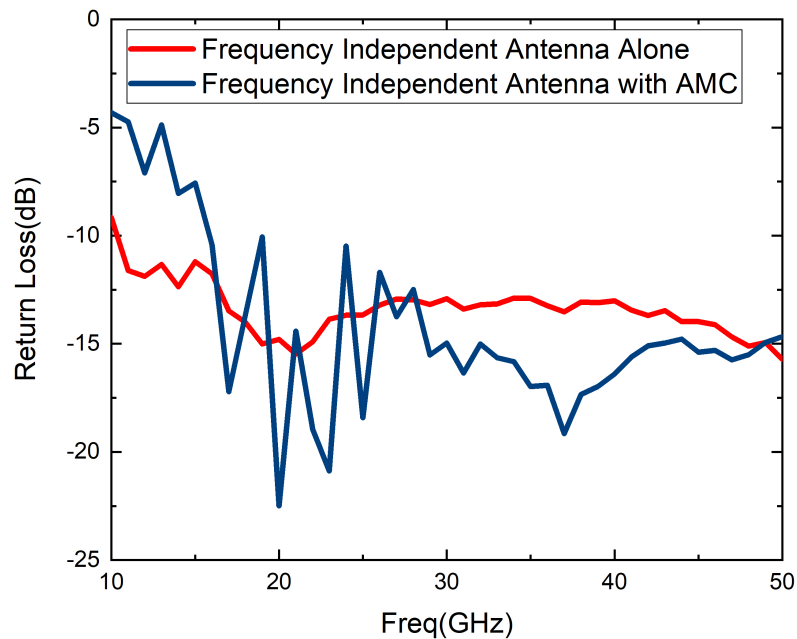


Figure 7.11: Return Loss Comparison for a Frequency Independent Antenna with and without Mushroom AMC

Patch to Patch Mushroom AMC

The structure and phase of reflection are shown in 7.13

The gains of the circular and spiral antenna with the AMC are plotted as in 7.14

It is observed that within the in-phase band, the peak gains are enhanced, and out of the band, the peak gains are reduced differently.

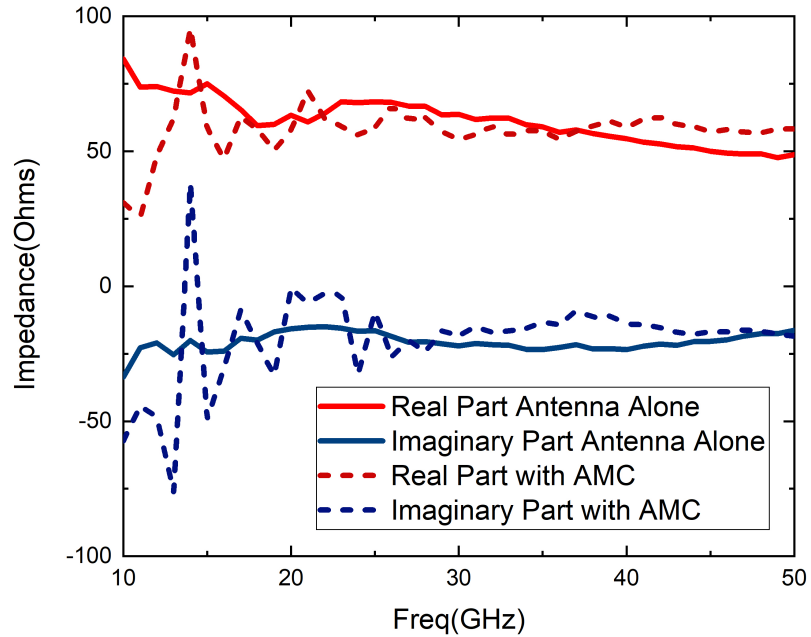


Figure 7.12: Impedance Comparison for a Frequency Independent Antenna with and without Mushroom AMC

Table 7.3: Parameters for Patch to Patch AMC

Parameter	Value(unit)
Cubic Sidelength	0.9mm
Top Gap Width	0.01mm
Top Patch Radius	0.4491mm
Ground Patch Radius	0.4425mm
Top Ground Distance	0.855mm
Superstrate Material	Air
Superstrate Dielectric Constant	1
Substrate Material	RO4350
Substrate Dielectric Constant	3.66

Non-Mushroom Vertical Crossed Rings Structure AMCs

The parameters of the vertical crossed rings with a crossed stop sign structure are listed in the table below, and the return losses and gains are shown here,

The structure and phase of reflection are shown in 7.15

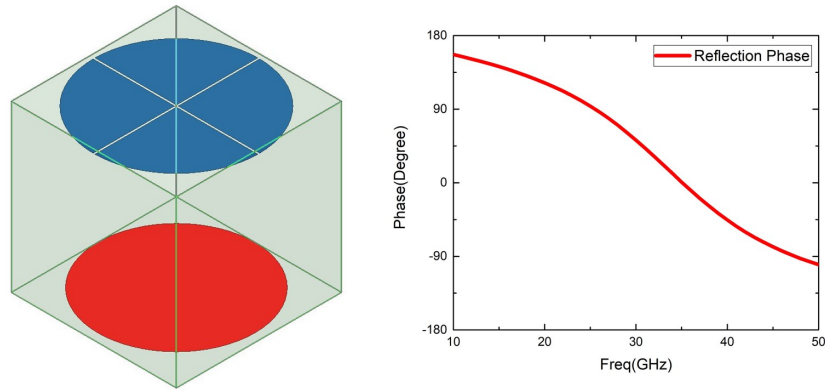


Figure 7.13: Patch to Patch Millimeter Wave AMC

Table 7.4: Parameters for Vertical Crossed Rings AMC

Parameter	Value(unit)
Ring Width	0.045mm
Middle Gap Width	0.27mm
Gap Between Rings	0.036mm
Unit Cubic Sidelength	0.9mm
Middle Stop Sign Sidelength	0.226mm
Substrate Material	RO4350
Substrate Dielectric Constant	3.66
Substrate Material	RO4350
Substrate Dielectric Constant	3.66
Substrate Thickness	0.11mm

The gains of the circular and spiral antenna with the AMC are plotted as in 7.16

It is observed that within the in-phase band, the peak gains are enhanced, and out of the band, the peak gains are reduced differently.

After making a comparison of the gains with and without the AMC, the AMC is proved to be able to increase the peak gain by 1.5dB - 3.5dB across the in-phase bandwidth, and out of the in-phase bandwidth, we observe a clear and significant decrease of peak gain. This model of AMC is also defined as effective.

Meanwhile, in order to show that our AMCs work also work with the narrow-band/single frequency antennas, we present a series of planar bowtie antennas at

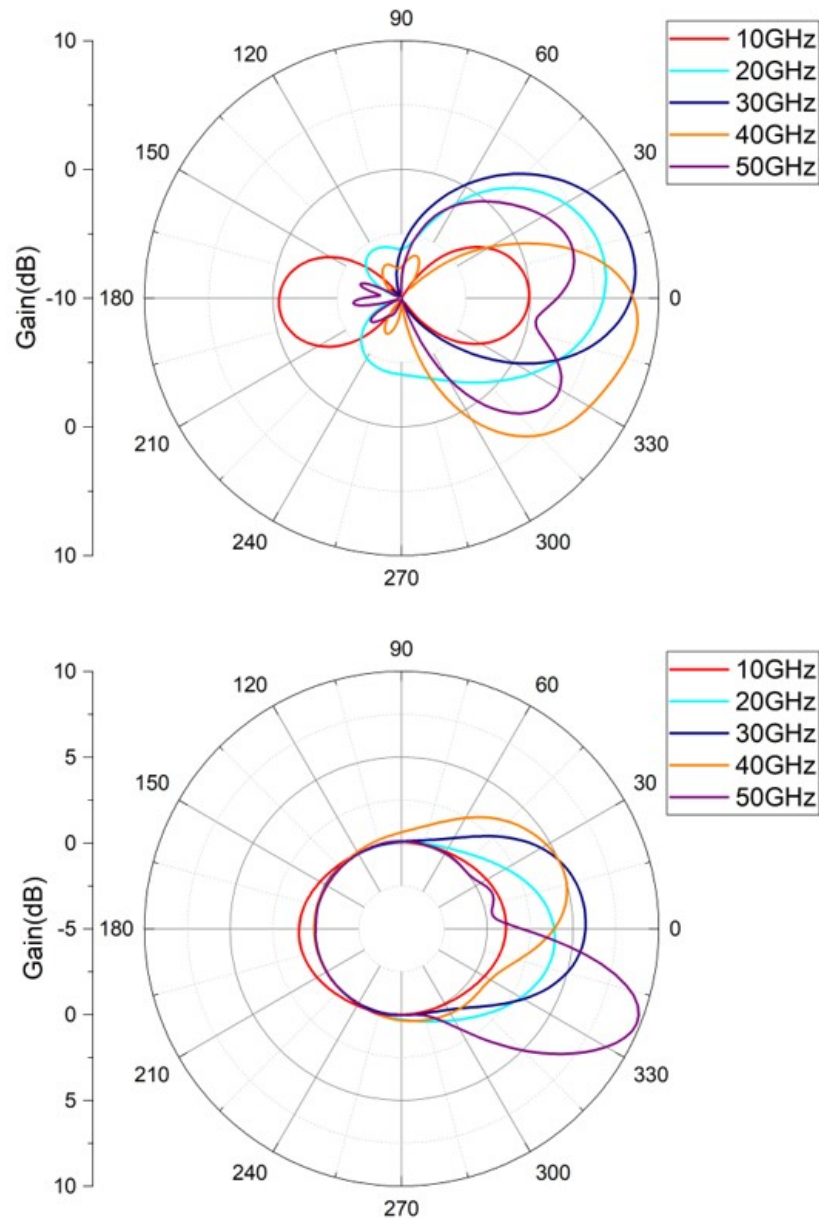


Figure 7.14: Gains With Patch to Patch AMC

last. In the purposing of reducing the reactive interaction between the AMC and the planar bowtie antennas, we make the bowtie antennas with wire structures. The resonant frequencies of the wire planar bowtie antennas are selected to be 30GHz, 35GHz, and 40GHz, all within the millimeter wave spectrum. 7.17

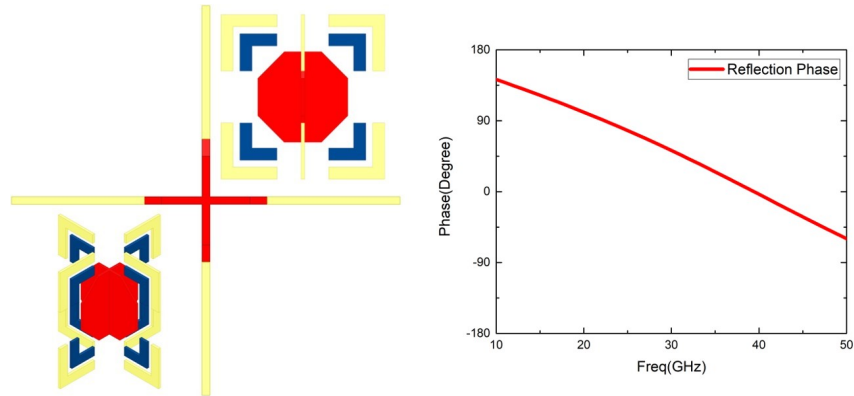


Figure 7.15: Vertical Cross Millimeter Wave AMC

The AMC structure selected here is the simplest mushroom structure AMC. The phase of reflection and gain comparison are shown in 7.18.

From 7.18, it is observed that the AMC presented works well with the wire planar bowtie antennas as expected, we also find that the average improvement of peak gain is around 3-4dB. The performance of 30GHz is best for it is almost the 0° crossing point of the AMC, while the 40GHz performs the worse for the phase of reflection at that frequency is -57° .

At this point, the principle of AMC discussed, the practical ways of designing AMCs, as well as the interaction between the AMC and antennas when required conditions are satisfied, are all proved to be valid. And generally speaking, it is easier and better to use the offset dual layer circular spiral antennas for the millimeter wave applications.

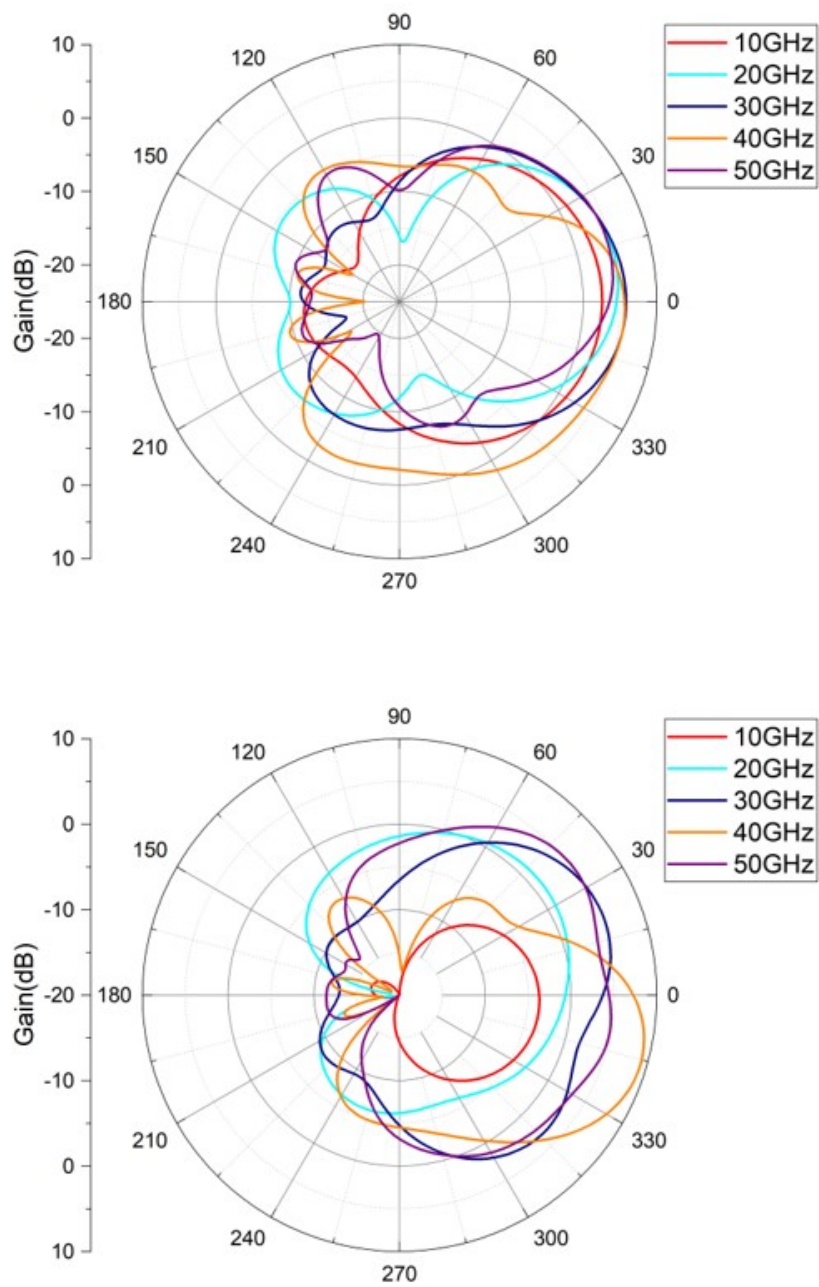


Figure 7.16: Gains With The Vertical Cross AMC

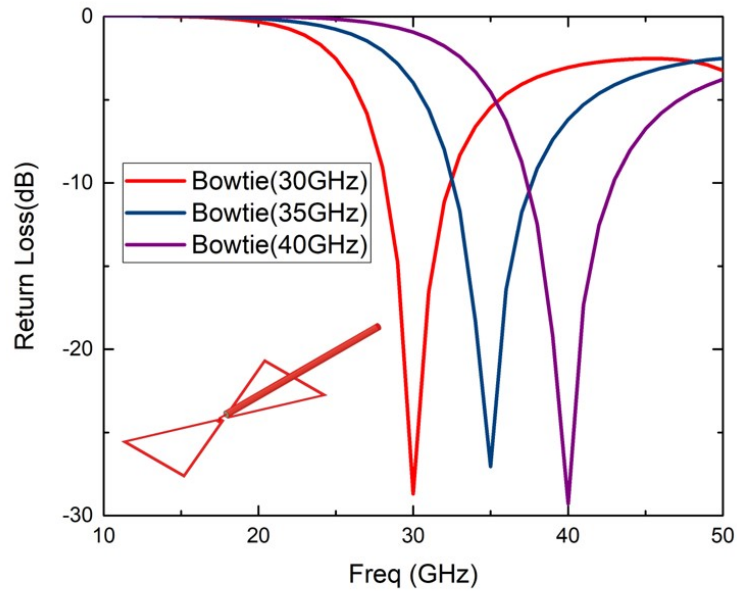


Figure 7.17: The Structure of Return Losses of the Wire Bowtie Antennas

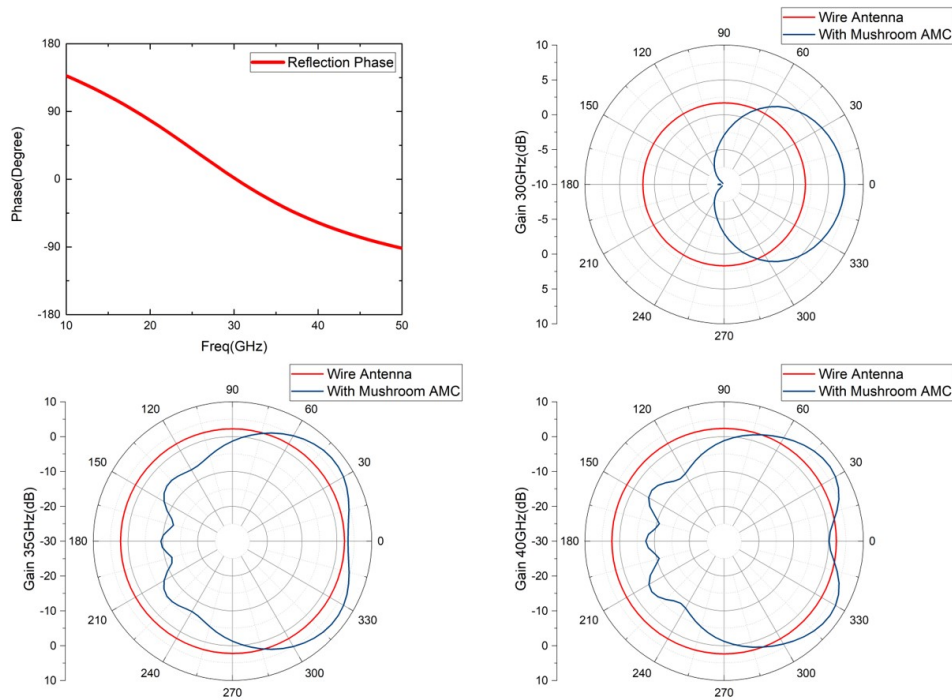


Figure 7.18: AMC Phase of Reflection and Gain With Bowtie

CHAPTER 8: Summary and Perspection

8.1 Summary

In this dissertation, we discussed the principles of AMCs, such as how can the permittivity and permeability be tuned. We also look into the interaction between the AMC and antennas placed very close to it and explain why they are still effective within the reactive near field. Using the summarized theories, we design a number of AMCs works under different spectrums, especially for the millimeter wave bandwidth, which is a very promising spectrum in development the 5G wireless communication technologies. We also use wideband antennas to prove that they are working as theoretically expected.

The AMCs presented in this dissertation, throws a light upon the future research of the 5G technologies. As known at this moment, the two key characters of the greatest importance of the 5G wireless communications are MIMO(Multiple In and Multiple Out) antenna systems and the Millimeter Wave Communications. The research presented here is expected to work for both of them. The ultra-wideband antennas can receive and send signals to come with slightly different frequencies simultaneously, and the associated AMC can enhance the radiation towards certain directions of the millimeter waves.

These millimeter wave AMCs, although demonstrated only with antennas, the application are not limited to antenna enhancement or even the on-chip antenna enhancement. These AMCs can be used to replace the absorption cavity wherever the radiation is not wanted. This transformation is very significant, for the AMC in 5G wireless communication technologies has two advantages over the cavity.

1. AMC helps certain directions to receive strong enough signals with less energy

cost, which means longer battery life for portable devices.

2. AMC reflects the radiation instead of absorbing it, and that means it will not produce as much heat as the cavity does. As known, the heat is one of the most dangerous enemies of the electronic devices, especially for the coming 5G portable devices whose internal space is even more crowded.

8.2 Future Work

Most of the charming prosperities shown in this dissertation of the AMCs are demonstrated only with simulation in HFSS. Although the HFSS has been long proved and trusted as a precise simulation tool which fits the measurement results well. A literally fabricated AMC and measurement results are still the most persuasive answer. Time permitted, we do want the designs to be fabricated and measured as many as possible.

Meanwhile, for some of the AMC designs, especially those for the 5G millimeter wave applications, we at this moment, are not very clear about how they can be fabricated, they may need the photolithography or deposition process in the clean room, which is not yet within our reach. However, that will undoubtedly, lead to a very bright future, and by the progress of the exploration towards the tomorrow of the 5G wireless communication technologies.

REFERENCES

- [1] Brian, R.M. Cohen, R.S *Hans Christian Orsted and the Romantic Legacy in Science*, Boston Studies in the Philosophy of Science, Vol. 241. 2007
- [2] James C. Maxwell, *A Dynamical Theory of the Electromagnetic Field*.1865
- [3] Xuehe Wang, Ryan S. Adams, *A Novel Ultra-Wide Band (UWB) Artificial Magnetic Conductor (AMC)*.
- [4] Xuehe Wang, Ryan S. Adams, *A Novel Ultra-Wide Band (UWB) Artificial Magnetic Conductor (AMC) For Millimeter Waves*.
- [5] Dip R. Thakar, Ryan S. Adams, *Implementation of a Self-matched 40:1 two arm Archimedean Spiral Antenna*. 2017
- [6] NASA, *OPEN DOCUMENT PUBLIC DOMAIN*
- [7] Feynman, *The Feynman Lectures on Physics Vol II* , Addison Wesley Longman, England, 1970.
- [8] Author James Maxwell, Editor Niven, M.A., F. R. S. *The Scientific Papers of James Clerk Maxwell, Volume 1*, Dover Publication, INC, NY, USA, 1965
- [9] David M.Pozar *Microwave Engineering, 4th Edition*,John Wiley and Sons, Inc., USA, 2011.
- [10] David M. Poaze, Stephen D. Targoniski, H.D. Syrigos, *Design of Millimeter Wave Microstrip Reflectarrays*, IEEE TRANSACTIONS ON ANTENNAS AND PROPAGATION, VOL. 45, NO. 2, USA, 1997.
- [11] Constantine A. Balanis *Advanced Engineering Electromagnetics, 2nd Edition*,John Wiley and Sons, Inc., USA, 2012.
- [12] Warren L. Stutzman, Gary A. Thiele *Antenna Theory, and Design, 2ND Edition*,John Wiley and Sons, Inc., USA, 1998.
- [13] Engheta, Nader; Richard W. Ziolkowski. *Metamaterials: physics and engineering explorations*, Wiley and Sons, USA, 2006.
- [14] Sir William Thomson Lord Kelvin. *The Molecular Tactics of a Crystal*, Clarendon Press, United Kingdon, 1894

- [15] Ikonen, Pekka. *Artificial Dielectrics and Magnetics in Microwave Engineering: A Brief Historical Revisit*, Helsinki University of Technology, Helsinki, Finland, 2005.
- [16] Pendry, J.B.; Holden, A.J.; Stewart, W.J.; Youngs, I. *Extremely Low Frequency Plasmons in Metallic Microstructures*, Phys. Rev. Lett, United Kingdom, 1996
- [17] Pendry, Holden, Robbins, Stewart. *Magnetism from Conductors, and Enhanced Non-Linear Phenomena*, IEEE Trans. Microwave Theory Tech, 1999.
- [18] V. G. Veselago, *The electrodynamics of substances with simultaneously negative values of ϵ and μ* , Sov. Phys. Usp, former USSR, 1967(8)
- [19] Sheldon Schultz. *Left handed metamaterials and intrinsic negative index of refraction*, UCSD Science and Engineering, CA, USA 2010
- [20] D. Schurig, J. J. Mock, B. J. Justice, S. A. Cummer, J. B. Pendry, A. F. Starr, D. R. Smith. *Metamaterial electromagnetic cloak at microwave frequencies*, Conference on Quantum Electronics and Laser Science (QELS) - Technical Digest Series, v 74, p 13, 2002
- [21] D. Sievenpiper, S. Kim, J. Long and J. Lee, *Advances in nonlinear, active, and anisotropic artificial impedance surfaces*, 2016 46th European Microwave Conference (EuMC), London, 2016, pp. 799-802. doi: 10.1109/EuMC.2016.7824464
- [22] William M. Daley, Secretary of US Department of Commerce, etc. *Federal Radar Spectrum Requirements*, 2000, USA
- [23] Ari Sihvola, *Metamaterials in electromagnetics*, Invited Review of Metamaterials, 2007
- [24] Nader Engheta. *Metamaterials With Negative Permittivity and Permeability: Background, Salient Features, and New Trends*, IEEE MTT-S International Microwave Symposium Digest, Invited paper, 2003.
- [25] Dan Sievenpiper, James Schaffner, Robert Loo, Gregory Tangonan, Samuel Ontiveros, and Rick Harold, *A Tunable Impedance Surface Performing as a Reconfigurable Beam Steering Reflector*, IEEE TRANSACTIONS ON ANTENNAS AND PROPAGATION, 2002
- [26] G. H. Schennum, *Frequency Selective Surface of Multiple Frequency Antennas*, Microwave Journal, USA, 1973
- [27] G. H. Schennum, *Design of frequency selective surfaces using a waveguide simulator technique*, Antennas and Propagation Society International Symposium, USA, 1975

- [28] Y. J. Yang, T. G. Dziura, S. C. Wang, and R. Fernandez, *Large CW Power, Very-Low-Threshold, Single Transverse Mode Operation of Vertical Cavity Mushroom Structure Surface Emitting Lasers*, IEEE TRANSACTIONS ON ELECTRON DEVICES, VOL. 38. NO 1, 1991
- [29] A. G. Cha, C. C. Chen and D. T. Nakatani, *AI OFFSET CASSEGRAINIAN REFLECTOR ANTENNA SYSTEM WITH A FREQUENCY SELECTIVE SUBREFLECTOR*, , Antennas and Propagation Society International Symposium, 1975
- [30] Dan Sievenpiper, Lijun Zhang, Romulo F. Jimenez Broas, Nicholas G. Alexopolous, Eli Yablonovitch, *High-Impedance Electromagnetic Surfaces with a Forbidden Frequency Band*, , IEEE TRANSACTIONS ON MICROWAVE THEORY AND TECHNIQUES, VOL. 47, NO. 11, 1999
- [31] Constantine A. Balanis *Antenna Theory Analysis and Design*, John Wiley and Sons, Inc., USA, 2005.
- [32] John Volakis *Antenna Engineering Handbook, 4th Edition*, McGrawHills, Inc., USA, 2007.
- [33] Daniel. J. Gregoire, Carson. R. White, Joseph. S. Colburn *Wideband Artificial Magnetic Conductors Loaded With Non-Foster Negative Inductors*. IEEE ANTENNAS AND WIRELESS PROPAGATION LETTERS, VOL. 10, 2011, Page 1586-1589
- [34] Daniel. J. Gregoire, Carson. R. White, Joseph. S. Colburn *Wideband Artificial Magnetic Conductors Loaded With Non-Foster Negative Inductors*. 978-1-4673-0037-7/12 2012 IEEE Page 237-240
- [35] Horold A. Wheeler *Transmission-Line Properties of Parallel Wide Strips by a Conformal-Mapping Approximation*, IEEE TRANSACTIONS ON MICROWAVE THEORY AND TECHNIQUES., Page 289 USA, 1964.
- [36] Brian C. Wadell *Transmission Line Design Handbook*, Artech Home, Inc. USA, 1991
- [37] Hisamatsu Nakano, Kazuo Hitosugi, Naoki Tatsuzawa, Daisuke Togashi, Hiroaki Mimaki, Junji Yamauchi *Effects on the Radiation Characteristics of Using a Corrugated Reflector With a Helical Antenna and an Electromagnetic Band-Gap Reflector With a Spiral Antenna*, IEEE TRANSACTIONS ON ANTENNAS AND PROPAGATION. VOL. 53, NO. 1, JANUARY 2005
- [38] Hidetoshi Ebara, Takao Inoue, Osamu Hashimoto *Measurement method of complex permittivity and permeability of a Powdered material using a waveguide in microwave band*, Science and Technology of Advanced Materials 7 (2006) 77-83

- [39] M. Moukanda, F. Ndagijimana, J. Chilo, P. Saguet *Complex Permittivity Extraction Using Two Transmission Line S-Parameter Measurements*, African Physical Review (2008) 2 Special Issue(Microelectronics)030.
- [40] Stephen D. Stearns *Non-Foster Circuits and Stability Theory*, 978-1-4244-9561-0/11 2011 IEEE, Page 1942-1945
- [41] Daniel. J. Gregoire, Carson. R. White, Joseph. S. Colburn *A Coaxial TEM Cell for Direct Measurement of UHF Artificial Magnetic Conductors*. IEEE Antennas and Propagation Magazine, Vol. 54, No. 2, April 2012
- [42] Filippo Costa, Simone Genovesi, Agostino Monorchio *On the Bandwidth of High-Impedance Frequency Selective Surfaces*, PROCEEDING OF THE I-R-E, 1955, Page 179-185
- [43] R. E. COLLIN *Theory and Design of Wide-Band Multisection Quarter-Wave Transformers*. IEEE Antennas and Propagation Magazine, Vol. 54, No. 2, April 2012
- [44] Ryan Gordon Quarfoth *Anisotropic Artificial Impedance Surfaces* . P.hD Dissertation, 2014, University of California, San Diego
- [45] J. S. Colburn*, D. F. Sievenpiper, B. H. Fong, J. J. Ottusch, J. L. Visher and P. R. Herz *Advances in Artificial Impedance Surface Conformal Antennas*. HRL Laboratories LLC, Malibu, CA, USA
- [46] Olli Luukkonen *ARTIFICIAL IMPEDANCE SURFACES*. Helsinki University of Technology, 2009
- [47] C. M. Tran, H. Hafdallah Ouslimani, L. Zhou and A. C. Priou *HIGH IMPEDANCE SURFACES BASED ANTENNAS FOR HIGH DATA RATE COMMUNICATIONS AT 40 GHz*. Progress In Electromagnetics Research C, Vol 13, 217229, 2010
- [48] S. A. Tretyakov and C. R. Simovski *WIRE ANTENNAS NEAR ARTIFICIAL IMPEDANCE SURFACES*. MICROWAVE AND OPTICAL TECHNOLOGY LETTERS / Vol. 27, No. 1, October 5 2000